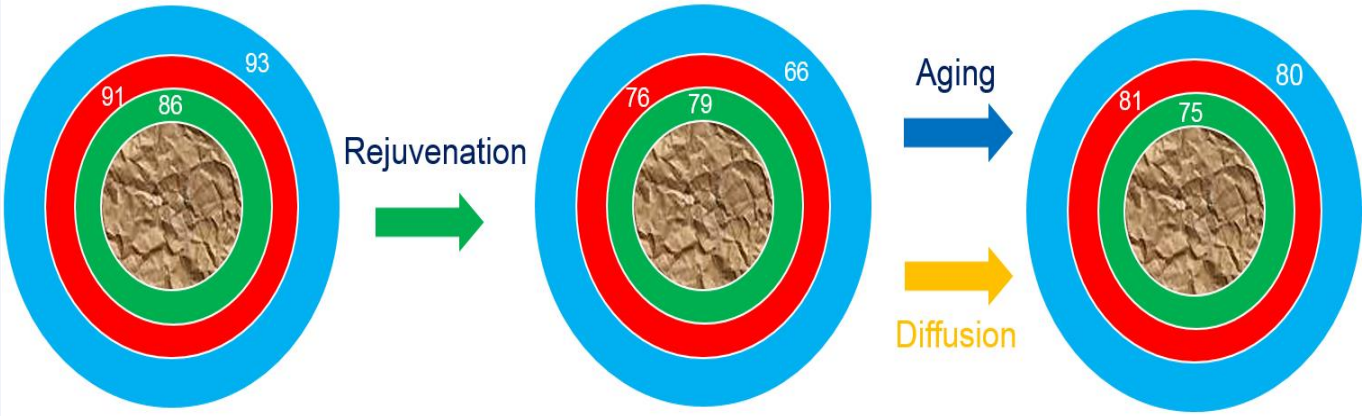

Final Report

Evaluation of the Effect of Homogeneity of the Asphalt Binder on Performance of a Recycled Mix

Contract Number: BDV29-977-35

Submitted by

Hesham A. Ali, Ph.D.,
Louay Mohammad, Ph.D.,
Mojtaba Mohammadafzali, Ph.D.,
Farshad Haddadi and
Moses Akentuna, Ph.D.

Civil and Environmental Engineering Department
Florida International University
10555 W. Flagler Street, Room EC3602, Miami, FL 33172
Phone: (305) 348-6755, Fax: (305) 348-2802, E-mail: heaali@fiu.edu

Submitted to

The Florida Department of Transportation
Research Center
605 Suwannee Street, MS 30
Tallahassee, FL 32399

March 29 2019

DISCLAIMER

The contents of this report reflect the views of the authors, who are solely responsible for the facts and accuracy of the data, the opinions, findings, and conclusions presented herein. The contents do not necessarily reflect the official views or policies of the State of Florida Department of Transportation, Florida International University, or Louisiana State University.

CONVERSION TABLE

SI* (MODERN METRIC) CONVERSION FACTORS

APPROXIMATE CONVERSIONS TO SI UNITS

Symbol	When You Know	Multiply By	To Find	Symbol
		LENGTH		
in	inches	25.4	Millimeters	mm
ft	feet	0.305	Meters	m
yd	yards	0.914	Meters	m
mi	miles	1.61	Kilometers	Km
		AREA		
in^2	square inches	645.2	Square millimeters	mm^2
ft^2	square feet	0.093	Square meters	m^2
yd^2	square yard	0.836	Square meters	m^2
ac	acres	0.405	Hectares	ha
mi^2	square miles	2.59	Square kilometers	km^2
		VOLUME		
fl oz	fluid ounces	29.57	Milliliters	mL
gal	gallons	3.785	Liters	L
ft^3	cubic feet	0.028	cubic meters	m^3
yd^3	cubic yards	0.765	cubic meters	m^3
	NOTE: volumes greater than 1000 L shall be shown in m^3			
		MASS		
oz	ounces	28.35	Grams	g
lb	pounds	0.454	Kilograms	kg
T	short tons (2000 lb)	0.907	megagrams (or "metric ton")	Mg (or "t")
		TEMPERATURE (exact degrees)		
°F	Fahrenheit	5 (F-32)/9 or (F-32)/1.8	Celsius	°C
		ILLUMINATION		
fc	foot-candles	10.76	Lux	lx
fl	foot-Lamberts	3.426	$candela/m^2$	cd/m^2
		FORCE and PRESSURE or STRESS		
lbf	poundforce	4.45	Newtons	N
lbf/in^2	poundforce per square inch	6.89	Kilopascals	kPa

APPROXIMATE CONVERSIONS FROM SI UNITS

Symbol	When You Know	Multiply By	To Find	Symbol
		LENGTH		
mm	millimeters	0.039	Inches	in
m	meters	3.28	Feet	ft
m	meters	1.09	Yards	yd
km	kilometers	0.621	Miles	mi
		AREA		
mm^2	square millimeters	0.0016	square inches	in^2
m^2	square meters	10.764	square feet	ft^2
m^2	square meters	1.195	square yards	yd^2
ha	Hectares	2.47	Acres	ac
km^2	square kilometers	0.386	square miles	mi^2
		VOLUME		
mL	Milliliters	0.034	fluid ounces	fl oz
L	liters	0.264	Gallons	gal
m^3	cubic meters	35.314	cubic feet	ft^3
m^3	cubic meters	1.307	cubic yards	yd^3
		MASS		
g	grams	0.035	Ounces	oz
kg	kilograms	2.202	Pounds	lb
Mg (or "t")	megagrams (or "metric ton")	1.103	short tons (2000 lb)	T
		TEMPERATURE (exact degrees)		
°C	Celsius	1.8C+32	Fahrenheit	°F
		ILLUMINATION		
lx	lux	0.0929	foot-candles	fc
cd/m^2	$candela/m^2$	0.2919	foot-Lamberts	fl
		FORCE and PRESSURE or STRESS		
N	newtons	0.225	Poundforce	lbf
kPa	kilopascals	0.145	poundforce per square inch	lbf/in^2

*SI is the symbol for the International System of Units. Appropriate rounding should be made to comply with Section 4 of ASTM E380 (Revised March 2003)

Technical Report Documentation Page

1. Report No.	2. Government Accession No.	3. Recipient's Catalog No.
4. Title and Subtitle Evaluation of the Effect of Homogeneity of the Asphalt Binder on Performance of a Recycled Mix		5. Report Date March, 29, 2019 6. Performing Organization Code
7. Author(s) Hesham Ali, Louay Muhammad, Mojtaba Mohammadafzali, Farshad Haddadi and Moses Akentuna		8. Performing Organization Report No. Test Report No. BDV29-977-35
9. Performing Organization Name and Address Florida International University 10555 W. Flagler Street, Room EC3602, Miami, FL 33172		10. Work Unit No. (TRAIS) 11. Contract or Grant No.
12. Sponsoring Agency Name and Address State of Florida Department of Transportation 605 Suwannee Street, M.S. 75 Tallahassee, FL 32399-0450		13. Type of Report and Period Covered Draft Final Report 14. Sponsoring Agency Code
15. Supplementary Notes		

16. Abstract

The road to sustainability passes through the process of recycling a greater amount of asphalt pavement. Inclusion of additional amounts of reclaimed asphalt pavement (RAP) in new mixes has become a prominent method to promote sustainability. This research addresses some of the challenges related to high RAP content mixes. Among the factors considered are the impact of rejuvenator diffusion on binder stiffness, stiffness gradient, performance grade, homogeneity, and ultimately, their effects on mix performance.

In this project, an experiment was conducted to evaluate the effects of the rejuvenator type, dosage rate, and mix-aging protocol on recycled binder homogeneity and mix performance. Another experiment was conducted to evaluate the ability of several simulated aging protocols to produce a binder stiffness and stiffness gradient similar to those observed in natural aging. The results show that the target high temperature grade of a recycled mix should be set at 6^{o}C higher than that of virgin mixes. In general, mixes with a high temperature grade of 6^{o}C higher than a virgin mix performed better in rutting and comparably in cracking. There is a strong correlation between binder stiffness gradient and cracking performance. The best simulated aging protocol was to heat the mix to 110^{o}C for 4 days. These results were based on five mixes and a total of 15 mix/aging protocol combinations.

17. Key Word	18. Distribution Statement		
Reclaimed asphalt, homogeneity, durability, aging, performance, rejuvenation, performance grade	Copyrighted. Not to be copied or reprinted without consent from the Florida International University.		
19. Security Classif. (of this report) Unclassified	20. Security Classif. (of this page) Unclassified	21. No. of Pages 88	22. Price n/a

EXECUTIVE SUMMARY

The road to sustainability passes through the process of recycling a greater amount of asphalt pavement. Inclusion of additional RAP in new mixes has been a prominent method for promoting sustainability. This research reviews some of the challenges related to high RAP content mixes. Among the factors considered are the impact of rejuvenator diffusion on binder stiffness, stiffness gradient, performance grade, homogeneity, and ultimately, their effects on mix performance.

In this project, an experiment was conducted to evaluate the effects of the rejuvenator type, dosage rate, and mix-aging protocol on recycled binder homogeneity and mix performance. The experimental design consisted of 15 cells, which represent three aging protocols and five mixes: one virgin mix (control), one mix recycled with an RA1 rejuvenator to the same Superpave Performance Grading (PG) as the control; one mix recycled with an RA1 rejuvenator to a 6°C higher high-temperature PG (HTPG) than the control; one mix recycled with an RA2 rejuvenator to the same HTPG as the control; and one mix recycled with an RA2 rejuvenator to a 6°C higher HTPG than the control. The RA1 rejuvenator was selected to represent good rejuvenation, and the RA2 was selected to represent a lower quality rejuvenation from the perspective of durability and homogeneity. The materials used for preparing the samples included locally supplied RAP, two rejuvenators, limestone aggregates of the same gradation as the RAP and a PG 67-22 virgin binder.

The testing program included the Hamburg loaded-wheel test (LWT), semicircular bend test (SCB), and Florida indirect tension test (IDT). All mixes were tested at three aging levels: one short-term aging level and two long-term aging levels. The short-term aging process consisted of placing the loose mix in a conventional oven at 165°C for one hour. The second and third aging levels involved placing compacted asphalt specimens in a conventional oven at 85°C for five and ten days, respectively. The performance of the samples was compared, and the correlation between homogeneity and performance parameters was evaluated.

The results show the target HTPG of a recycled mix should be set at 6°C higher than virgin mixes. In general, mixes with a HTPG of 6°C higher than a virgin mix performed better in rutting and comparably in cracking. There is a strong correlation between binder stiffness gradient and cracking performance. It is suggested the target HTPG of the recycled mix be selected to optimize rutting and cracking performance.

The effectiveness of rejuvenation can be evaluated using critical Pressure Aging Vessel (PAV) time and homogeneity index. Both rejuvenators used in this study had a PAV critical time of more than 50 hours and a homogeneity index of more than 0.9. However, RA1 had a slightly better homogeneity than RA2. In general, RA1 had a rutting performance similar to RA2, and both performed better than the virgin mix. Based on SCB J_c and IDT $DCSE_f$ parameters, RA1 had a better cracking performance than RA2, but the virgin mix had better cracking performance than the recycled mixes. However, the Energy Ratio (ER) parameter showed that the mix with RA1 rejuvenator had a better cracking performance than the virgin mix, and RA1 mixes performed better than the RA2 mixes.

The average rut depth for recycled mixes with HTPG of the same as virgin mix was 10.46 mm and with recycled mixes with 6°C higher HTPG was 2.84 mm. This indicates that overall rutting performance of the control mix was almost the same as recycled mix when the HTPG are the same. Also, this indicates that recycled mixes had an overall better rutting resistance than the virgin mix when its HTPG was 6°C higher than the virgin mix.

Based on $DCSE_f$ values, the virgin mix had the best performance, with an average $DCSE_f$ value of 4.36 kJ/m^3, followed by mixes recycled with RA1, with an average $DCSE_f$ value of 2.58 kJ/m^3, followed by mixes recycled with RA2, with an average $DCSE_f$ value of 2.48 kJ/m^3. This order of performance is the same as that established by SCB Jc. All mixes had $DCSE_f$ values higher than the critical value of 0.75 kJ/m^3, indicating satisfactory crack initiation resistance behavior. According to ER values, the mix recycled with RA1 had the best performance, with an average ER value of 5.87, followed by the virgin mix, with an average ER value of 4.86, and further followed by mixes recycled with RA2, with an average ER value of 4.83. All mixes exhibited ER values higher than the critical value of 1, indicating satisfactory crack initiation resistance behavior.

Another experiment was conducted to evaluate the ability of several simulated long-term aging protocols to produce a similar binder stiffness and stiffness gradient, as observed in natural aging. The best simulated aging protocol was to oven-heat the loose mixes to 110^{o}C for 4 days. It was observed that heating to 135^{o}C, as commonly done, leads to a different stiffness gradient than the one seen in naturally aged mixes.

TABLE OF CONTENTS

LIST OF FIGURES

LIST OF TABLES

Chapter 1 : INTRODUCTION AND LITERATURE REVIEW

Increasing the quantity of reclaimed asphalt pavement (RAP) in the construction of asphalt pavements is an important approach for improving the sustainability of roadway systems (Ali and Sobhan 2012; Alkins et al., 2008; Silva et al. 2012). Using a higher proportion of RAP leads to reducing the consumption of energy and raw material for pavement construction (Zaumanis et al., 2014a; Dony et al., 2013). However, due to the uncertainty of the performance of high-RAP asphalt mixes, most agencies limit the RAP content for pavement surface layers (Al-Qadi et al., 2007). The main reasons for this hesitation are the difficulties in the aggregate gradation control, the aging of the RAP binder, and the blending between the aged binder, the new binder, and the rejuvenator, if used. The focus of current research is on the blending concerns.

Generally, the amount of blending that occurs between the aged binder within the RAP and the recycling agent or virgin binder that is added to it is unknown. In many cases, a complete blending is assumed. However, the reliability of this assumption has not been verified. The three scenarios considered in the literature that express the blending of the old and the new binder are the following (Bowers et al., 2013):

- *No Blending (black rock):* In this scenario, it is assumed no blending occurs between the aged and new binders. Therefore, the RAP aggregate and aged binder together function as a black rock.
- *Complete Blending:* It is assumed the aged and the new binder blend completely and form a uniform asphalt mastic.
- *Partial Blending*: In this case, although the aged and the new binder blend, the blending is not complete. Therefore, portions of the aged asphalt do not participate in the blending process effectively.

Although some experiments show the black rock theory is applicable when the RAP content is low (under 20%), it cannot be applied when the RAP content is higher. Generally, previous research show partial blending is often true, but the extent of blending is unknown (, Zaumanis et al., 2014b). Figure **1-1** presents the previously mentioned scenarios schematically.

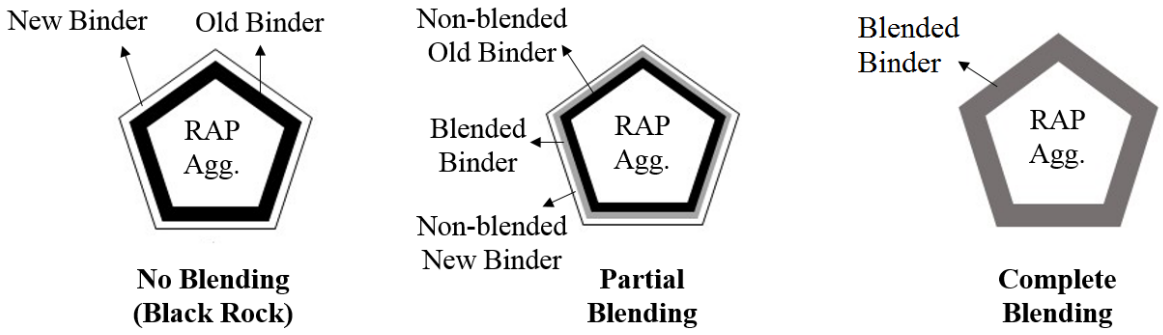

Figure 1-1. Three Scenarios for Blending of the Aged and the Virgin Binders.

1.1 Methods to Measure the Level of Blending

Several methods have been used to evaluate the blending of the aged and the new binders. These methods can be categorized as stage extraction methods, binder marking methods, and chemical identification methods. In these methods, it is assumed the aggregates are surrounded by a film of asphalt that does not necessarily have similar properties throughout its thickness, and its inner layers can be different from its outer layers.

1.1.1 Stage Extraction Method

In stage extraction methods, the asphalt film that surrounds aggregates is extracted using a solvent in several stages. The idea is that the first stage of the extraction, which is done in a relatively short time, provides a sample of the outer layers of the asphalt film, and subsequent extractions recover inner layers of asphalt. Therefore, several samples are obtained, each representing a different layer. Those samples are then characterized by performance or chemical methods. Figure ***1-2*** shows a three-stage extraction method schematically.

The stage extraction method was first introduced by Zearley (Zearley, 1979) and Carpenter and Wolosick (Carpenter and Wolosick, 1980). In those experiments, the binder was extracted in three stages, and Trichloroethylene was used as the solvent. The samples were characterized by their viscosity and penetration grade. The same method was used in work of Noureldin and Wood with four stages of extraction and in work of Kooij and Verburg with very hard RAP (Noureldin and Wood, 1987; Kooij and Verburg, 1996). Karlsson and Isacsson used a Fourier transform infrared spectroscopy with an attenuated total reflectance (FTIR-ATR) method to characterize the aging of the sample obtained from stage extraction (Karlsson and Isacsson, 2003). FTIR is a spectroscopy method that yields an infrared spectrum of absorption or emission of a substance. Fourier-transform is needed to convert the raw data from the infrared scanning to a spectrum. Components are associated with particular ranges of bandwidth to be identified.

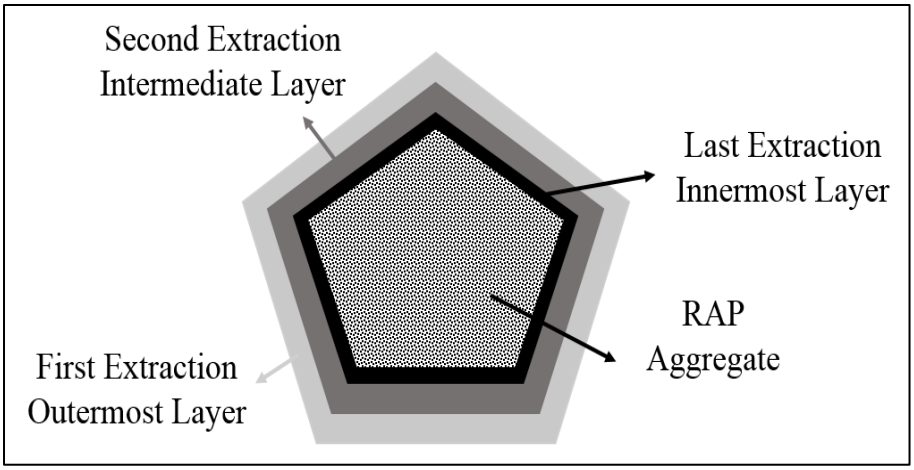

Figure 1-2. Schematic Illustration of a Stage Extraction Method.

There are concerns regarding the reliability of the stage extraction method. A possible flaw is that the remaining solvent from a previous extraction affects the result the subsequent ones. The type of the solvent can also be influential. It is possible that a particular type of solvent dissolves lighter components of the aged binder during the first few extraction stages and dissolves heavier binder components in the last extraction stages. Thus, the extracted binder with more heavier binder components will show more aging properties than the one with more lighter binder components (Xu et al., 2014; Zhao et al., 2016). A study to investigate some of these possible flaws was reported in (Bowers et al. 2014). A six-stage extraction was performed on a homogeneous sample of aged asphalt using four different solvents, trichloroethylene, tetrahydrofuran, toluene, and decalin. The samples were compared based on their carbonyl index, which was measured by FTIR. Carbonyl index is the ratio of the area beneath the Carbonyl (C=O) band in the FTIR spectrum to the area of the saturated C-C band. While the saturated C-C band is not affected by the aging process, the oxidation increases the amount of Carbonyl. Therefore, an increase in the Carbonyl index is an indication of aging. Since no meaningful difference was observed in the samples from different extractions, it was concluded that the mentioned flaws are not significant. Also, this study showed that Trichloroethylene had the best performance as the solvent for stage extraction. A modified stage extraction procedure was employed in work of Zhao et al. In this procedure, an almost equal quantity of the binder was recovered in each stage of extraction.

1.1.2 Binder Marking Methods

In binder marking methods, the binder molecules are manipulated to facilitate their ability to be detected. A possible manipulation approach is to alter the atoms. However, this method did not yield satisfactory results in asphalt studies (Navaro et al., 2012).

An alternative approach is to make small changes in the chemical composition of the material. In an experiment that utilized this approach, Energy-Dispersive X-ray Spectroscopy (EDXS) with titanium was used to observe the blending of the binders (Lee, 1983). EDXS is a technique for

microanalysis of the chemicals, which uses the microscope primary beam to generate X-rays and detect the emission of sample X-rays.

The image processing technology is also applicable for observing the diffusion process. In a study, samples of mixed RAP and virgin binder were photographed. Iron oxide pigment was used to change the color of the virgin asphalt to red (Nguyen, 2009). In another study, the image analysis was performed under white light and ultraviolet (UV) light. The virgin binder was manipulated to be detectable by UV light. Navaro et al. (2012) and Cavalli et al. (2016) performed multi-scale study on the distribution of the components within a high RAP asphalt mix. Energy dispersive X-ray spectroscopy was used to visualize the binder film thickness at the microscale. This technique provided detailed information about the structure of the aggregate surface and near-surface microstructure. It was shown that the thickness of the RAP binder film decreases with an increase in the mixing temperature. Although the use of microscopy and image processing techniques for studying the mixing process has been limited, the few conducted studies that used these approaches provided a better understanding of the microstructure of the mixes and the diffusion process.

1.1.3 Chemical Identification Methods

In chemical identification methods, the variations in the composition of the binder within its body are detected and identified. FTIR is the most popular method used for this purpose (Karlsson and Isacsson, 2003; Zhao et al., 2016; Ding et al., 2016). However, there are several other methods that have been used successfully and are reported in the literature, including gel permeation chromatography, gas chromatography, atomic force microscopy, and differential scanning calorimetry.

In the studies on asphaltic material that use FTIR, some indices such as Carbonyl Index and Sulfoxide Index are often used to determine the level of aging. In many cases, FTIR is used with stage extraction methods (Bowers et al., 2014).

Gel permeation chromatography is a variation of size exclusion chromatography that facilitates separation of different components in a solution by analyzing the molecular weight distribution (Bowers, 2013) . Gas chromatography is another chromatography technique that uses a vaporized substance to analyze a compound (Tang and Isacsson, 2005). Atomic force microscopy is a very high-resolution microscopy technique that facilitates the examination of surface topography and phase separation of the material, as well as properties such as stiffness and adhesion. This method has been used to study the microstructure of the bituminous material (Allen et al.,,, 2012). In a differential scanning calorimetry method, the amount of heat that increases the temperature of a component is used for its identification. This method can be used to study the time-dependent behavior of asphalt (Zhi-ling et al., 2005; Masson et al., 2002).

1.2 Blending of the Aged Asphalt and the Recycling Agent

The blending of the new binder or recycling agent with the aged asphalt is a time-dependent process. Initially, as a general description, the aggregate that is coated with a layer of aged asphalt is surrounded by a relatively low viscosity layer of recycling agents. Further, the recycling agent penetrates the outer hard asphalt layers and causes a reduction in their viscosity. As the diffusion continues toward inner layers, the viscosity of the outer layers increases and that of the inner layers decreases. If the mixing is complete, an equilibrium can be reached, and most of the body of the recycled asphalt has almost consistent viscosity. Only the thin layer at the interface of binder and aggregate might remain relatively hard (Carpenter and Wolosick, 1980). Previous research has shown that the diffusion process can continue up to six months after the construction of the pavement (Xu, et al., 2014; Huang et al., 2005).

A study that used FTIR to identify the level of aging showed that the temperature has a significant impact on the rate of diffusion as higher temperature accelerates the diffusion process. The study also indicated that Fick's law could express the diffusion process (Karlsson and Isacsson, 2003). Another research that used a similar method claimed that warm mixes had a higher blending effectiveness compared to hot mixes that used rejuvenators (Ding et al., 2016). This is in contrast with the existing knowledge that a higher temperature accelerates the diffusion process (Karlsson and Isacsson, 2003).

A finite element model developed for the plant mixing process indicated that the dosage of the recycling agent also influences the time it takes the mix to reach equilibrium (Zaumanis et al. 2014). A study that used a molecular dynamics model showed that in addition to the temperature, the molecular weight of asphaltic molecules affects the rate of diffusion. It was concluded from the simulation model that rejuvenator application sequence is influential. While the mixing of the rejuvenator with the virgin binder did not improve the blending effectiveness, adding the rejuvenator to the aged asphalt accelerated the diffusion process significantly (Ding, et al., 2016). Another study that used Dynamic Shear Rheometer (DSR) to characterize the binder confirmed the effect of mixing temperature and concluded that a temperature less than 100°C results in insufficient blending. It also indicated that the asphalt chemical composition affects the diffusion rate (Rad et al., 2014).

Karlsson and Isacsson (2003) investigated the effects of aging on the diffusion process. Their study showed no significant effects from the Rolling Thin Film Oven short-term aging. Results indicated that bitumen distillation increased the polarity and molecular size of the maltenes and reduced the diffusion rate. Despite the fact that the viscosity of the maltenes that form the diffusing media could not be obtained precisely, the output from the Stoke-Einstein equation yielded a good correlation with diffusion data (Karlsson and Isacsson 2003).

1.3 The Effect of Binder Homogeneity on the Performance of the Pavement

An incomplete blending of the recycling agent and the aged asphalt results in a non-homogeneous composite-layered binder mastic that consists of layers with different properties. Such a condition

can influence the performance of the pavement significantly. Despite the importance of such an issue, limited research has been conducted on this subject. Research by Huang et al. (2005) showed that mixing of the RAP with a recycling agent produces a composite layered structure with a stiffer binder in the layers that are immediately attached to the aggregate and a softer binder in outer layers. Such a structure was concluded to be favorable to improve the performance of the pavement by decreasing the stress concentration (Huang et al. 2005). However, as the diffusion process continues, such an effect diminishes a few months after the pavement construction. Therefore, premature deterioration might occur while initial performance evaluations have passed the acceptance criterion. Figure 1-3 shows variations of the degree of blending with time and its possible effects on the performance of the mix (Xu. et al., 2014). This study also presented a method to predict the level of blending using performance parameters, including dynamic modulus and tensile strength. However, if a rejuvenator is applied, opening the road to traffic before allowing sufficient time for the diffusion can cause premature rutting and cracking.

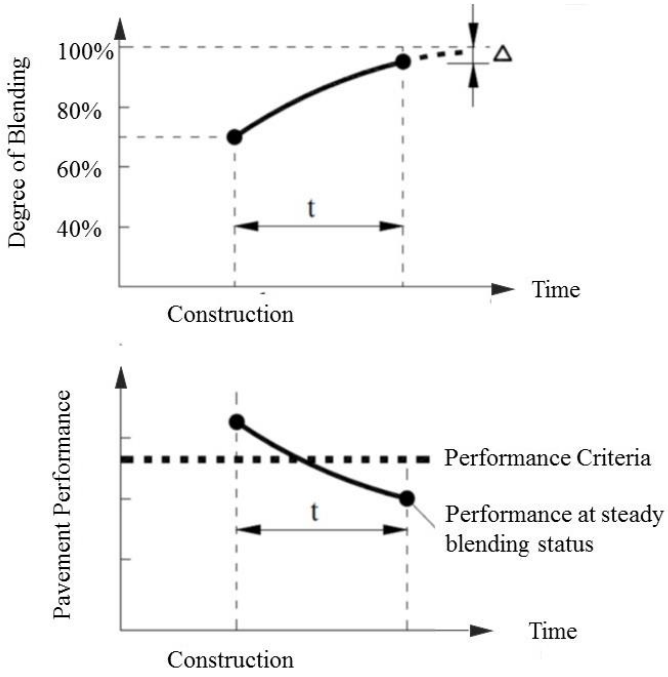

Figure 1-3. Potential Effect of the Blending Status on the Performance of the Pavement.

Coffey et al. (2013) used mechanistic-empirical design principles to investigate the impact of the degree of blending on the performance of the RAP. Results showed that the degree of blending was 85% to 90% for three RAP samples that were tested. The degree of blending did not affect the rutting performance significantly in this study (Coffey et al., 2013). However, if a rejuvenator is applied, opening the road to traffic before allowing sufficient time for the diffusion of the rejuvenator may compromise the pavement stability, because the outer layers are still too soft (Zaumanis et al., 2014). A study on the effects of production stages or binder blending was performed using the rheological properties of the RAP mixes. Dynamic modulus and creep compliance were the performance parameters that were tested. Results showed that the degree of

blending is more influential on intermediate temperature properties of the mix compared to its low-temperature properties. It was proposed that the optimum storage time for high RAP mixes with rejuvenators should be determined so that enough time is allowed for the diffusion process without causing excessive aging (Zhang and Muhunthan, 2017).

1.4 Summary

The uncertainty about the blending process between the old and the new binder is a source of concern regarding the performance of high RAP content asphalt mixes. Generally, it is believed that although some blending occurs, the mixing is often incomplete and the binder remains non-homogeneous. The degree of blending is often unknown.

Several techniques have been used to investigate the blending process, including binder marking methods, chemical identification methods, and the stage extraction method. Among these, the stage extraction method is the most widely used, and its applicability has been confirmed by several researchers. This method divides the asphalt film into separate layers and can be implemented along with performance measurements such as DSR tests or chemical identification methods such as FTIR.

It has been indicated in several studies that the diffusion continues for a long time after the initial mixing and gradually homogenizes the asphalt matrix. An increase in the temperature accelerates the diffusion process.

The existing knowledge about the effects of binder homogeneity and the diffusion process on the performance of the pavement is limited and insufficient. Generally, previous research shows that the composite layered structure present in recycled mixes improves pavement performance. However, even if that is true, such an improvement diminishes when the diffusion process continues and alters the initial conditions of the asphalt film. These circumstances might lead to a rapid drop in the performance of the pavement. In addition, some extent of diffusion is necessary to prevent the instability of the pavement. Therefore, especially in cases where the material is placed immediately after mixing, such as in in-place recycling methods, a sufficient amount of time should be allowed before opening the pavement to traffic.

As a part of phase I of the current research, the effects of aging on the structure of the binder film was investigated. To the best of the authors' knowledge, there is no published study on this effect reported in the literature.

1.5 Research Objectives

The objective of this research is to evaluate the effects of binder homogeneity and durability on the performance of recycled mixes. It is known from previous research that binder diffusion, rejuvenation and aging influence the structure of the binder film that coats aggregates. This research aims to gain a better understanding of the effects of these parameters on binder homogeneity and consequently, the performance of the mix.

The homogeneity index was used as a measure of asphalt binder's homogeneity. This parameter is obtained by separating different layers of the asphalt film that coat the aggregates, using the stage extraction method, and then determining the high temperature performance grade (HTPG) of each layer. Five samples, including one virgin mix and four recycled mixes, were tested for their rutting susceptibility, moisture resistance and fatigue cracking resistance at three aging levels. The performance of the samples was compared, and the relationship between homogeneity and performance parameters was evaluated.

Previous research work showed that if an effective rejuvenator is used, the rejuvenated binder would have two advantages over virgin asphalt: It ages slower and the resultant binder is more homogeneous. When virgin mixes age, their outer layers harden more quickly and their fatigue resistance drops. In a properly recycled mix, after five days of oven aging at 85°C, the HTPG of the outer layer is almost similar to the average HTPG of the binder. In addition, if a proper rejuvenator is used, the rejuvenated binder ages at a slower rate. In theory, by using an appropriate rejuvenator, the long-term performance of the recycled mix can match or even exceed that of new mixes. These advantages can be used as a basis for designing high RAP mixes with acceptable performance. This study has four hypotheses:

1. The effectiveness of rejuvenators can be evaluated using critical PAV time and the homogeneity index. The acceptable limits for these parameters should be determined after further studies with additional rejuvenators. However, the following tentative limits were used in this research to distinguish between proper and improper rejuvenators in this study:
    - Critical PAV Time $\geq$ 50 hours
    - $I_h \geq 0.9$
2. A recycled mix rejuvenated by a proper rejuvenator has a better long-term performance in comparison with a new mix with a virgin binder with a similar HTPG. This is based on the observation that the outer layer of the virgin binders, which highly contribute to cracking resistance, is stiffer due to aging.
3. The target HTPG for a recycled mix can be set 6°C higher than virgin mixes, without compromising the performance. In other words, a recycled mix can have a similar long-term performance to that of a virgin mix, with a 6°C lower HTPG.
4. If an improper rejuvenator is used, the recycled mix will have worse long-term performance compared to a virgin mix.

1.6 Report Organization

This report consists of seven chapters. Chapter 1 reviews the most recent studies on the performance of recycled mixes and diffusion of rejuvenators. Chapter 2 describes the sample preparation procedure. Chapter 3 describes the laboratory protocol used to determine binder homogeneity and stiffness gradient. Chapter 4 describes the mix performance testing procedures. Chapter 5 presents the analyses of the results from Chapters 3 and 4 and explores the correlations

between homogeneity and performance parameters. Chapter 6 presents the aging protocol evaluation. Chapter 7 summarizes the important findings of the research.

Chapter 2 : MIX PREPARATION

2.1 Introduction

This section presents the process of sample preparation. The RAP was recycled using two different rejuvenators: one possessed desirable durability and diffusion characteristics, while the other had fewer desirable properties. In addition, two different target PG values were considered for the rejuvenated samples. The samples underwent three levels of aging: short-term aging and two levels of long-term aging.

An important consideration in the sample preparation process was to produce samples with consistent aggregate gradations and air-void values, despite their different compositions. To achieve this goal, several trial mixes were produced and tested.

2.2 Material

One type of RAP, two rejuvenator types, one virgin binder, and virgin aggregate were used to prepare the samples. One of the rejuvenators was selected based on experience from earlier phases of this research, and the other was selected from four nominated products, based on the homogeneity index.

2.2.1 RAP

A RAP sample weighing approximately 3,000 pounds was obtained from a RAP stockpile and was mixed thoroughly to produce a consistent sample. Three samples of RAP were tested to characterize the material. The aggregate was extracted from the samples, and the binder content was determined using an ignition oven, in accordance with ASTM D6307. In addition, the maximum specific gravity (G_{mm}) of the samples was determined in accordance with ASTM D2041.

The RAP binder was recovered using a centrifuge extractor and a rotary evaporator, in accordance with ASTM D2172 and ASTM D5404. The HTPG of the recovered binder was determined using the DSR, in accordance with AASHTO T315.

Table ***2-1*** shows the gradation, binder content, G_{mm}, and HTPG of the samples and the average values.

Table 2-1. Gradation, Binder Content, Maximum Specific Gravity, and High-Temp. PG of the RAP

Sieve Size	RAP1	RAP2	RAP3	Average
19 mm	100.00	100.00	100.00	**100.00**
12.5 mm	99.62	99.15	99.48	**99.42**
9.5 mm	97.08	91.01	92.46	**93.52**
No.4	76.15	56.49	69.15	**67.26**
No.8	57.99	47.56	51.01	**52.19**
No. 16	46.19	33.05	40.59	**39.94**
No. 30	36.1	28.66	34.05	**32.94**
No. 50	25.9	18.89	21.55	**22.11**
No. 100	8.09	7.16	7.04	**7.43**
No 200	4.79	5.03	4.66	**4.83**
Binder Content (%)	7.65	6.63	7.43	**7.24**
Gmm	2.423	2.408	2.414	**2.415**
High-Temp. PG (˚C)	90.55	89.63	88.41	**89.53**

2.2.2 Rejuvenator

Two rejuvenator types were used in the preparation of the test specimens. RA1 represents rejuvenators with desirable durability and diffusion characteristics. A commercial rejuvenator with desirable properties, which were observed in the previous phases of this research (Hydrolene H90T), was selected as the RA1. RA2 was chosen to represent less effective rejuvenators. Four products were considered to represent the less desirable rejuvenators (RA2, RA3, RA4 and RA5). These rejuvenator properties were measured in the previous phases of this study and in other studies (Ali and Mohammadafzali, 2015). To investigate their diffusion performance, stage extractions were performed on rejuvenated samples prepared with these rejuvenators, and the products were evaluated based on their homogeneity index. Table ***2-2*** shows the rejuvenators that were evaluated in this study.

Table 2-2. Rejuvenators

Commercial Name	Tag	Product Description
Hydrolene H90 T	RA1	A dark yellow heavy paraffinic oil with a high aromatic content that provides good softening power. The rejuvenator contains no Asphaltene.
Kendex MNE	RA2	Kendex MNE is an oil extract that contains about half aromatic and half naphthenic molecules to maintain compatibility between the asphalt and the rejuvenator oil.
EcoAddz	RA3	A semi-solid black substance with an asphalt odor. This product is manufactured by re-refining used oils through vacuum distillation and is a Re-refined Engine Oil Bottom (REOB)
Silvaroad	RA4	A Polyolester pine chemical derived from a co-product of the pulp and paper industry; a light-yellow oil.
Hydrogreen S	RA5	This semi-fluid rejuvenator is a mix of long-chain and tricyclic organic acids, resin acids, fatty acids, esterified fatty acids and vegetable oils.

In order to find the rejuvenator content that produces a binder with a HTPG value similar to that of the virgin asphalt, rejuvenator softening curves were established, as shown in Figure 2-1.

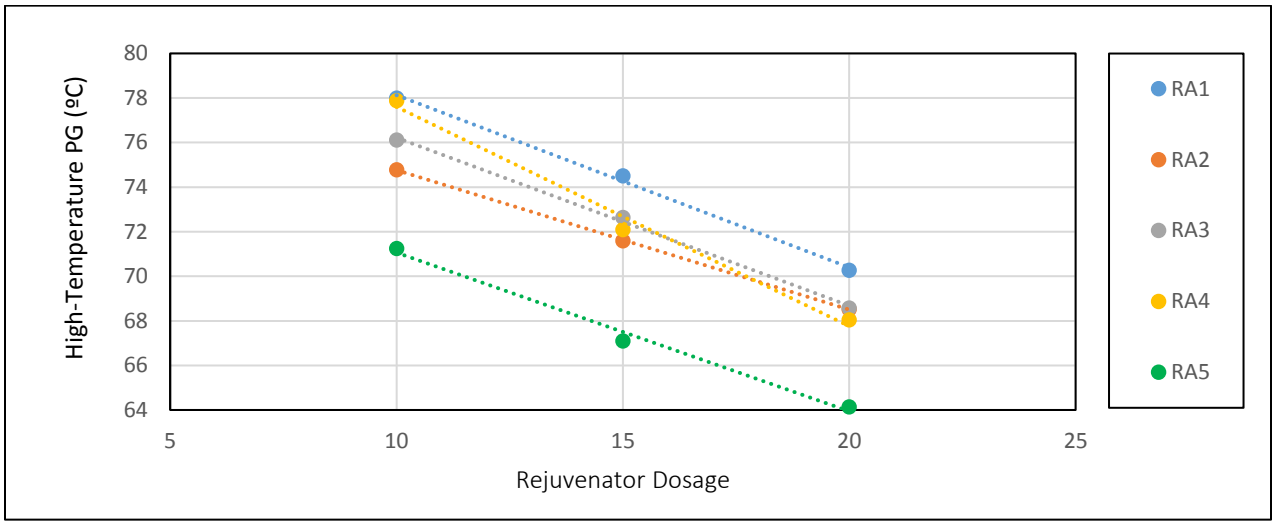

Figure 2-1. Rejuvenator Softening Curves.

The stage extraction process was performed on the rejuvenated samples after five days of oven aging at 85ºC. Table ***2-3*** shows the results of the stage extractions and resulting homogeneity indices (I_h). RA2 had the lowest homogeneity index. This shows that this rejuvenator has relatively inferior diffusion properties. Therefore, RA2 was selected as a rejuvenator with less desirable diffusion and durability properties.

Table 2-3. Stage Extractions for Rejuvenator Selection Process

Rejuvenator	Extraction No.	Recovered Binder		PG_i	PG_{ave}	$PG_i - PG_{ave}$	$\frac{PG_i}{PG_{ave}}$	I_h
		(grams)	(proportion)					
RA1	1	32.72	0.54	78.19	78.34	-0.15	1.00	0.95
	2	15.50	0.26	80.39		2.05	1.03	
	3	12.32	0.20	76.16		-2.18	0.97	
RA2	1	33.18	0.57	81.91	78.87	3.04	1.04	0.91
	2	14.20	0.24	74.83		-4.04	0.95	
	3	11.02	0.19	74.93		-3.95	0.95	
RA3	1	38.62	0.60	78.92	79.09	-0.18	1.00	0.93
	2	13.52	0.21	81.83		2.74	1.03	
	3	12.16	0.19	76.62		-2.48	0.97	
RA4	1	37.12	0.59	81.12	80.54	0.57	1.01	0.94
	2	15.29	0.24	81.56		1.02	1.01	
	3	10.12	0.16	76.89		-3.65	0.95	
RA5	1	28.17	0.48	79.99	79.13	0.86	1.01	0.96
	2	18.25	0.31	79.69		0.56	1.01	
	3	12.85	0.22	76.45		-2.68	0.97	

2.2.3 Virgin Asphalt and Aggregate

A sample of virgin binder was obtained from a local asphalt producer (General Asphalt). Upon DSR testing of this binder, its HTPG was 74.2ºC. In addition, samples of local limestone virgin aggregate products were obtained from the same asphalt producer. Table ***2-4*** shows the gradation of these aggregate products.

Table 2-4. Virgin Aggregate Gradations (Percent Passing)

Sieve Size	C51	F22 (Screening)	C41- M
19 mm	100	100	100
12.5 mm	100	100	100
9.5 mm	97	100	17
No.4	44	100	7
No.8	10	92	7
No. 16	5	72	5
No. 30	4	56	5
No. 50	3	41	5
No. 100	2	13	4
No. 200	2	2.3	5.7

2.3 Sample Design

The rejuvenated samples to be tested in this study used different rejuvenators with different dosages. The control used virgin aggregate and virgin asphalt. Table ***2-5*** shows the general composition of the samples and the aging that they underwent. In order to investigate the hypothesis explained in Section 2.2, the HTPG of samples R3 and R4 was 6°C higher than that of the control.

Table 2-5. Factorial Design of the Experiment

Sample Name	Composition	Target High-Temperature PG (°C)	Cell Number		
			Aging		
			No Additional Aging	5 Days at 85 °C	10 Days at 85 °C
Control	RAP Aggregate + Virgin Binder	74.2°C ± 1°C	1	2	3
R1	RAP + Rejuvenator 1	74.2°C ± 1°C	4	5	6
R2	RAP + Rejuvenator 2	74.2°C ± 1°C	7	8	9
R3	RAP + Rejuvenator 1	80.2°C ± 1°C	10	11	12
R4	RAP + Rejuvenator 2	80.2°C ± 1°C	13	14	15

In order to make a valid comparison between the performances of the samples and evaluate the effects of rejuvenators, it is necessary to keep some parameters consistent between samples. In particular, the aggregate gradation, binder content, binder PG, and air voids should remain within an acceptable range for all samples. To achieve this purpose, several trial mixes were made and their air voids were determined.

2.3.1 Rejuvenated Samples

Rejuvenated samples consisted of RAP, rejuvenator and screenings (Table ***2-4***) when necessary to facilitate the adjustment of the air voids. After making several trial samples, it was concluded that adding the screenings with a quantity almost equal to that of the rejuvenator leads to consistent air void values (between three to four percent). The gradation of the screening sand that was used for this purpose is presented in Table ***2-4*** (F22). It is a well-graded limestone aggregate with a low passing #200 content. The air void values were determined after compacting the samples by 50 gyrations using a gyratory compactor. The amount of rejuvenator added to each sample was determined using the softening curves presented in Figure 2-1. Table ***2-6*** shows the composition of the samples, the G_{mm}, and air void values.

Table 2-6. Composition and Volumetric Properties of the Rejuvenated Samples

Sample	Rejuvenator	Rejuvenator Content		Screening Content	Relative Density (% Gmm)	Air Voids
		By binder weight	By mix weigh			
R1	RA1	15.7%	1.14 %	1.14 %	96.52%	3.48%
R3		11.3%	0.87%	0.87%	96.98%	3.02%
R2	RA2	7.9%	0.57%	0.57%	96.94%	3.06%
R4		6.5%	0.29%	0.20 %	96.31%	3.69%

2.3.2 Control (Virgin Samples)

The control samples consisted of virgin asphalt and virgin aggregate. The aggregates were sieved to individual sizes and were combined to obtain the same gradations as the average gradation for the RAP

Table ***2-1***). The only deviation was that the percentage of passing #200 for control samples was 3.5%, while that of the RAP was 4.8%. This deviation was made to account for the aggregate degradation that occurs in the ignition oven when extracting aggregates from the RAP. Also, the air void value would drop too low if a higher #200 content was used. Table ***2-7*** shows the composition and volumetric properties of the control samples, and Table ***2-8*** shows the gradation of the aggregate.

Table 2-7. Composition and Volumetric Properties of the Control Samples

Sample	Passing #200	Binder Content	Gmm	Gmb	Relative Density (%Gmm)	Air Voids
Control	3.5%	6.4%	2.352	2.273	96.64%	3.36%

Table 2-8. Gradation of the Control Mix

Sieve Size	% Passing (Target)	% Passing (Actual)
19 mm	**100.00**	**100.00**
12.5 mm	**99.42**	**99.67**
9.5 mm	**93.52**	**93.24**
No.4	**67.26**	**66.87**
No.8	**52.19**	**52.34**
No.16	**39.94**	**40.16**
No.30	**32.94**	**32.18**
No.50	**22.11**	**21.54**
No.100	**7.43**	**7.09**
No 200	**3.50**	**3.47**

2.4 Preparation of the Specimens

The rejuvenated samples were prepared by mixing the RAP with designed quantities of rejuvenator and screenings. The loose RAP was heated in a 165ºC oven for one hour. Further, the rejuvenator was introduced and the sample was mixed in a bowl mixer for five minutes. The control mix was produced by mixing heated aggregate (with a gradation that is presented in Table ***2-8***) with 6.4% of virgin binder by weight of mix. The control sample was then heated in an oven at 165ºC for one hour and was then mixed once again to ensure proper consistency.

Samples prepared for performance tests, as shown in Table 2-9, were compacted to an air void level of 7.0 ± 0.5 percent. All specimens were 150 mm diameter cylinders and their heights are shown in

Table ***2-9***. The indirect tensile test specimens were initially fabricated as 160-mm-height X 150 mm diameter and then sawn into three 38-mm-height samples. The mass that produced a sample with those dimensions with a relative density of 93.0% was determined. Further, the sample was compacted using a gyratory compactor until the specified height was achieved. This procedure ensured the production of each specimen to an air void level of 7.0 ± 0.5 percent.

Table 2-9. Specimens for Performance Tests

	Loaded Wheel Tester (LWT)	Semi Circular Bend Test (SCB)	Indirect Tension Test (IDT)
Specification	AASHTO T324	ASTM D8044	Draft AASHTO (UF, Roque)
Number of replicates, short-term aged	4	4	3
Number of replicates, 5 days aged at 85ºC	4	4	3
Number of replicates, 10 days aged at 85°C	4	4	3
Height of each sample (mm)	60	57	160

The process for fabricating the specimens by a gyratory compactor included heating the mixes to 165ºC for one hour. This exposure was considered short-term aging that all specimens were exposed to. Performance tests were conducted on specimens in three aging conditions. The first set of samples were tested without any long-term aging. The second and third sets of samples underwent long-term aging by heating compacted samples in an 85ºC oven for five and ten days, respectively (Table 2-9).

Chapter 3 : STAGE EXTRACTION

3.1 Introduction

This chapter examines the diffusion of rejuvenators into aged asphalt, as measured by the stiffness gradient of the rejuvenated binder film surrounding the RAP aggregates. The goal is to study the performance of recycled mixes and determine if it is correlated to the degree of the diffusion and stiffness gradient of the recycled binder. This evaluation is reported in Chapter 5. After adding the rejuvenator to the aged mix, the outer binder layer is immediately exposed to the rejuvenator, which gradually diffuses into the inner layers. The rate of penetration of the rejuvenator into the aged binder depends on different parameters such as type of material, temperature and mixing efficiency. Based on previous research conducted by the project team, aged recycled mixes were more homogeneous than virgin mixes with the same aging time (Mohammadafzali et al. 2017).

3.2 Methodology and Sample Preparation

To prepare samples for binder extraction, the RAP and aggregates were heated to 165ºC for 45±5 minutes. The rejuvenator or binder was then added to the heated RAP or aggregate samples and mixed for five minutes. The extraction sample weight was 1100±20 grams. The RAP binder was recovered using a centrifuge extractor and a rotary evaporator

Figure 3-1), in accordance with ASTM D2172 and ASTM D5404, respectively. The extraction was done in three stages for each of the 15 cells shown in Table 3-1. At each stage, the samples were soaked in trichloroethylene for a specific time, as shown in Table 3-2.

Further, the binder dissolved in trichloroethylene is obtained using the centrifuge extractor. The extracted liquid was then placed into a centrifuge with an 800 relative centrifugal force (RCF) for 30 minutes to make suspended fine aggregate sediment. The rotatory evaporator was used to separate the solvent from the binder.

Figure 3-2 shows the appearance of the sample during each stage of extraction. Before the first extraction, aggregates are completely coated by a relatively thick layer of asphalt. The first extraction washes a large portion of the asphalt film away, leaving a thinner layer. After the second extraction, only a very thin layer of asphalt remains on the aggregates. During the last stage of extraction and after the samples were soaked in trichloroethylene for 45 minutes and extracted, the remaining aggregates were soaked in trichloroethylene again for 15 minutes to ensure that almost all of the remaining binder was extracted. The binder extracted from the first, second and third stages represents the outer, intermediate and inner layers of the binder film coating the aggregates, respectively.

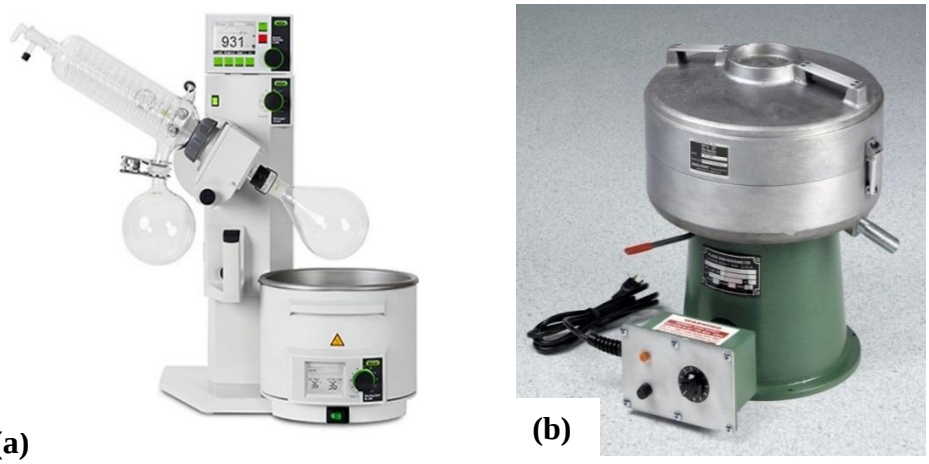

Figure 3-1. Binder Recovery Apparatus: (a) Rotary Evaporator and (b) Centrifuge Extractor.

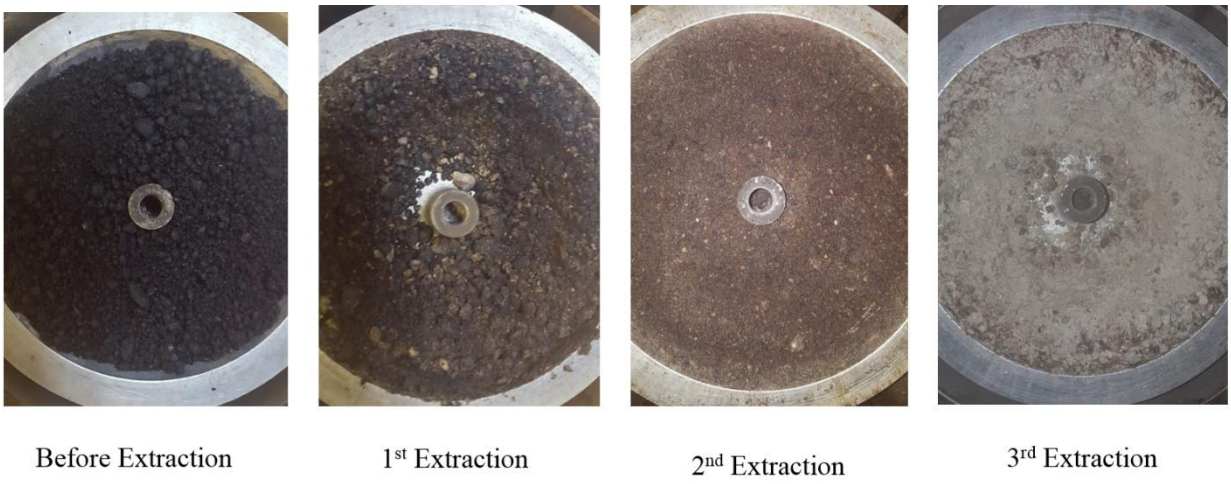

Figure 3-2. The Appearance of Samples at each Stage of the Extraction Process.

Virgin binder was obtained from General Asphalt, a local asphalt producer in Miami, Florida. The high-temperature PG (HTPG) of this binder, determined by DSR testing, was 74.2ºC. As explained in Chapter 2, the rejuvenator dosage for each target HTPG and each type of rejuvenator was determined using the softening curve shown in Figure 3-3. The target HTPG of the samples and dosage of each rejuvenator type are shown in Table 3-1. The weight of the rejuvenator was determined by multiplying the dosage percent obtained from the softening curve by the binder content of the mix. It is noted that RA2 is slightly more effective in softening the asphalt than RA1, as shown by a lower curve, indicating that at the same dosage, RA2 is capable of obtaining a softer asphalt (lower HTPG). To keep the HTPG constant, an additional quantity of RA1 is used to achieve the same HTPG, as shown in Table 3-1.

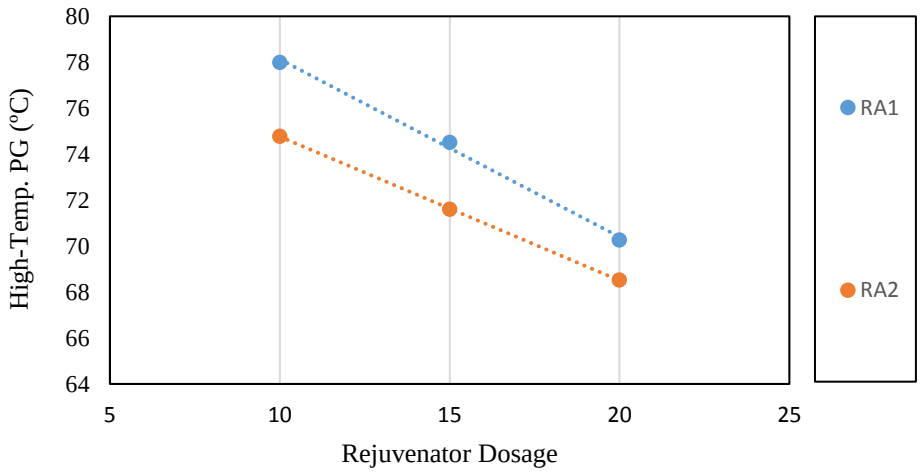

Figure 3-3. Softening Curves of Rejuvenators.

Table 3-1. Experiment Factorial Design

Sample Name	Composition	Target High-Temperature PG (°C)	Cell Number		
			Aging		
			No Additional Aging (Only short-term aging)	5 Days at 85°C	10 Days at 85°C
Control	Virgin Aggregate + Virgin Binder	74.2°C ± 1°C	1	2	3
R1	RAP + 15.7% RA1	74.2°C ± 1°C	4	5	6
R2	RAP + 11.3% RA2	74.2°C ± 1°C	7	8	9
R3	RAP + 7.9% RA1	80.2°C ± 1°C	10	11	12
R4	RAP + 6.5% RA2	80.2°C ± 1°C	13	14	15

Table 3-2. Extraction Stages and Corresponding Times

Extraction Number	Solvent Soaking Time	Asphalt Layered Sampled
X1	1 Minute	Outer
X2	3 Minutes	Intermediate
X3	45 Minutes	Inner

Finally, the binder extracted at each stage was tested by the DSR to determine the HTPG values at the outer, intermediate, and inner layers, according to AASHTO M320 criterion. Homogeneity indices and stiffness gradient factors were calculated based on the HTPG of each layer.

3.3 Results

Three stage extractions were conducted on all 15 samples, and then two DSR tests were performed to measure HTPG at each extracted layer. Equation 3-1 is used to calculate the weighted average HTPG of the samples adjusting for the individual layer mass.

$PG_{ave} = a_1 PG_{x1} + a_2 PG_{x2} + a_3 PG_{x3}$ Equation 3-1

In which:

$$a_i = \frac{The\ mass\ of\ the\ binder\ recovered\ in\ i^{th}\ stage\ of\ extraction}{The\ mass\ of\ total\ recovered\ binder}$$ Equation 3-2

PG_{xi} = The high-temperature PG of the i^{th} layer

To compare the stiffness of asphalt layers, the following parameters are presented in Table 3-3:

- $PG_i - PG_{ave}$: The difference between the high-temperature PG of *i*th layer and the average high-temperature PG of all layers.
- $\frac{PG_i}{PG_{ave}}$: The normalized high-temperature PG of each layer.
- $PG_{max} - PG_{min}$: The difference between the minimum and the maximum high-temperature PGs.

To quantify the stiffness gradient and homogeneity of the samples, two parameters, Stiffness Gradient Factor (SGF) and Index of Homogeneity (I_h), are introduced and defined by Equations 3-3 and 3-4, respectively:

Stiffness Gradient Factor (SGF) = $\frac{PG_1 - PG_3}{PG_{ave}} \times 100\%$ Equation 3-3

The SGF is a measure of the stiffness gradient of the asphalt film coating the aggregates and shows how stiff the outer layer is in comparison with the inner layer. A positive value of SGF means that the outer layer is harder, while a negative SGF indicates that the outer layer is relatively softer.

$$I_h = 1 - \frac{Maximum\ PG_i - Minimum\ PG_i}{PG_{ave}}$$ Equation 3-4

The I_h shows the degree of homogeneity of the binder coating the aggregates. An I_h of 1 represents the most homogenous coating, and a smaller I_h indicates less homogeneity. Based on the former research results, the I_h value could vary between 0.75 to 0.99, depending on the type of material and level of aging (Mohammadafzali 2017). The results are summarized in Table ***3-3***.

Table 3-3. Results of DSR Tests on Stage Extracted Binder

Cell No.	Extraction No.	Binder Recovered (grmas)	ai	PGi	PGave	PGi-PGave	PGi/PGave	PGmax-PGmin	Ih	SGF
1	X1	35.25	0.52	84.21	80.81	3.40	1.04	9.12	0.89	11.3%
	X2	19.50	0.29	78.46		-2.35	0.97			
	X3	12.90	0.19	75.09		-5.73	0.93			
2	X1	40.23	0.55	86.86	83.51	3.35	1.04	10.58	0.87	12.7%
	X2	21.35	0.29	81.00		-2.50	0.97			
	X3	11.28	0.15	76.28		-7.23	0.91			
3	X1	39.60	0.56	88.25	84.69	3.26	1.04	11.93	0.86	14.1%
	X2	19.66	0.28	82.15		-2.54	0.97			
	X3	10.87	0.15	76.32		-8.37	0.90			
4	X1	32.12	0.49	79.20	79.32	-0.12	1.00	5.31	0.93	3.8%
	X2	20.31	0.31	81.52		2.20	1.03			
	X3	13.08	0.20	76.21		-3.11	0.96			
5	X1	38.32	0.58	81.34	80.60	0.74	1.01	6.60	0.92	7.6%
	X2	18.29	0.28	81.84		1.24	1.02			
	X3	9.54	0.14	75.24		-5.36	0.93			
6	X1	30.56	0.51	82.04	81.00	1.04	1.01	6.00	0.93	7.4%
	X2	21.58	0.36	81.21		0.21	1.00			
	X3	7.32	0.12	76.04		-4.96	0.94			
7	X1	39.30	0.61	81.45	80.76	0.69	1.01	6.20	0.92	6.4%
	X2	14.06	0.22	82.45		1.69	1.02			
	X3	11.30	0.17	76.25		-4.51	0.94			
8	X1	36.30	0.57	84.12	82.73	1.39	1.02	6.89	0.92	8.3%
	X2	15.23	0.24	83.85		1.12	1.01			
	X3	12.22	0.19	77.23		-5.50	0.93			
9	X1	35.66	0.57	85.14	83.94	1.20	1.01	7.19	0.91	8.6%
	X2	16.32	0.26	85.10		1.16	1.01			
	X3	10.32	0.17	77.95		-5.99	0.93			
10	X1	35.00	0.56	87.21	86.51	0.70	1.01	5.90	0.93	5.7%
	X2	15.10	0.24	88.21		1.70	1.02			
	X3	12.01	0.19	82.31		-4.20	0.95			
11	X1	36.80	0.54	88.25	87.79	0.46	1.01	6.23	0.93	5.7%
	X2	20.40	0.30	89.47		1.68	1.02			
	X3	11.30	0.16	83.24		-4.55	0.95			
12	X1	39.36	0.56	89.05	88.54	0.51	1.01	6.63	0.93	6.6%
	X2	22.31	0.31	89.84		1.30	1.01			
	X3	9.21	0.13	83.21		-5.33	0.94			
13	X1	35.20	0.57	90.24	89.55	0.69	1.01	9.14	0.90	8.1%
	X2	16.30	0.26	92.14		2.59	1.03			
	X3	10.20	0.17	83.00		-6.55	0.93			
14	X1	39.21	0.58	93.21	91.90	1.31	1.01	11.17	0.88	11.1%
	X2	18.37	0.27	94.18		2.28	1.02			
	X3	10.50	0.15	83.01		-8.89	0.90			
15	X1	36.88	0.52	94.21	92.47	1.74	1.02	9.27	0.90	9.7%
	X2	19.87	0.28	94.48		2.01	1.02			
	X3	14.35	0.20	85.21		-7.26	0.92			

3.4 Analysis

Table ***3-4*** shows the average SGF and I_h of the three aging levels of each sample. As expected, the average I_h of the RAP samples containing RA1 (R1 and R3) were highest, and the control samples made of virgin binder resulted in the lowest I_h. This indicates that there is only a small difference in layer stiffness and thus a better homogeneity in samples R1 and R3. Furthermore, considering that the HTPG of the inner layer for samples of the same target HTPG are roughly the same, lower SGF of the R1 and R3 compared to R2 and R4 indicates a better diffusion ability of RA1 compared to RA2. The I_h of 0.87 for the control samples shows that the outer layer of the virgin samples ages much faster than the other layers, which makes a non-homogeneous coat of binder after aging. This is attributed to more exposure of the outer layer to air, causing faster oxidation and evaporation of the binder's volatile material (Mohammadafzali et al., 2017).

Table 3-4. Average SGF and I_h of the Three Aging Levels of each Sample Type.

Sample name	Control	R1	R2	R3	R4
I_h	0.87	0.93	0.92	0.93	0.89
Average SGF	12.68%	6.25%	7.78%	5.99%	9.64%

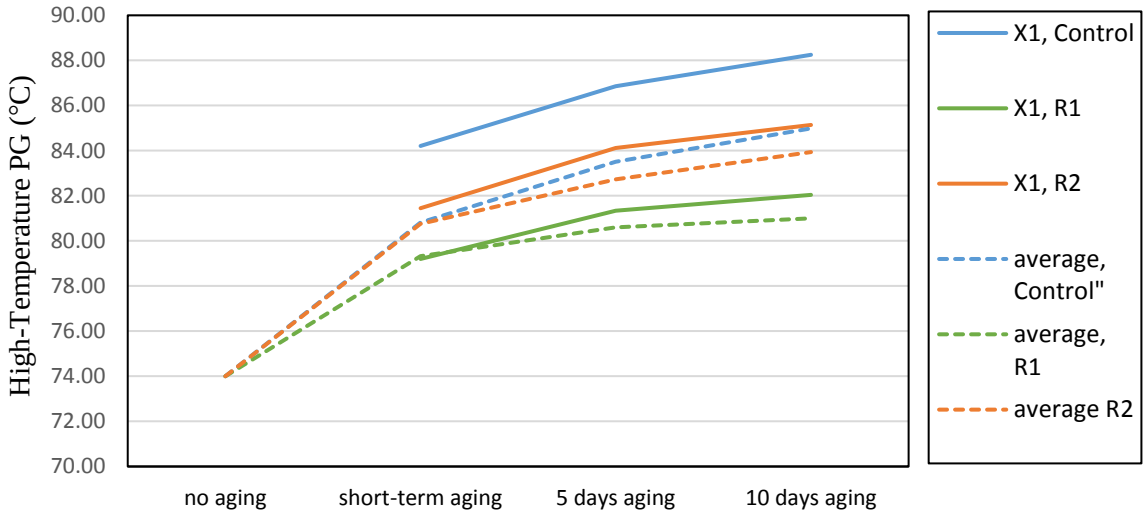

Figure 3-4. Comparison of Average and Outer Layer (X1) HTPG Values of the Samples with Initial HTPG of 74°C.

The high-temperature PG of the outer layer (X1 HTPG) of R1, R3 and the Control after 10 days of aging was compared, Figure 3-5. While the X1 HTPG of the Control was 88.25°C, that of the

R1 was 6.2ºC lower (82.04ºC), and that of the R3 (with a 6ºC higher initial HTPG), was only 0.8ºC higher (89.05ºC).

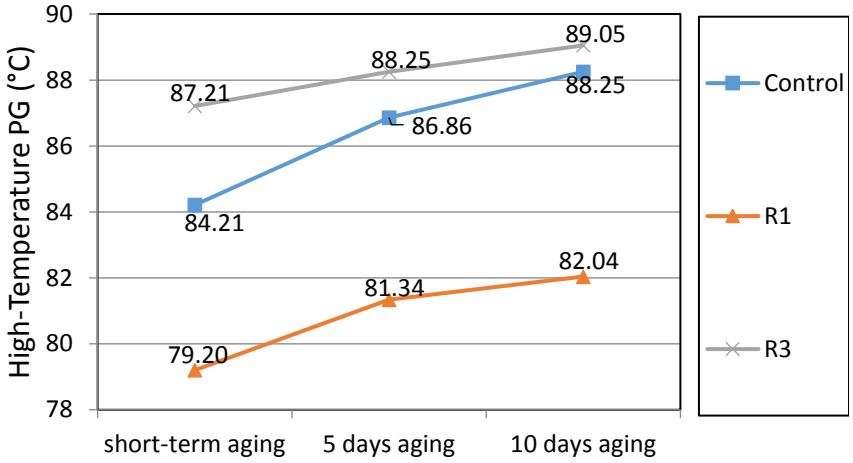

Figure 3-5. HTPG of the X1 Layer of the R1, R3, and the Control Samples at Different Aging Levels.

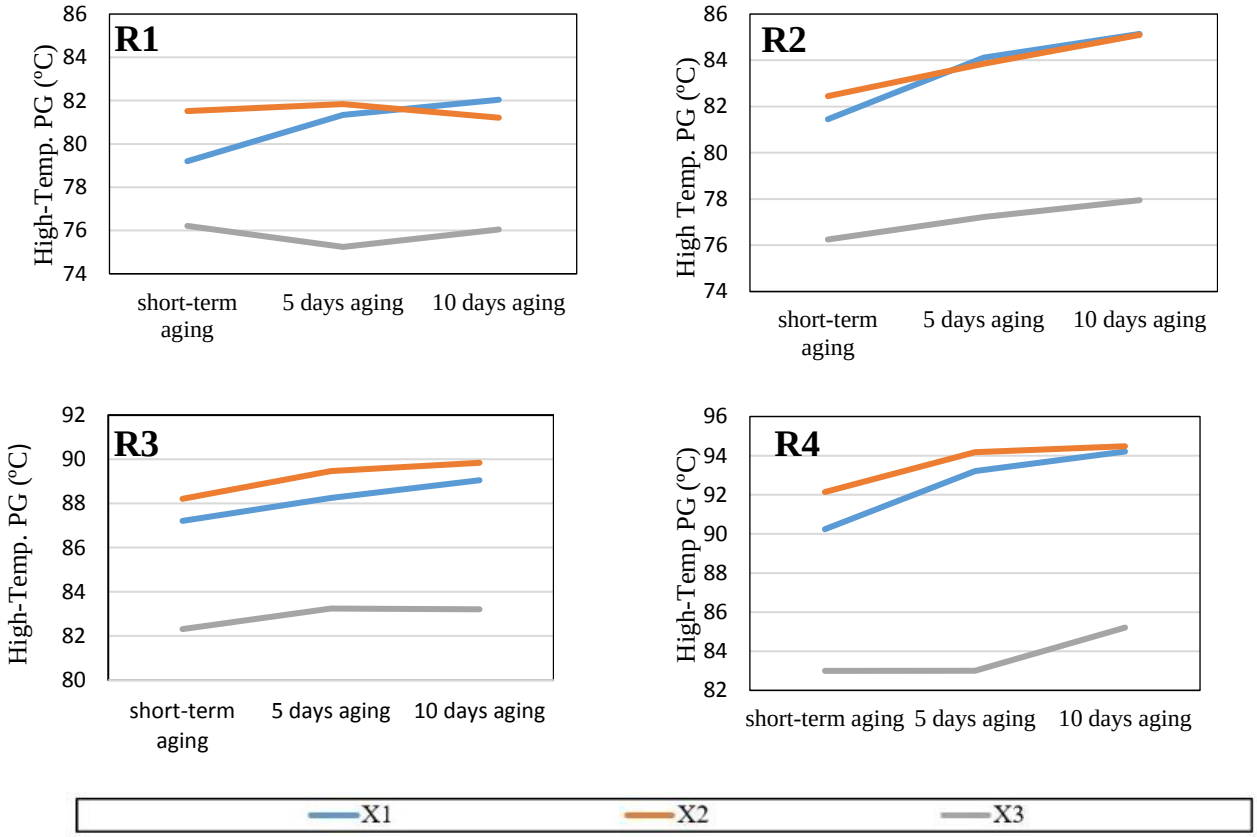

Figure 3-6. High-Temperature PG of the Layers of the R1, R2, R3, and R4 at Different Aging Levels.

Considering that both the diffusion and the aging occur from the outside to the inside, these two processes can balance each other and make a more homogeneous coating, as long as efficient mixing took place. As shown in Figure 3-6, at the short-term aging stage, the high-temperature PG (HTPG) value of the X1 layers in all samples is lower than the HTPG value of the X2 layer. This could be attributed to the softening effect of the rejuvenator at the beginning of the aging process. However, as the samples undergo more aging, diffusion occurs and causes the X2 layer to become softer, to the extent that for the R1 sample, after ten days of aging, the X2 layer is even softer (lower HTPG) than the X1 layer. In fact, for the R1 sample, the X1 layer becomes more aged, while the diffusion softens the inner layers. In other samples (R2, R3 and R4), after ten days of aging, the HTPG of the X1 and X2 layers get close to each other. The inner layer is barely affected by aging.

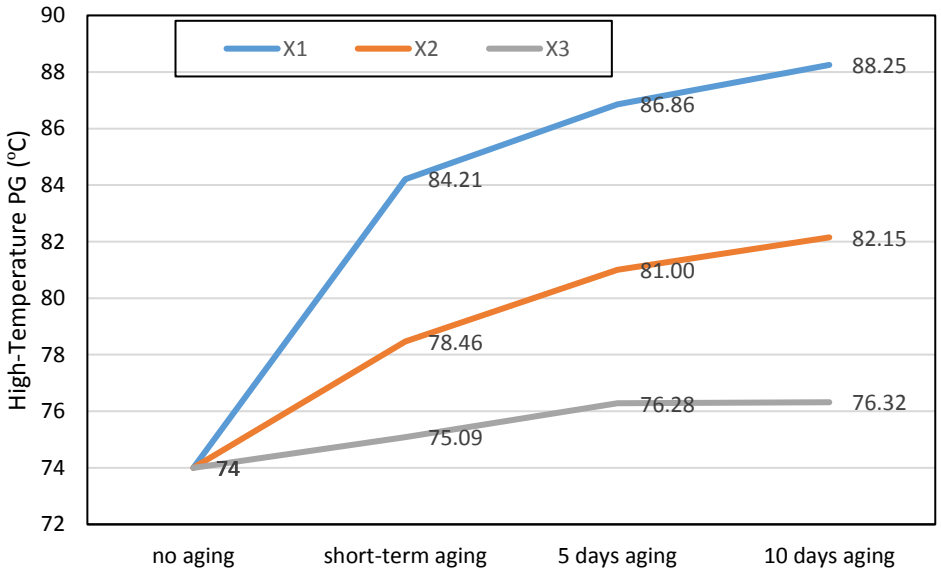

Figure 3-7. Comparing HTPG of the Different Layers of the Control Sample.

Figure 3-7 shows the stiffness expressed in terms of the HTPG, as well as the asphalt layers of the control sample as they age. The outer layer of X1 is most exposed to the elements and exhibits the most aging (HTPG 74 to HTPG 88). The trend is lessened as the process proceeds to the intermediate layer, X2 and is even further lessened in the inner layer, X3, all of which was expected (Mohammadafzali 2017). It is noted that the inner layer, X3, shows a stabilization of aging at a point not too far from the initial condition (HTPG 74 to HTPG 76). Further analysis of the results and correlation with performance data will be presented in Chapter 5, Data Analysis.

Chapter 4 : PERFORMANCE TESTS

4.1 Introduction

This chapter describes sample preparation and performance test procedures used for this research study.

4.2 Test Procedures

4.2.1 Sample Preparation

The material used for preparing the samples included RAP, two rejuvenator types (RA1 and RA2), limestone aggregate and a PG 67-22 virgin binder. The control specimens consisted of virgin binder and aggregate, and the rejuvenated samples R1, R2, R3, and R4 consisted of RAP and different dosages of rejuvenators, as indicated in Table **4-1**. Staff at Florida International University (FIU) transported materials to the Louisiana Transportation Research Center laboratory and prepared the samples to facilitate the regulation of the time between the preparation and testing of specimens, as well as to prevent possible damage during transportation. The details of sample preparation process is provided in in Chapter 3.

The testing program included the LWT, SCB, and IDT. LWT was conducted to characterize the rutting and moisture susceptibility at high temperatures, and SCB and IDT tests were aimed at evaluating the intermediate temperature cracking resistance. All mixes were tested at three aging levels, as shown in Table **4-1**, namely, one short-term aging level and two long-term aging levels. Both short- and long-term aging levels were performed in accordance with AASHTO R30, "*Standard Practice for Mixture Conditioning of Hot Mix Asphalt.*" The short-term aging (level 1) process included placing the loose mix in a conventional oven at 165°C for one hour. . Subsequently, cylindrical specimens were fabricated using a Superpave gyratory compactor (SGC) to a target air void level of 7.0% ± 0.5%. The second and third aging levels were comprised of placing compacted asphalt specimens in a conventional oven at 85°C for five and ten days, respectively. The three aging levels were performed in order to provide insight into the progression of rejuvenator diffusion into RAP mixes over time at higher temperatures and its effects on the performance of RAP mixes.

Table ***4-2*** presents a summary of the performance tests performed during this study.

Table 4-1. Factorial Design of Test Cells

Sample Name	Mix Composition	High-Temperature PG (°C)	Cell Number		
			Aging Level		
			STA (Loose Mix)	LTA (Compacted Mix)	
			1hr, 165°C	5 Days, 85 °C	10 Days, 85 °C
Control	Virgin Aggregate + Virgin Binder	74.2°C ± 1°C	1	2	3
R1	RAP + 7.9% RA1	80.2°C ± 1°C	4	5	6
R2	RAP + 15.7% RA1	74.2°C ± 1°C	7	8	9
R3	RAP + 6.5% RA2	80.2°C ± 1°C	10	11	12
R4	RAP + 11.3% RA2	74.2°C ± 1°C	13	14	15

RAP: 100% Recycled Asphalt Pavement; RA1: Hydrolene rejuvenator; RA2: Kendex rejuvenator; STA: Short-term aging; LTA: Long-term aging.

Table 4-2. Mix Performance Tests

Test	Temperature	Protocol	Specimen Geometry	Evaluation of	Engineering Properties
LWT	50°C	AASHTO T324	Circular, ϕ150 mm × 60 mm	Rutting and moisture damage	Rut depth and Stripping inflection point
SCB	25°C	ASTM D8044	Semicircular, ϕ150 mm × 57 mm	Crack propagation	Critical strain energy release rate
IDT	10°C	Roque and Buttlar (1992), Buttlar and Roque (1994), Roque et al. (2004)	Circular, ϕ150 mm × 38 mm	Crack initiation	Dynamic Modulus Creep compliance Indirect tensile strength Dissipated creep strain energy Energy Ratio

4.2.2 Loaded Wheel Test (LWT)

The loaded wheel test (LWT) was conducted in accordance with AASHTO T 324 "Standard Method of Test for Hamburg Wheel-Track Testing of Compacted Hot Mix Asphalt (HMA)." This test is considered a torture test that produces damage by rolling a 703 N (158 lb.) steel wheel across the surface of cylindrical specimens (150 mm diameter by 60 mm thick) that is submerged in 50°C water for 20,000 passes, at 56 passes per minute. Four specimens (two specimens for each wheel) were tested. Rut depth measurements were recorded at 11 locations across the cylindrical specimen until failure, as shown in Figure 4-1. Then, rut depth measurements at four middle locations were averaged. Additionally, rut depth at 20,000 cycles was computed and used in the analysis.

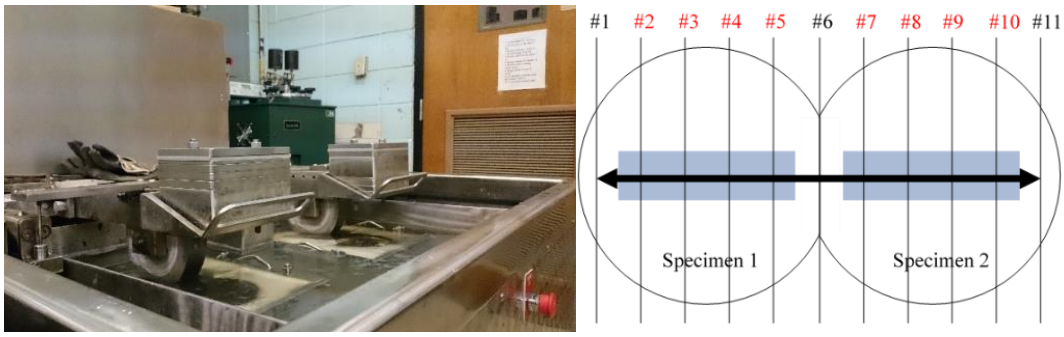

Figure 4-1. Setup of Loaded Wheel Tracking Test, 50°C Wet.

The stripping inflection point (SIP), which is a measure of the potential for moisture damage, was also determined for all mixes. The rut depth and load cycle output data were initially fit to a typical curve. The SIP, which is the inflection point of the fitted curve, was determined by finding the second derivative of the curve and equating it to zero (Figure 4-2).

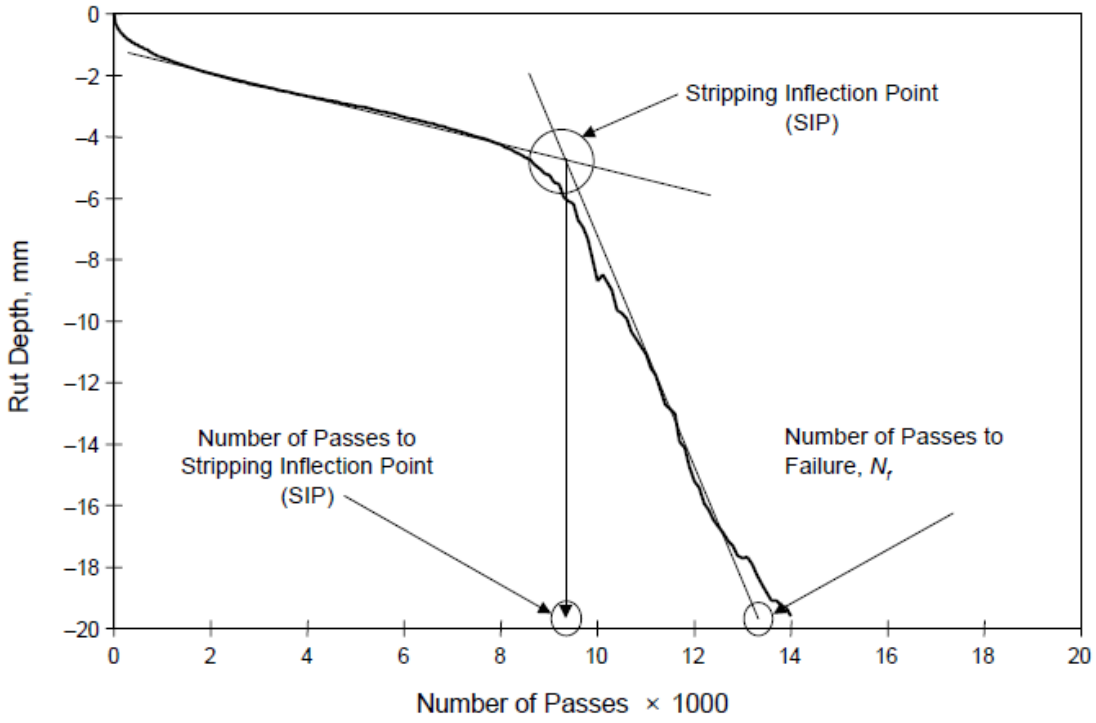

Figure 4-2. Hamburg Curve with Test Parameters (AASHTO T324).

4.2.3 Semi-Circular Bend (SCB) Test

The Semi-Circular Bend (SCB) test was performed according to ASTM D 8044 "Standard Test Method for Evaluation of Asphalt Mixture Cracking Resistance using the SCB at Intermediate Temperatures." This test characterizes the fracture resistance of asphalt mixes based on fracture mechanics principles by measuring the critical strain energy release rate, also called the critical value of J-integral, or Jc. To determine the critical value of J-integral (J_c), semicircular specimens with at least two different notch depths need to be tested for each mix. In this study, two notch

depths of 25.4 mm and 38 mm were selected. This test was conducted at a temperature of 25°C. The semicircular specimen is loaded monotonically until fracture failure occurred under a constant cross-head deformation rate of 0.5 mm/min in a three-point bending load configuration, as shown in Figure 4-3. The load and deformation are continuously recorded, and the critical value of J_c is determined using the following equation:

$$J_c = \left(\frac{U_1}{b_1} - \frac{U_2}{b_2}\right) \frac{1}{a_2 - a_1} \qquad \text{Equation 4-1}$$

where:
J_c = critical strain energy release rate (kJ/m^2),
b = sample thickness (m),
a = notch depth (m), and
U = strain energy to failure (kJ).

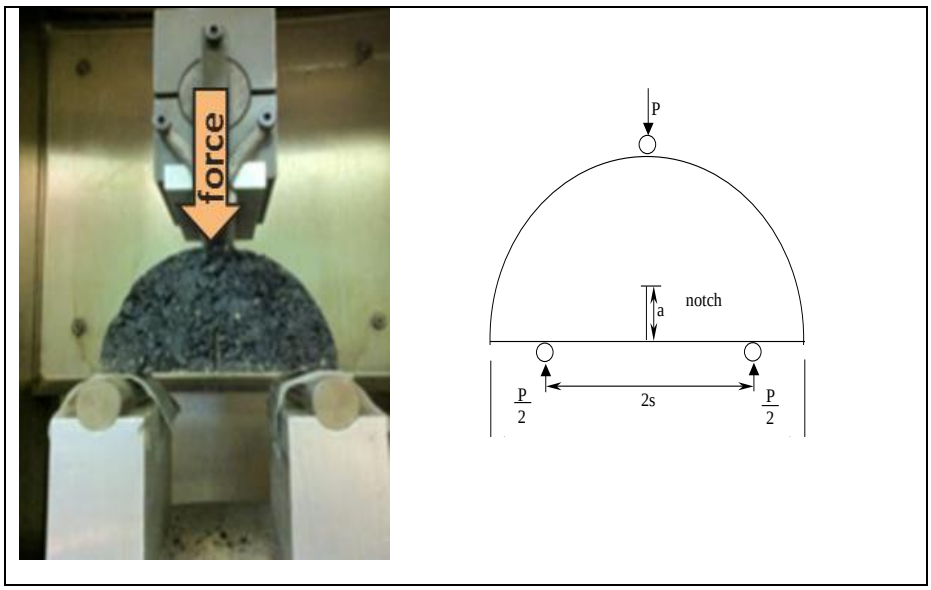

Figure 4-3. Setup of Semi-Circular Bending Test.

The higher the J_c value of a mix, the higher its fracture resistance at intermediate temperatures and vice versa. Mix specimens used for SCB testing were compacted to a target air void content of 7.0 ± 0.5% in this study. The cracking resistance of asphalt mixes conditioned for the three aging levels previously discussed was determined.

4.2.4 Florida Indirect Tension (IDT) Test

4.2.4.1 Dynamic Modulus

The Florida IDT test was conducted according to the University of Florida draft AASHTO test method, "*Standard Method of Test for Tensile Creep Compliance, Tensile Failure Limits and Energy Ratio of Asphalt Mixtures Using the Superpave Indirect Tension Test.*"". This test characterizes the intermediate temperature cracking resistance of asphalt mixes at 10°C, and it involves the performance of three individual tests on three replicate test specimens, as described below.

Three replicate specimens were first subjected to dynamic modulus testing in indirect tension mode, according to the draft test procedure proposed by Kim et al. (Kim et al. 2004). This test was conducted by applying sinusoidal compressive stress to the diametric axis of a 38-mm-thick test specimen at a temperature of 10°C and a frequency of 10 Hz, as shown in Figure 4-4. The sinusoidal compressive stress was applied to each sample to achieve target strain levels of 50 to 70 microstrains horizontally and 100 microstrains vertically to ensure that measurements are in the linear viscoelastic region. Equation 4-2 presents the mathematical relationship for the determination of the dynamic modulus:

$$|E^*| = 2\left(\frac{P_0}{\pi a d}\right)\left(\frac{\beta_1\gamma_2 - \beta_2\gamma_1}{\gamma_2 V_0 - \beta_2 U_0}\right) \qquad \text{Equation 4-2}$$

where:

$P_0 =$ Load amplitude,

$U_0 =$ Horizontal displacement amplitude,

$V_0 =$ Vertical displacement amplitude,

$a =$ Loading strip width,

$d =$ Specimen diameter,

β_1, β_2, γ_1, and γ_2 = geometric constants

The geometric constants are functions of gauge length, specimen diameter, and loading strip width (Kim et al., 2004).

The average values of the Dynamic Modulus (E*) and the Poisson's ratio of the three replicate specimens were computed, recorded, and used in the analysis.

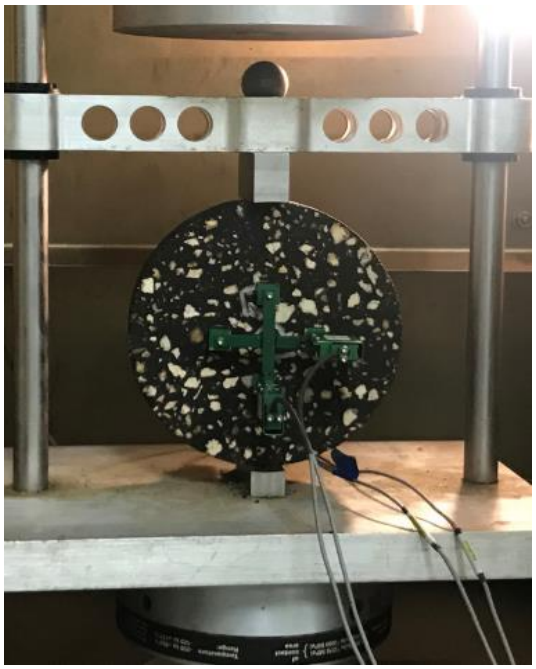

Figure 4-4. IDT Test Setup.

4.2.4.2 The Creep Compliance Test

Subsequent the dynamic modulus test, a static load was applied to the test specimen for 1,000 seconds. The horizontal deformations were kept between 0.0025 mm and 0.0040 mm (100-150 micro-inches) at 100s and below 0.020 mm (750 micro-inches) at 1000s. The horizontal and vertical deformations measured during testing were then used to compute the mix creep compliance as a function of time, as expressed in Equation 4-3:

$$D(t) = \frac{\Delta H \times h \times D \times C_{compliance}}{P \times GL} \quad \text{Equation 4-3}$$

where:

$\Delta H =$ Trimmed average horizontal deformation,

$h =$ Average thickness of specimens,

$D =$ Average diameter of specimens,

$C_{compliance} =$ Creep compliance correction factor,

$P =$ Average applied creep load, and

$GL =$ Gauge length

The calculated creep compliance values were then fitted to the power function expressed as shown in Equation 4-5 to determine parameters D_0, D_1, and m.

$$D(t) = \sigma D_0 + \sigma D_1 t^m \quad \text{Equation 4-4}$$

The creep compliance rate (CR) of the mixes were determined as shown below:

$$CR = \quad m\sigma \mathrm{D}_1 \mathrm{t}^{(\mathrm{m}-1)}$$ Equation 4-5

4.2.4.3 The IDT Tensile Strength Test

The IDT tensile strength test was conducted in the displacement control mode by applying a constant rate of displacement of 50 mm/min along the specimen's vertical diametrical axis until failure. The tensile stress in the test specimen during testing was expressed as shown below (Buttlar and Roque, 1994; Roque et al., 2004):

$$\sigma(t) = \frac{2 \times P(t)}{\pi \times h \times D} \times C_{sx}$$ Equation 4-5

where:

$\sigma(t) =$ Stress,

$P(t) =$ Load at time t, and

$C_{sx} =$ Stress correction factor for each specimen.

$h =$ Average thickness of specimens, and

$D =$ Average diameter of specimens.

The strains generated in the test specimen were also computed, as illustrated by Buttlar and Roque (1994). A stress-strain plot was prepared as shown in Figure 4-5, for the determination of the asphalt mix failure limits.

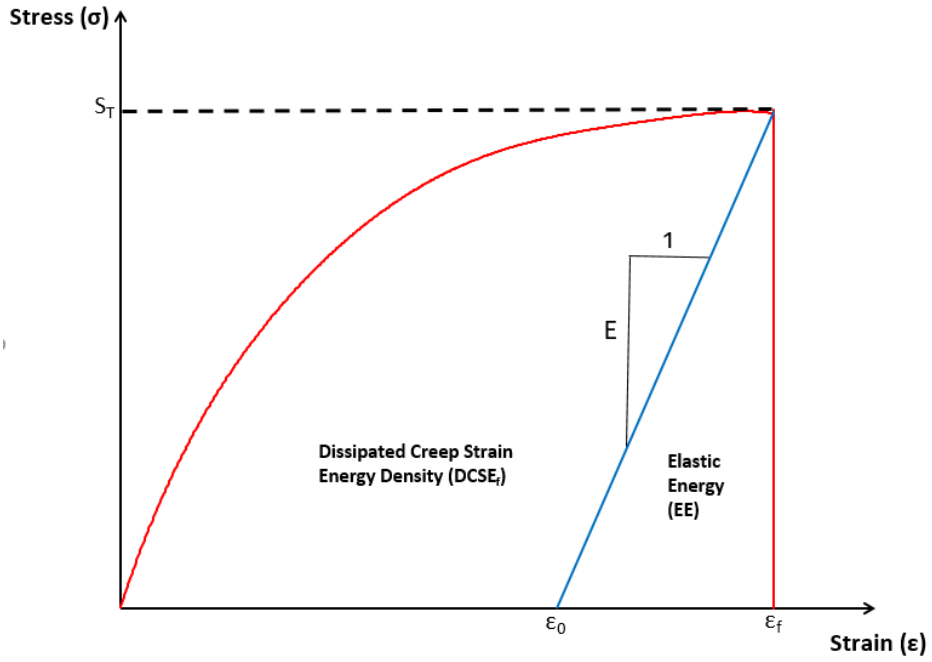

Figure 4-5. Asphalt Stress-Strain Plot and Failure Limits.

The Fracture Energy Density Failure Limit (FE_f) is determined as the area under the stress-strain curve up to the point of fracture. The elastic energy of each specimen was expressed as shown below (Kim et al. 2004):

$$EE = \frac{1}{2}\frac{(S_T)^2}{E} = \frac{1}{2}S_T(\varepsilon_f - \varepsilon_0) \quad \text{Equation 4-6}$$

where:

$EE =$ Elastic energy of the specimen,

$S_T =$ Indirect tensile strength of the mix,

$\varepsilon_f =$ Failure strain, and

$E =$ Dynamic modulus of the specimen measured at 10°C and at a frequency of 10 Hz.

The dissipated creep strain energy density ($DCSE_f$), which is the portion of the total energy that is not recoverable, was expressed as shown in Equation 4-8.

$$DCSE_f = FE_f - EE \quad \text{Equation 4-7}$$

Roque et al. introduced the dimensionless Energy Ratio (ER) parameter as a means to characterize asphalt pavements into those that exhibited cracking and those that did not. Mixes with better cracking performance were reported to have higher ER values, whereas those with relatively poorer cracking performance exhibited lower ER values. The ER parameter was expressed as:

$$ER = \frac{DCSE_f}{\frac{m^{2.98} \times D_1}{A}} \quad \text{Equation 4-8}$$

where:

$D_1, m =$ Tensile creep compliance parameters.

$A =$ Parameter that is a function of the a tensile strength (S_T) and tensile stress in asphalt pavement (σ =1 MPa, when tensile stress is unknown). For stress and strength recorded in MPa, $DCSE_f$ in kJ/m^3 and D_1 in GPa^{-1}, A (in MPa^{-2}) was calculated as:

$$A = 8.64 \times 10^{-4} \times \frac{(6.36 - S_T)}{\sigma^{3.1}} + 3.57 \times 10^{-3} \quad \text{Equation 4-9}$$

Chapter 5 : DATA ANALYSIS

5.1 Introduction

This chapter provides results of the performance tests introduced in Chapter 4 and explores their correlation between homogeneity and high-temperature PG (HTPG) of different layers provided in Chapter 3. Performance parameters of virgin mixes are compared with those of recycled mixes. The hypotheses of the study are evaluated based on the results.

The previous parts of this study (Mohammadafzali et al. 2017) showed that if proper rejuvenation (as defined below) is used, the rejuvenated binder would have two advantages over a virgin asphalt: It ages slower, and the resultant binder is more homogeneous. When a virgin mix ages, its binder outer layer hardens more quickly relative to its inner layer, and its fatigue resistance drops. In a properly recycled mix, however, after five days of oven aging at 85°C, the HTPG of the outer layer is almost similar to the average HTPG of the binder. These advantages can be used as a basis for designing 100% recycled mixes with acceptable performance.

Also, the relationship between mix performance and binder homogeneity parameters is assessed. The variables to be statistically correlated are presented in Table 5-1.

Table 5-1. Binder Homogeneity and Mix's Performance Variables

Dependent Variables	Independent Variables
• Rutting Performance parameters • Cracking Performance parameters	• X_1 - Outer Layer Stiffness (or HTPG) • X_2 - Intermediate Layer Stiffness (or HTPG) • X_3 - Inner Layer Stiffness (or HTPG) • PG_{ave} - Average Stiffness (or HTPG) • SGF - Stiffness Gradient Factor • I_h - Homogeneity Index

5.2 Loaded Wheel Testing- Results and Discussion

Figure 5-1 presents rut depth measurements at 20,000 passes for mixes evaluated. Table 5-2 shows the average rut depth at 20,000 passes, along with the coefficient of variation (COV) and statistical ranking of mixes evaluated. The average COV was 18.6%, with a range of 5% - 30%. Table 5-3 summarizes the average stripping inflection point (SIP), along with the statistical ranking of mixes evaluated. The average SIP COV was 12.1%, with a range of 6% - 22%.

The short-term aged virgin mix and recycled mixes with high rejuvenator dosage rates (RAP+15.7% RA1 and RAP + 11.3% RA2) exhibited higher rut depths than similar mixes that were long-term aged at five and ten days. However, the evaluated aging levels did not seem to affect the rut depths for recycled mixes at lower rejuvenator dosage levels (RAP+7.9% RA1 and RAP + 6.5% RA2). This indicates that the higher rejuvenator dosage was effective in softening the recycled binder and thereby increases rutting potential. This observation is consistent with the

binder HTPG presented in Table 4-1. The softening effect is short-term, and the mix rutting performance improves with aging. It is noted that the RAP +7.9% RA1 mix aged for ten days was damaged and was not tested. This is shown in Tables 5-2 and 5-3 as Not Measured (NM).

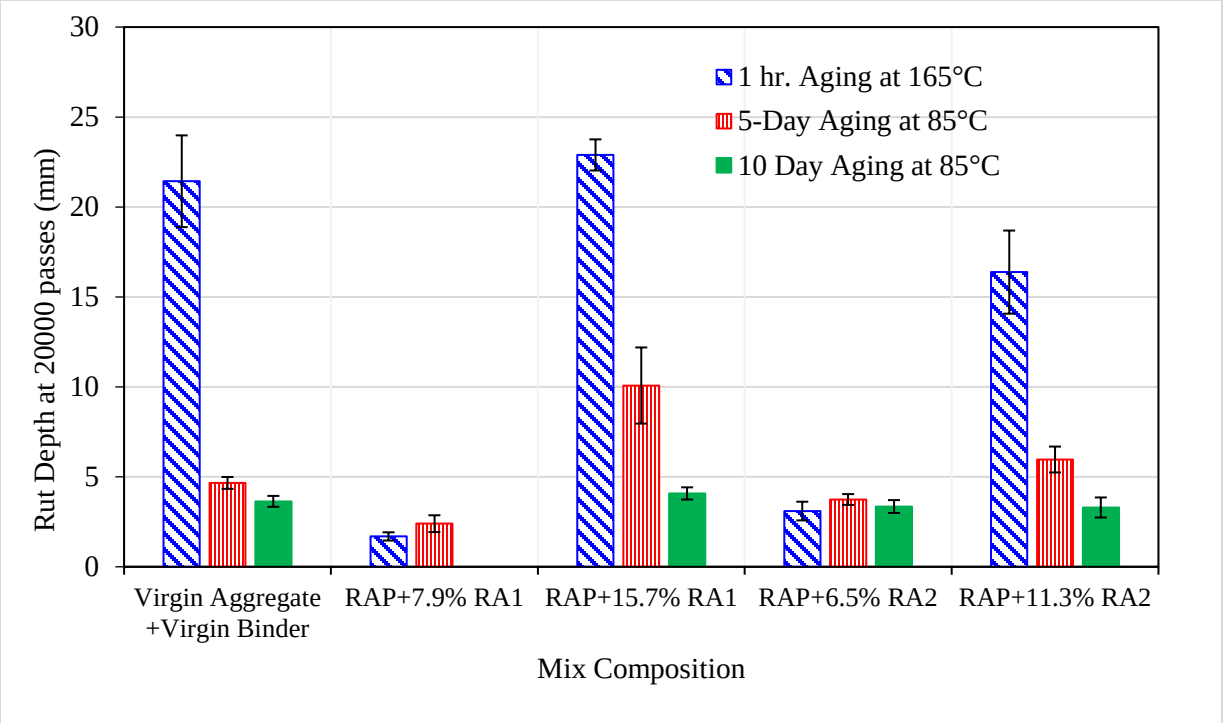

Figure 5-1. LWT Test Results, 50°C Wet.

Effects of aging on moisture susceptibility is reported as the Stripping Inflection Point (Table 5-3). An increased aging level improved moisture damage resistance for recycled mixes with a higher rejuvenator dosage rate. It is noted that for RAP samples with a 6°C higher HTPG than virgin mix and for samples 2, 3, 9 and 15 (Table 4-1), no stripping inflection was observed within 20,000 passes.

Table 5-2. LWT Rut Depth Test Results, 50°C Wet

Mix Aging Level	Mix Composition	Rut Depth at 20000 Passes (mm)		
		Average	Std. Dev.	Groupings
1 hr. aging at 165°C	Virgin Aggregate +Virgin Binder	21.4	3.6	C
	RAP + 7.9% RA1	1.7	0.3	A
	RAP + 15.7% RA1	22.9	1.2	C
	RAP + 6.5% RA2	3.1	0.7	A
	RAP + 11.3% RA2	16.4	3.3	B
5 Days aging at 85°C	Virgin Aggregate +Virgin Binder	4.7	0.5	B/C
	RAP + 7.9% RA1	2.4	0.7	A
	RAP + 15.7% RA1	10.1	3.0	D
	RAP + 6.5% RA2	3.7	0.4	A/B
	RAP + 11.3% RA2	6.0	1.0	C
10 Days aging at 85°C	Virgin Aggregate +Virgin Binder	3.6	0.4	A/B
	RAP + 7.9% RA1	NM	NA	NA
	RAP + 15.7% RA1	4.1	0.5	B
	RAP + 6.5% RA2	3.3	0.5	A
	RAP + 11.3% RA2	3.3	0.8	A

Mix Aging Level	Rejuvenator Type	Rejuvenator Dosage (%)	Rut Depth at 20000 Passes (mm)		
			Average	COV (%)	Groupings
1 hr. aging at 165°C	RA1	7.9	1.7	19	A
		15.7	22.9	5	B
	RA2	6.5	3.1	24	A
		11.3	16.4	20	B
5 Days aging at 85°C	RA1	7.9	2.4	28	A
		15.7	10.1	30	B
	RA2	6.5	3.7	11	A
		11.3	6.0	17	B
10 Days aging at 85°C	RA1	7.9	NM	NA	NA
		15.7	4.1	12	NA
	RA2	6.5	3.3	15	A
		11.3	3.3	24	A

NA: Not applicable; NM: Not measured as sample was damaged; COV: Coefficient of Variation; Statistical groupings were based on Tukey analysis at a 95% confidence level.

Table 5-3. LWT Stripping Inflection Point Results, 50°C Wet

Mix Composition	Aging Level	Stripping Inflection Point (Number of Passes)		
		Average	COV (%)	Groupings
Virgin Aggregate +Virgin Binder	1 hr. Aging at 165°C	6225	10	B
	5-Day Aging at 85°C	20000*	NA	A
	10-Day Aging at 85°C	20000*	NA	A
RAP+7.9% RA1	1 hr. Aging at 165°C	20000*	NA	A
	5-Day Aging at 85°C	20000*	NA	A
	10-Day Aging at 85°C	NM	NA	NA
RAP+15.7% RA1	1 hr. Aging at 165°C	5683	12	C
	5-Day Aging at 85°C	14344	22	B
	10-Day Aging at 85°C	20000*	NA	A
RAP+6.5% RA2	1 hr. Aging at 165°C	20000*	NA	A
	5-Day Aging at 85°C	20000*	NA	A
	10-Day Aging at 85°C	20000*	NA	A
RAP+11.3% RA2	1 hr. Aging at 165°C	11238	6	C
	5-Day Aging at 85°C	15790	9	B
	10-Day Aging at 85°C	20000*	NA	A

NA: Not applicable (mixes did not strip after 20000 passes); NM: Not measured as sample was damaged; COV: Coefficient of Variation; Statistical groupings were based on a Tukey analysis at a 95% confidence level.

5.2.1 Correlations

Rutting results for all 15 samples are correlated with characteristics of the extracted binder, and the results are summarized in Table 5-4. The R-squared, adjusted R-squared and the significance level of the correlations are calculated using SPSS software. The R-squared measures the strength of the relationship between the model and the dependent variable on a convenient 0 – 1 scale. To balance the effect that the number of independent variables has on the coefficient of multiple determination, the adjusted R-squared is used. In fact, the adjusted R-squared becomes useful in comparing the correlations of the same variable with different sample sizes. The p-value for each term tests the null hypothesis that the coefficient is equal to zero (no effect). A low p-value (< 0.05) indicates that we can reject the null hypothesis. In other words, a predictor that has a low p-value is likely to be a meaningful addition to the model because changes in the predictor's value are related to changes in the response variable.

Table 5-4. Linear Correlation between Rut Depth and Independent Variables

		Linear regression (n=15)	
		R-squared	P-value
1	PG_{ave}	0.464	0.005
2	X_1	0.443	0.007
3	X_2	0.381	0.014
4	X_3	0.359	0.018
5	I_h	0.029	0.544
6	SGF	0.000	0.979

Layers X_1, X_2, and X_3 represent the outer, middle, and inner "layers" of the binder coating around the aggregates. As shown in Table 5-4, the PG_{ave} and X_1 have the most significant correlations with the rut depth, with 0.005 and 0.007 P-values, respectively. Stiffness of the second and third layers also somewhat correlated with rutting, which is consistent with expectation. The trend curve showed in Figures 5-2 to 5-5 demonstrates the inverse relation between variables 1 to 4 with the rut depth. This means that as the HTPG increases, the rutting susceptibility of the mix decreases.

The homogeneity Index (I_h) and the stiffness gradient (SGF) did not show any significant correlations with rutting. The power function ($y=a*X^b$) was also fitted to the data, which results in a higher R-squared. Parameters a, b, and R-squared for power function regression are presented in Table 5-5.

Table 5-5. Nonlinear Correlation between Rut Depth and Independent Variables

		R-squared	a	b
1	PG_{ave}	0.556	10^{25}	-12.59
2	X_1	0.500	3×10^{23}	-11.79
3	X_2	0.474	4×10^{19}	-9.784
4	X_3	0.513	10^{26}	-13.34

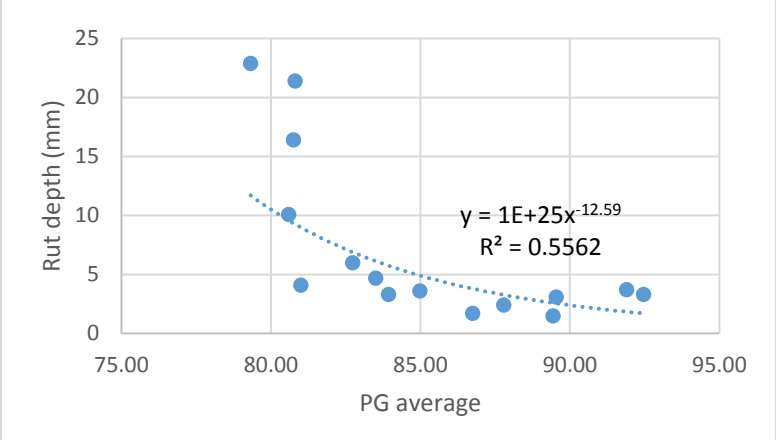

Figure 5-2. Correlation between PG_{ave} and Rut Depth (n=15).

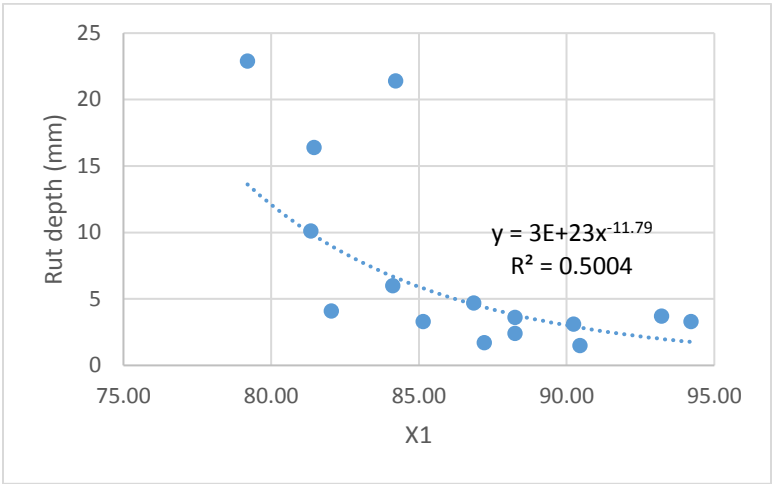

Figure 5-3. Correlation between X1 and Rut Depth (n=15).

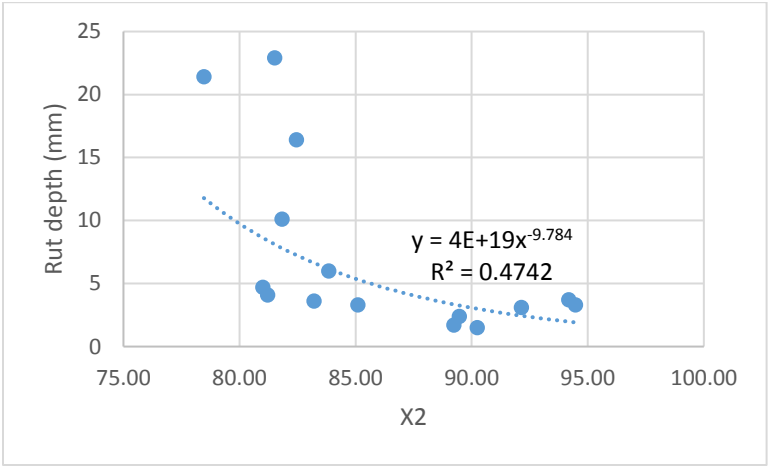

Figure 5-4. Correlation between X2 and Rut Depth (n=15).

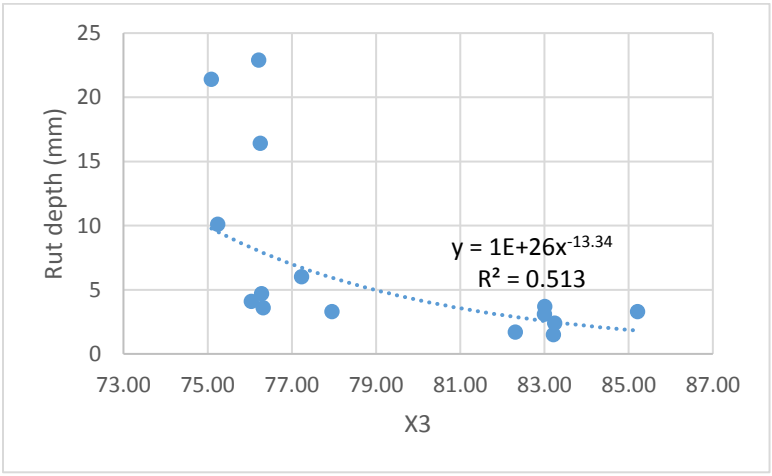

Figure 5-5. Correlation between X3 and Rut Depth (n=15).

5.3 Semi-Circular Bend (SCB) Test - Results

The SCB strain energy release rate (J_c [kJ/m^2]) of all the mixes was determined from the SCB test as a measure of the intermediate temperature cracking resistance of the asphalt mixes. J_c is mechanistically correlated to the mix resistance to crack propagation. Figure 5-6 shows the SCB J_c values for the mixes evaluated. Table 5-6 presents the average SCB J_c values along with the COV and statistical ranking of mixes considered. The average COV was 11.81%, with a range of 5% - 20%. SCB J_c values for the control mix decreased with an increase in aging level, indicating that the mix resistance to cracking decreased as the aging level increased. A similar trend was observed for recycled mixes with low dosage levels. However, recycled mixes with high dosage levels, in general, tended to possess higher SCB J_c values as aging levels increased, except for the RAP + 11.3% RA2 mix at the 10-day aging level. This may indicate that the higher rejuvenator dosage level was effective in improving the diffusion of rejuvenators into the aged RAP binder after long-term aging, thereby enhancing the mix's ability to resist crack propagation. A similar observation is reported elsewhere (Carpenter and Wolosick 1980; Noureldin and Wood 1987). It is worth noting that the short-term aged virgin mix had a Jc value equal to or greater than the Louisiana DOTD specified minimum value of 0.5 kJ/m^2 (2016 Louisiana DOTD Specifications for Roads and Bridges).

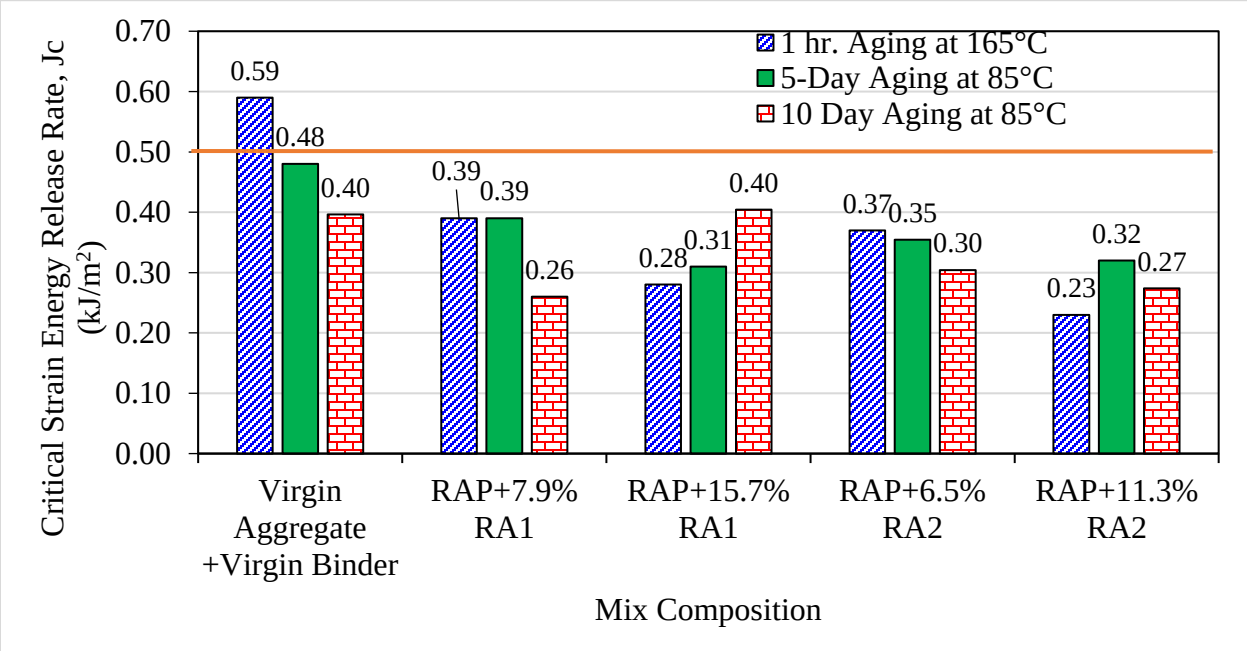

Figure 5-6. Semi-Circular Bend Test Results, 25°C.

Table 5-6. Semi-Circular Bend Test Results for Different Rejuvenator Dosages, 25°C

Mix Aging Level	Rejuvenator Type	Rejuvenator Dosage (%)	SCB Jc Value(kJ/m^2)		
			Average	COV (%)	Groupings
1 hr. aging at 165°C	RA1	7.9	0.39	10	A
		15.7	0.28	5	A
	RA2	6.5	0.37	5	A
		11.3	0.23	16	A
5 days aging at 85°C	RA1	7.9	0.39	20	A
		15.7	0.31	9	A
	RA2	6.5	0.35	12	A
		11.3	0.32	10	A
10 days aging at 85°C	RA1	7.9	0.26	6	A
		15.7	0.40	16	A
	RA2	6.5	0.30	18	A
		11.3	0.27	16	A

COV: Coefficient of Variation; Statistical groupings were based on a Tukey analysis at a 95% confidence level.

5.3.1 Correlations

Table 5-7 shows the results of correlations between the J_c and the independent variables for two different sample sizes of 15 and 9. The sample size of 9 is used to consider the difference in the initial HTPG of the samples. The correlation for all 15 samples shows that the homogeneity index and stiffness gradient are the only independent variables that have significance values close to 0.05. However, variables 1 to 4 do not have a meaningful correlation with the J_c.

Table 5-7. Correlation between SCB Jc Value (kJ/m2) and Independent Variables for Various Sample Sizes

		All samples (n=15)			Samples with Initial HTPG of 74.2°C ± 1°C (n=9)		
VAR No.	VAR name	R-squared	Adjusted R-squared	P-value	R-squared	Adjusted R-squared	P-value
1	PG_{ave}	0.014	-0.061	0.669	0.013	-0.128	0.771
2	X_1	0.003	-0.074	0.859	0.202	0.087	0.225
3	X_2	0.107	0.039	0.233	0.559	0.496	0.021
4	X_3	0.145	0.034	0.455	0.129	0.116	0.121
5	SGF	0.266	0.21	0.050	0.435	0.355	0.045
6	I_h	0.242	0.183	0.063	0.419	0.336	0.059

Although a higher HTPG means a stiffer binder and generally a stiffer binder is more brittle and susceptible to cracking, there is no significant correlation between the HTPG of the binder (variables 1 to 4) and intermediate cracking resistance of the asphalt mix (Jc).

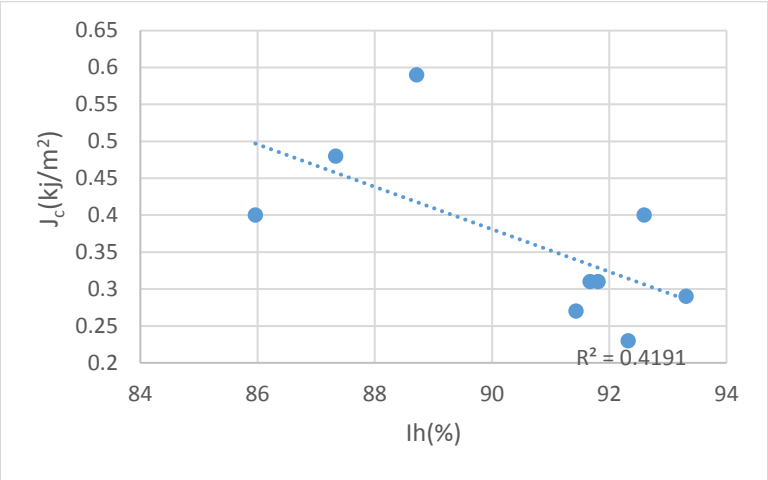

Figure 5-7. Correlation between I_h and J_c for the Samples with HTPG 74.2°C ±1°C (n=9).

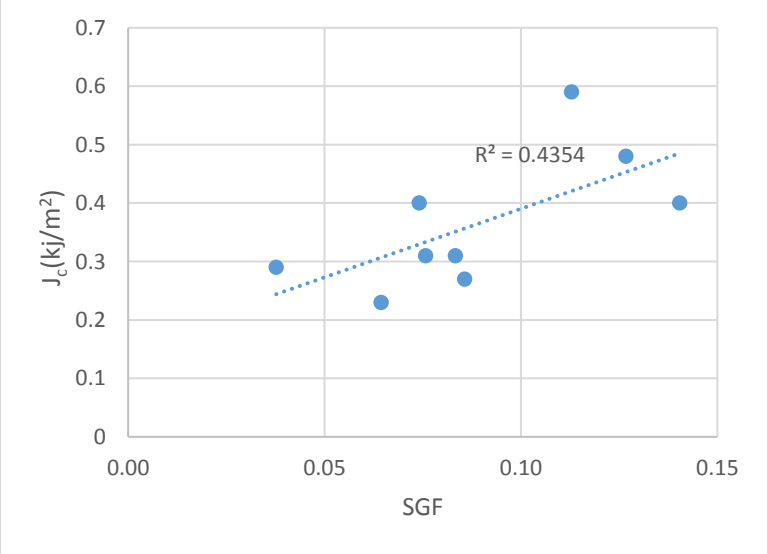

Figure 5-8. Correlation between SGF and J_c for the Samples with HTPG 74.2°C±1°C (n=9).

Figure 5-7 illustrates that as the I_h increases, the Jc decreases. This observation does not support the hypothesis that a more homogeneous binder coating could lead to a higher crack resistance of the mix. Figure 5-8 shows that as the SGF increases, the Jc increases. This indicates that the stiffer the outer layer relative to the inner layer, the better the cracking performance of the asphalt mix.

5.4 Florida Indirect Tension (IDT) Test: Results and Discussion

Table 5-8 presents the average dynamic modulus (|E*|), the tensile strength (S_T), m-value, creep compliance [D(t)], dissipated creep strain energy density failure ($DCSE_f$) limit values, the Energy Ratio (ER) and the respective COV values for mixes evaluated. The tensile stress at the bottom of the asphalt layer was assumed to be 150 psi (1MPa), as suggested by Roque et al. (1992, 2004).

The average COV of |E*|, S_T, and $DCSE_f$ was 7, 6, and 26%, respectively, with ranges of 2%-17%, 1%-11%, and 6%-49%, respectively. Figure 5-9 shows $DCSE_f$ values of the mixes evaluated. Table 5-9 presents the average $DCSE_f$ values, along with the COV and statistical ranking of recycled mixes with different rejuvenator dosage rates. $DCSE_f$ is considered a threshold for healable micro-damage. If this threshold is exceeded, macro-cracks start to initiate. Therefore, a high $DCSE_f$ value is desired for a crack-resistant mix.

Short-term aged virgin mix and recycled mixes with a low dosage rate of rejuvenator RA1 (RAP+7.9% RA1) exhibited higher $DCSE_f$ values than similar mixes long-term aged at 5 and 10 days. Low and high dosage rates of recycled mixes with rejuvenator RA2 (RAP+6.5% RA2 and RAP+11.3% RA2) also showed higher $DCSE_f$ values than similar mixes that were long-term aged at 5- and 10-day aging levels. Furthermore, the evaluated aging levels resulted in a progressive increase in the $DCSE_f$ values of the recycled mixes with the higher dosage of rejuvenator R1 (RAP+15.7% RA1). This may indicate that the higher dosage of rejuvenator RA1 was effective in enhancing the diffusion of rejuvenators into the aged RAP binder after long-term aging, thereby improving the intermediate temperature performance at 10°C. This observation is similar to the one observed from SCB Jc. All mixes had $DCSE_f$ values exceeding the threshold value of 0.75 kJ/m^3, indicating acceptable cracking performance. The energy ratio is a more effective method to characterize the fatigue performance of the asphalt mix than $DCSE_f$. The reason is that ER takes into account both the energy required to fracture HMA mixes and the dissipated energy accumulation in the mix. The higher the energy ratio, the better the crack resistance of the asphalt mix.

Table 5-8. Florida IDT Tests Results

Mix ID	Aging Level	Statistics	|E*| (MPa)	S_T (kPa)	*m-value*	D(t) (GPa^{-1})	$DCSE_f$ (kJ/m^3)	CR ($GPa^{-1}s^{-1}$)	Energy Ratio
Virgin Aggregate +Virgin Binder	1 hr, 165°C	Average	10,062	2,124	0.444	3.2	7.29	1.39	4.05
		COV (%)	8	3	-	-	6	-	-
	5-Days, 85°C	Average	10,871	2,355	0.42	1.1	2.83	0.44	4.57
		COV (%)	6	8	-	-	30	-	-
	10-Days, 85°C	Average	11,489	2,320	0.476	1	2.97	0.41	5.95
		COV (%)	8	10	-	-	37	-	-
RAP + 7.9% RA1	1 hr, 165°C	Average	11,370	2,497	0.467	1	3.85	0.42	7.17
		COV (%)	5	2	-	-	32	-	-
	5-Days, 85°C	Average	13,548	2,732	0.417	0.4	2.18	0.11*	12.90
		COV (%)	4	3	-	-	28	-	-
	10-Days, 85°C	Average	11,827	2,657	0.285	0.5	1.85	0.12*	8.85
		COV (%)	17	5	-	-	36	-	-
RAP + 15.7% RA1	1 hr, 165°C	Average	8,594	1,600	0.392	3.3	2.13	1.28	1.22
		COV (%)	8	5	-	-	24	-	-
	5-Days, 85°C	Average	9,177	1,633	0.354	2.3	2.56	0.83	2.13
		COV (%)	14	7	-	-	20	-	-
	10-Days, 85°C	Average	9,218	1,863	0.357	1.9	2.93	0.67	2.97
		COV (%)	5	11	-	-	8	-	-
RAP + 6.5% RA2	1 hr, 165°C	Average	11,211	2,059	0.385	1.3	3.31	0.50	4.54
		COV (%)	6	8	-	-	10	-	-
	5-Days, 85°C	Average	12,643	2,298	0.34	0.5	1.66	1.42	0.73
		COV (%)	3	7	-	-	47	-	-
	10-Days, 85°C	Average	13,145	2,590	0.307	0.5	1.47	0.12*	6.98
		COV (%)	5	1	-	-	20	-	-
RAP + 11.3% RA2	1 hr, 165°C	Average	7,746	1,543	0.665	1.5	4.25	0.85	8.57
		COV (%)	3	2	-	-	12	-	-
	5-Days, 85°C	Average	11,065	2,123	0.41	0.9	2.48	0.32	5.51
		COV (%)	7	5	-	-	26	-	-
	10-Days, 85°C	Average	9,751	1,646	0.37	1.3	1.72	0.45	2.66
		COV (%)	2	11	-	-	49	-	-

m-value: creep compliance power law constant, *CR:* creep compliance rate values, *: CR were outside the specified range of 0.23 to 6.16.

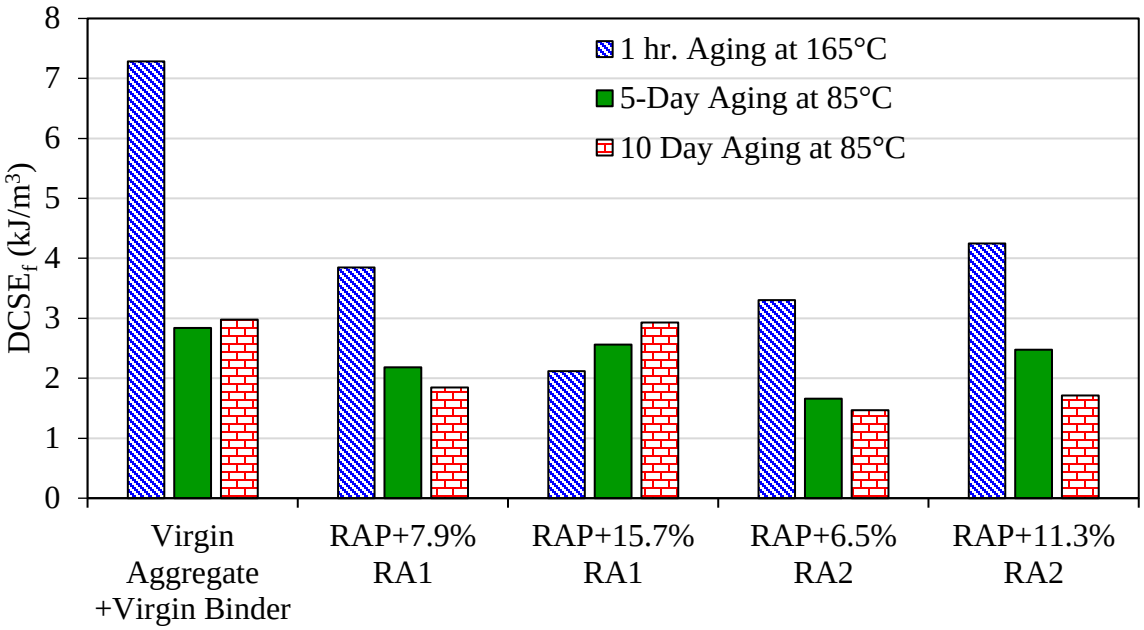

Figure 5-9. Dissipated Creep Strain Energy Density Failure Limit.

Table 5-9. IDT $DCSE_f$ Results for Different Rejuvenator Dosages, 10°C

Mix Aging Level	Rejuvenator Type	Rejuvenator Dosage (%)	$DCSE_f$ (kJ/m^3)		
			Average	COV (%)	Groupings
1 hr. aging at 165°C	RA1	7.9	3.8	32	A
		15.7	2.1	24	A
	RA2	6.5	3.3	10	B
		11.3	4.2	12	A
5 days aging at 85°C	RA1	7.9	2.2	28	A
		15.7	2.6	20	A
	RA2	6.5	1.7	65	A
		11.3	2.5	26	A
10 days aging at 85°C	RA1	7.9	1.8	36	B
		15.7	2.9	8	A
	RA2	6.5	1.5	20	A
		11.3	1.7	49	A

COV: Coefficient of Variation; Statistical groupings were based on a t-Test at a 95% confidence level.

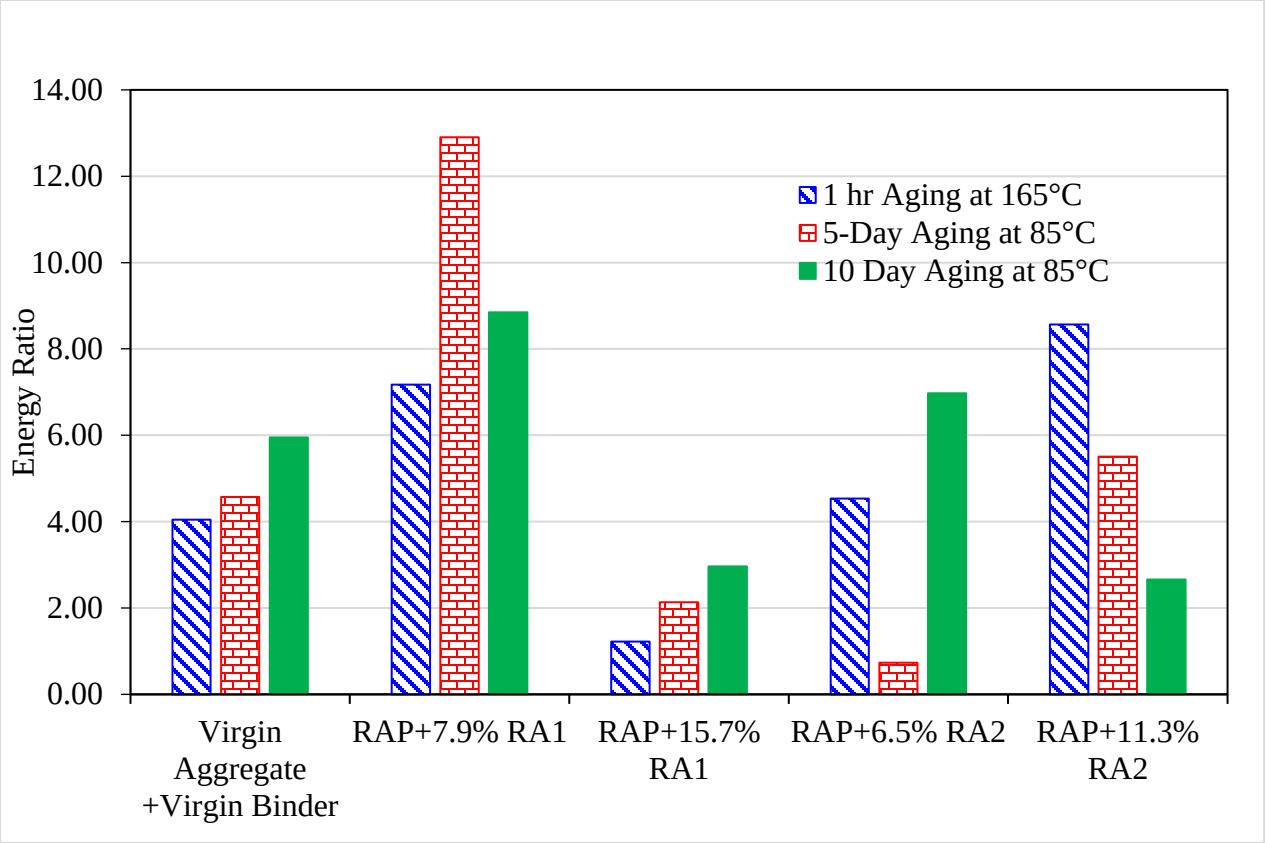

Figure 5-10. Florida IDT Energy Ratio Values, @ 10°C.

As shown in Figure 5-10, the energy ratio for the virgin asphalt mix is increased by aging. This trend was also observed in previous tests conducted on the asphalt mixes fabricated by highly absorptive limestone (Sholar et al., 2004). According to Figure 5-10, as the sample ages, the ER increases for samples containing RA1. However, the ER of the samples containing RA2 decreases as it ages, with the exception of the RAP+6.5% RA2 sample with 10-day aging. In previous sections, it was also observed that for long-term aged samples containing a 15.7% RA1, the J_c and $DCSE_f$ values improved as compared to short-term aged samples. This could be due to the better diffusion characteristic of the RA1 rejuvenator, which strengthens the idea of the positive effect of diffusion on the improvement of the crack performance of the asphalt mix.

5.4.1 Summary of IDT Results

Table 5-10 Summarizes $DCSE_f$ and ER values. According to $DCSE_f$ values, the virgin mix had the best performance, with an average $DCSE_f$ value of 4.36 kJ/m^3, followed by mixes recycled with RA1, with an average $DCSE_f$ value of 2.58 kJ/m^3, followed by mixes recycled with RA2, with an average $DCSE_f$ value of 2.48 kJ/m^3. This order of performance is the same as that established by the SCB Jc described earlier. All mixes had $DCSE_f$ values higher than the critical value of 0.75 kJ/m^3, indicating satisfactory crack propagation resistance behavior.

Table 5-10. Average $DCSE_f$ and ER Values

Mix	$DCSE_f$ (kJ/m^3)		ER	
	$DCSE_f$	Average	ER	Average
Virgin Aggregate +Virgin Binder	4.36	n/a	4.86	n/a
RAP + 7.9% RA1	2.63	2.58	9.64	5.87
RAP + 15.7% RA1	2.54		2.11	
RAP + 6.5% RA2	2.15	2.48	4.08	4.83
RAP + 11.3% RA2	2.82		5.58	

ER values reported in Table 5-10 showed that the mix recycled with RA1 had the best performance, with an average ER value of 5.87, followed by the virgin mix, with an ER value of 4.86, followed by mixes recycled with RA2, with an average ER value of 4.83. All mixes had an ER value higher than the critical value of 1.0, indicating satisfactory crack initiation resistance behavior. It is noted that ranking based on average values does not consider the statistical variability. A comparative statistical summary is presented in Section 5.5.

5.4.2 Correlations

5.4.2.1 $DCSE_f$

As shown in Table 5-11, there is no significant correlation between independent variables and $DCSE_f$. The analysis was repeated for different sample sizes to see if excluding variables like different initial HTPG, G_{mm} or binder content could result in a significant correlation. However, no significant correlations were found.

Table 5-11. Correlation between ($DCSE_f$) and Independent Variables for all Samples (n=15)

VAR No.	VAR name	R-squared	P-value
1	PG_{ave}	0.187	0.108
2	X_1	0.105	0.239
3	X_2	0.262	0.051
4	X_3	0.183	0.111
5	I_h	0.028	0.554
6	SGF	0.039	0.480

5.4.2.2 Energy Ratio

Correlation analysis between the independent variable and ER parameter is shown in Table 5-12. The outlier data are disregarded for the analysis. Contrary to the results of the $DCSE_f$, and J_c, the ER parameter is significantly correlated to variables 1 to 4. This indicates that the ER parameter is more sensitive to the stiffness of the binder than the other two parameters. The PG_{ave}, X_1, and X_2 show the most significant correlation with ER. However, the I_h and SGF are not correlated with ER.

Table 5-12. Correlation between ER and Independent Variables (n=12)

VAR No.	VAR name	R-squared	P-value
1	PG_{ave}	0.593	0.003
2	X_1	0.638	0.002
3	X_2	0.401	0.027
4	X_3	0.489	0.011
5	I_h	0.057	0.456
6	SGF	0.035	0.559

As shown in Figures 5-11 to 5-14, as the HTPG of the mix at different layers (variables 1 to 4) increases, the ER increases. This indicates that the stiffness of the binder is related to the fatigue performance of the mix.

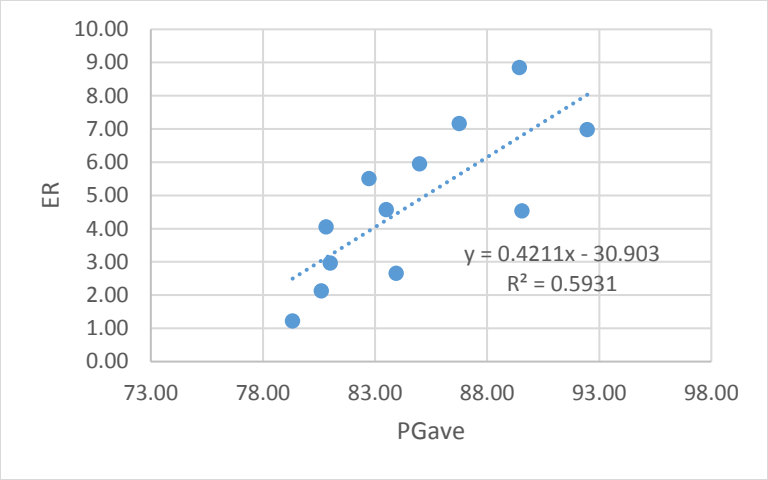

Figure 5-11. Correlation between PG_{ave} and ER (n=12).

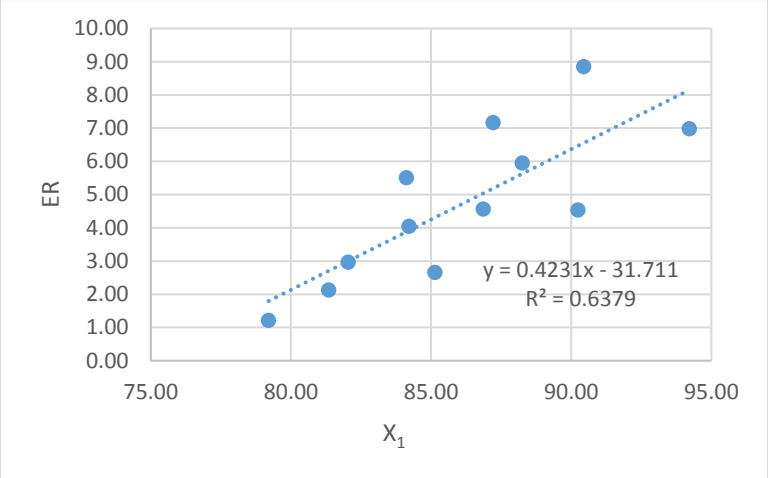

Figure 5-12. Correlation between X1 and ER (n=12).

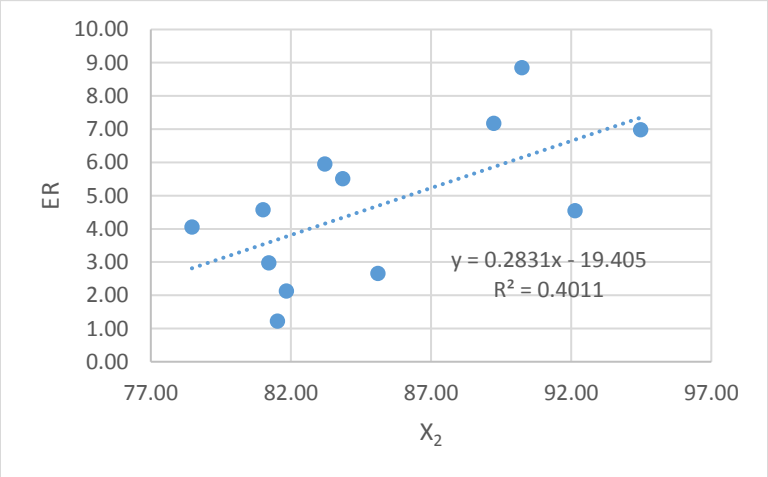

Figure 5-13. Correlation between X2 and ER (n=12).

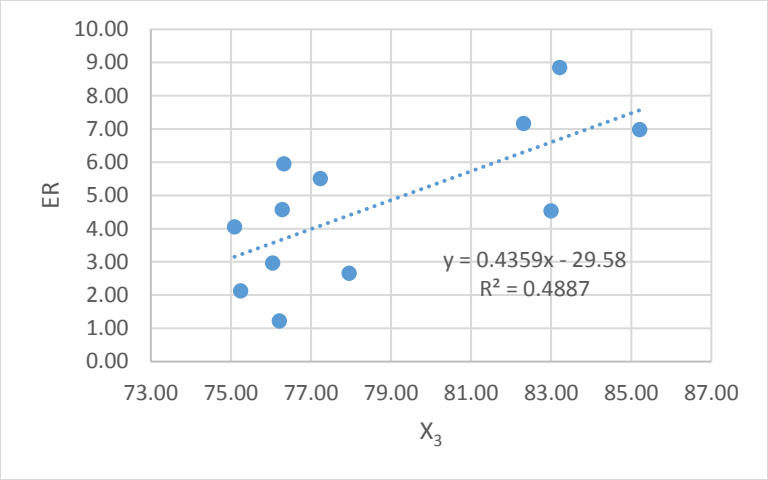

Figure 5-14. Correlation between X3 and ER (n=12).

5.4.2.3 Complex Modulus (|E*|)

Complex modulus is a fundamental property of asphalt used in the mechanistic-empirical methods to predict pavement response. As shown in Figures 5-15 to 5-18, as the HTPG of the binder increases, the Complex Modulus increases. Based on the results shown in Table 5-13, variables 1 to 4 have a strong correlation with the complex modulus. However, I_h and SGF do not have any significant correlation with |E*|, which is similar to the energy ratio. To address the difference of the initial HTPG of the samples and its possible effect on the outcome, the linear correlation for 9 samples with an initial HTPG of 74.2°C ± 1°C was also explored. For 9 samples, the correlation was significant for all variables except X_2 and X_3. For I_h and SGF parameters, the adjusted R-squared increased considerably (Table 5-13, Figures 5-19 and 5-20). This was also observed in the SCB test results, where samples with the same initial HTPG showed a stronger correlation with J_c compared to using all samples for the correlation.

Table 5-13. Correlation between Complex Modulus (|E*|) and Independent Variables.

		All Samples (n=15)			Samples with Initial HTPG of 74.2°C ± 1°C (n=9)		
VAR No.	VAR name	R-squared	Adjusted R-squared	P-value	R-squared	Adjusted R-squared	P-value
1	PG_{ave}	0.732	0.712	0.000	0.603	0.546	0.014
2	X_1	0.767	0.749	0.000	0.723	0.683	0.004
3	X_2	0.556	0.521	0.001	0.017	-0.123	0.735
4	X_3	0.623	0.594	0.000	0.043	-0.093	0.590
5	I_h	0.108	0.039	0.232	0.575	0.515	0.018
6	SGF	0.007	-0.069	0.762	0.652	0.602	0.008

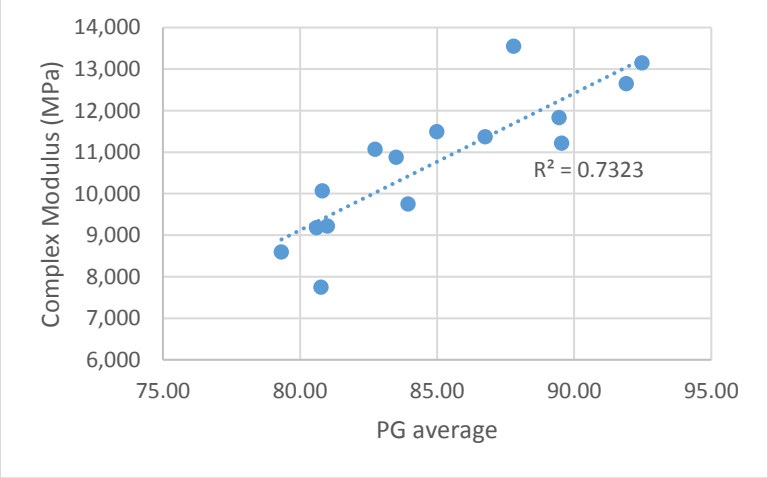

Figure 5-15. Correlation between PG_{ave} and Complex Modulus (|E*|) (n=15).

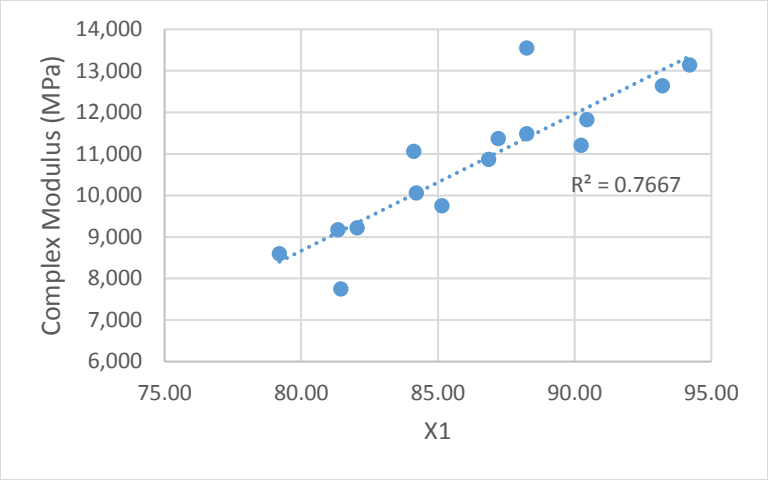

Figure 5-16. Correlation between X1 and Complex Modulus (|E*|) (n=15).

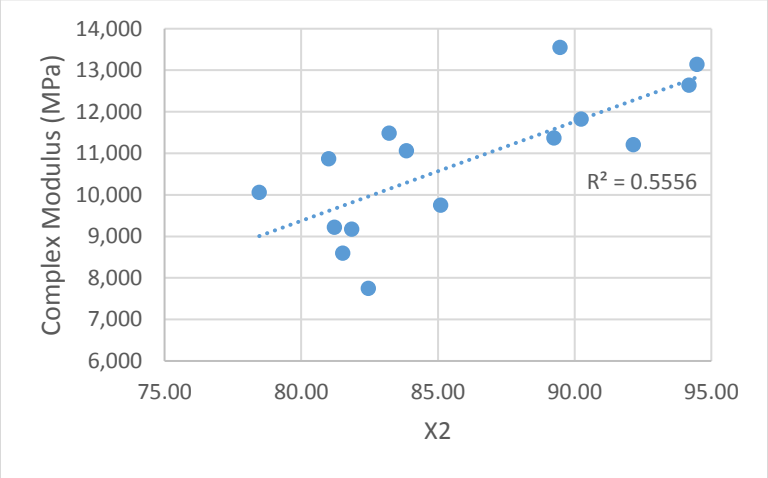

Figure 5-17. Correlation between X2 and Complex Modulus (|E*|) (n=15).

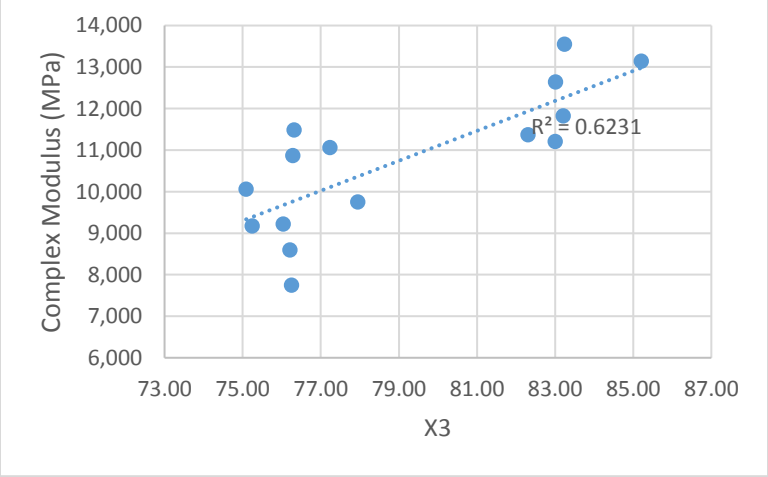

Figure 5-18. Correlation between X3 and Complex Modulus (|E*|) (n=15).

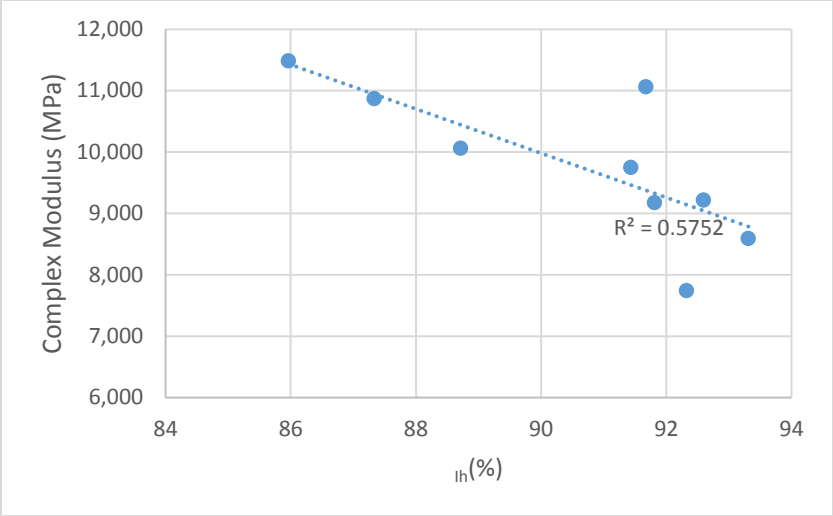

Figure 5-19. Correlation between Homogeneity Index and Complex Modulus (|E*|) for Samples with Initial HTPG 74.2°C±1°C (n=9).

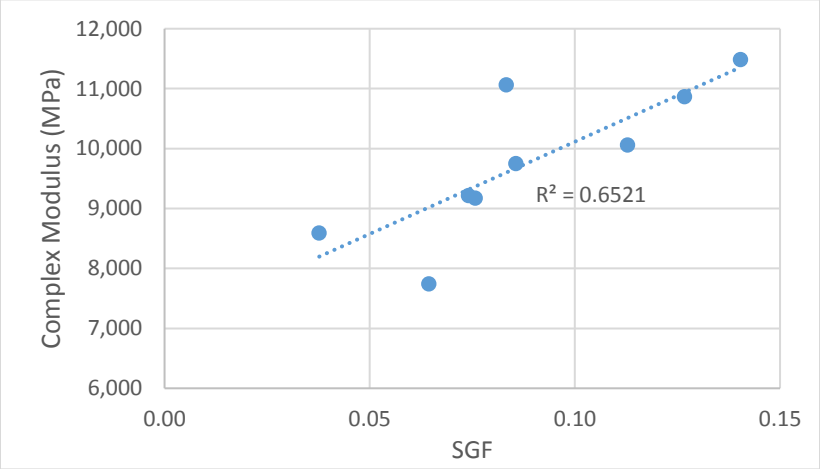

Figure 5-20. Correlation between SGF and Complex Modulus (|E*|) for Samples with Initial HTPG 74.2°C±1°C (n=9).

Figures 5-19 and 5-20 show similar trends observed for the correlation between the critical strain Jc of the SCB test with SGF and I_h (Figures 5-12 and 5-13).

5.4.2.4 Creep Compliance

Prior studies showed that the rate of creep compliance and the rate of micro-damage accumulation in asphalt mixes are directly related to each other. However, it should be considered that age-hardening of the asphalt mix not only reduces the rate of damage accumulation, but it can also reduce the $DCSE_f$ (Yan et al. 2016). Based on a bivariate analysis (Table 5-14), the correlations between creep compliance and HTPG of the samples are significant. The correlations between creep compliance and the homogeneity index and SGF were low. Figures 5-21 to 5-24 show an inverse relation between variables 1 to 4 and D(t). As the creep rate increases, the rate of micro-damage accumulation increases. As a result, the increases of HTPG of the binder coating the

aggregates decreases the resistance of the mix to fatigue cracking. However, as shown in the scatter plots in Figures 5-25 and 5-26, SGF and I_h show no correlation with D(t).

Table 5-14. Correlation between Creep Compliance [D(t)] and Independent Variables.

VAR NO.	VAR name	R-squared	P-value
1	PG_{ave}	0.601	0.001
2	X_1	0.573	0.001
3	X_2	0.519	0.002
4	X_3	0.493	0.004
5	I_h	0.003	0.516
6	SGF	0	0.960

The power function ($y=a*X^b$) was also fitted to the data, which resulted in a higher R-squared compared to linear correlation. Parameters a, b, and R-squared are presented in Table 5-15.

Table 5-15. Nonlinear Correlation between Creep Compliance and Independent Variables

		R-squared	a	b
1	PG_{ave}	0.7088	30×10^{20}	-11.08
2	X_1	0.658	30×10^{19}	-10.54
3	X_2	0.6187	80×10^{15}	-8.714
4	X_3	0.633	90×10^{20}	-11.55

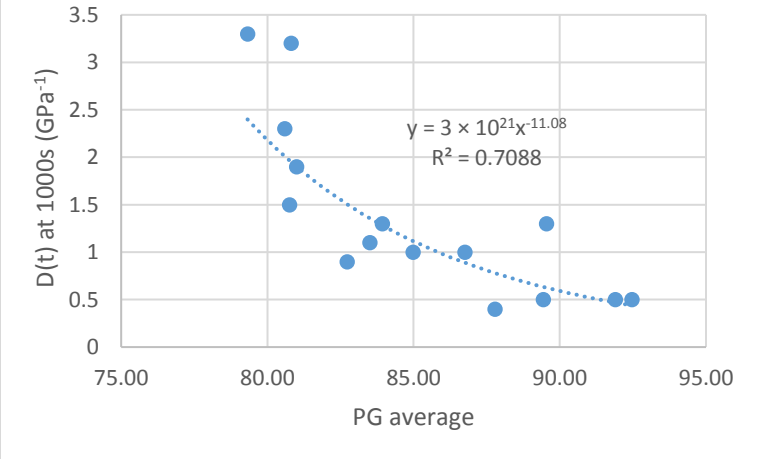

Figure 5-21. Correlation between PG_{ave} and D(t) (n=15).

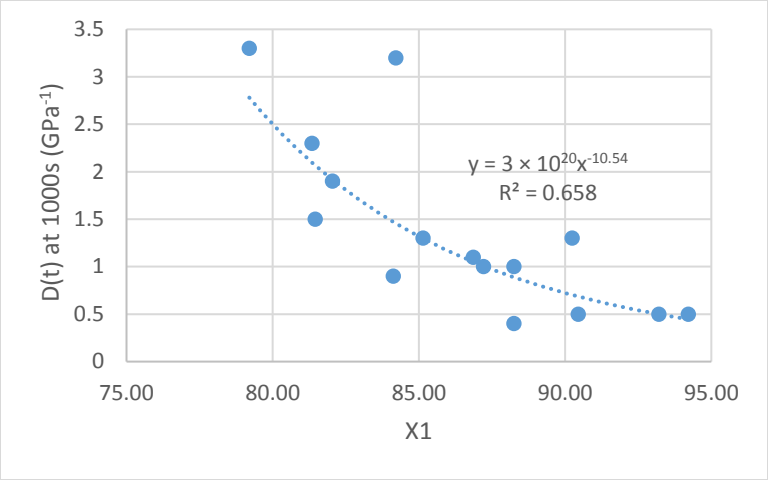

Figure 5-22. Correlation between X1 and D(t) (n=15).

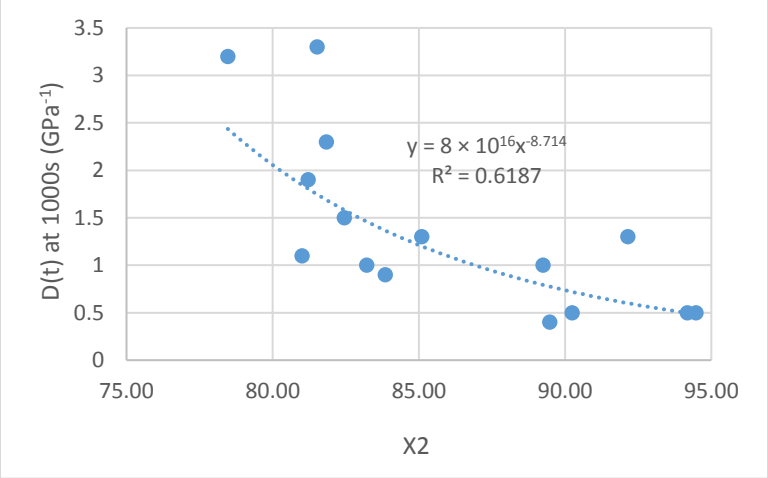

Figure 5-23. Correlation between X2 and D(t) (n=15).

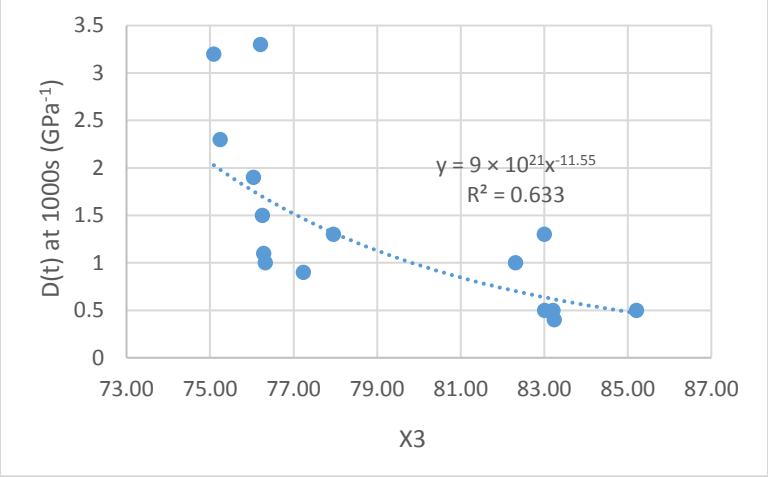

Figure 5-24. Correlation between X3 and D(t) (n=15).

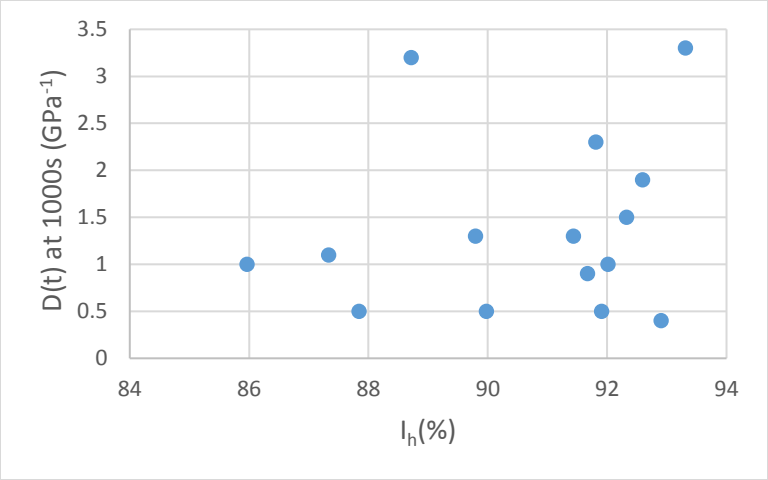

Figure 5-25. Homogeneity Index Versus Creep Compliance Plot.

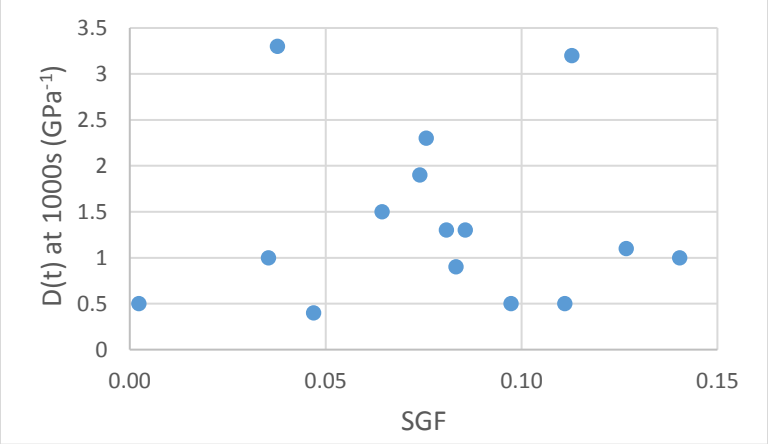

Figure 5-26. SGF Versus Creep Compliance Plot.

5.4.2.5 Tensile Strength (S_T)

Tensile strength (S_T) is the asphalt mix strength when subjected to tension. As shown in Table 5-16 and Figures 5-27 to 5-30, for the sample size of 15, S_T has a meaningful correlation with all independent variables, except for the homogeneity index and stiffness gradient. As the HTPG increases, the S_T increases. Based on previous research, RAP samples with higher S_T are more brittle and more susceptible to fatigue cracking (Shu et al., 2008). The correlation results for 9 samples with an initial HTPG of 74.2°C ± 1°C are also presented in Table 5-16. Based on Figures 5-31 and 5-32, increasing the homogeneity decreases the indirect tensile strength of the samples. On the other hand, an increase in the SGF increases the S_T. These trends are similar to those observed between |E*| and the independent variables. This is not surprising, as the elastic modulus and tensile strength are related.

Table 5-16. Correlation between Tensile Strength (S_T), and Independent Variables.

		All samples (n=15)			Samples with Initial HTPG of 74.2°C ± 1°C (n=9)		
VAR No.	VAR name	R-squared	Adjusted R-squared	P-value	R-squared	Adjusted R-squared	P-value
1	PG_{ave}	0.527	0.491	0.002	0.379	0.290	0.078
2	X_1	0.597	0.566	0.001	0.654	0.604	0.008
3	X_2	0.329	0.278	0.025	0.046	-0.090	0.577
4	X_3	0.479	0.439	0.004	.004	-0.138	0.871
5	I_h	0.085	0.014	0.293	.716	0.675	0.004
6	SGF	0.002	-0.075	0.872	.744	0.708	0.003

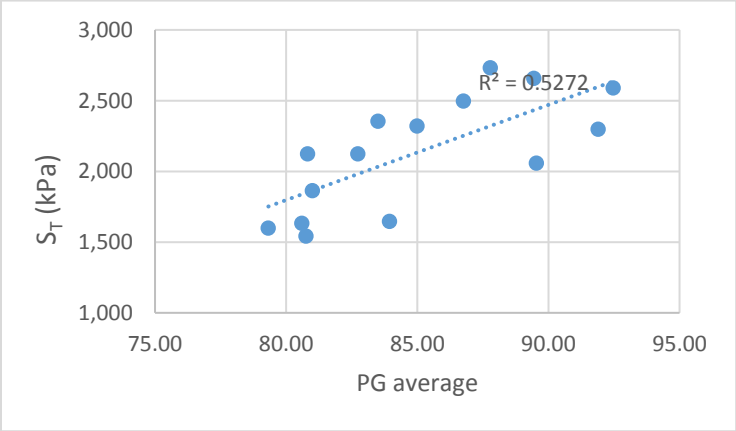

Figure 5-27. Correlation between PG_{ave} and S_T (n=15).

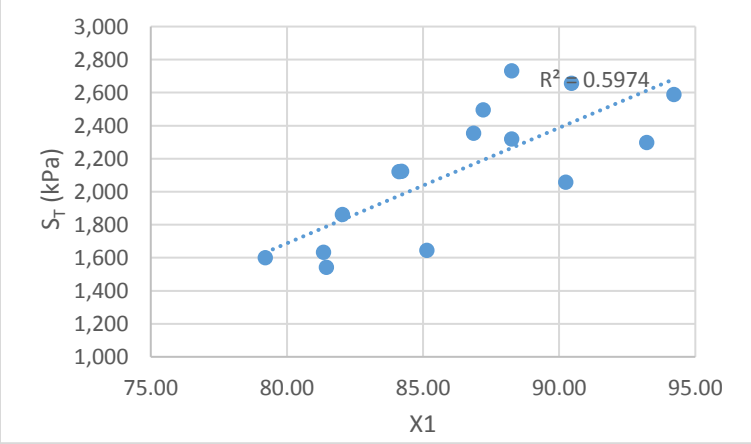

Figure 5-28. Correlation between X1 and S_T (n=15).

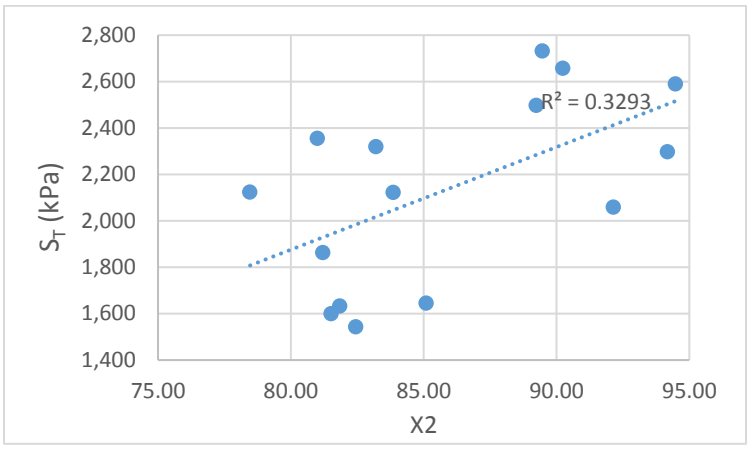

Figure 5-29. Correlation between X2 and S_T (n=15).

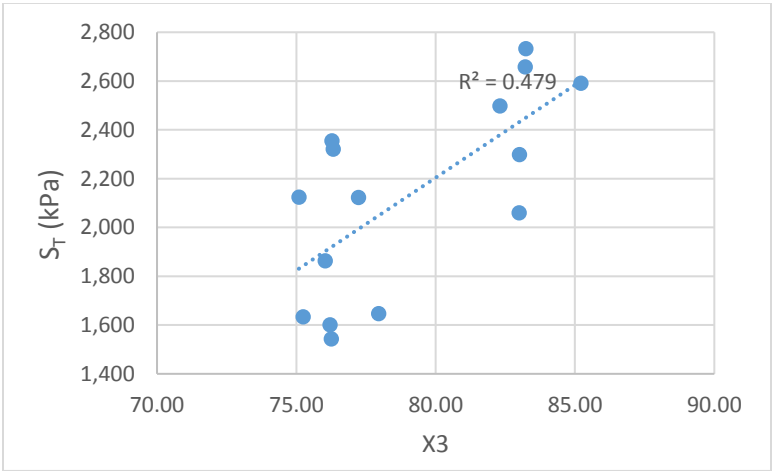

Figure 5-30. X3 Versus S_T Plot (n=15).

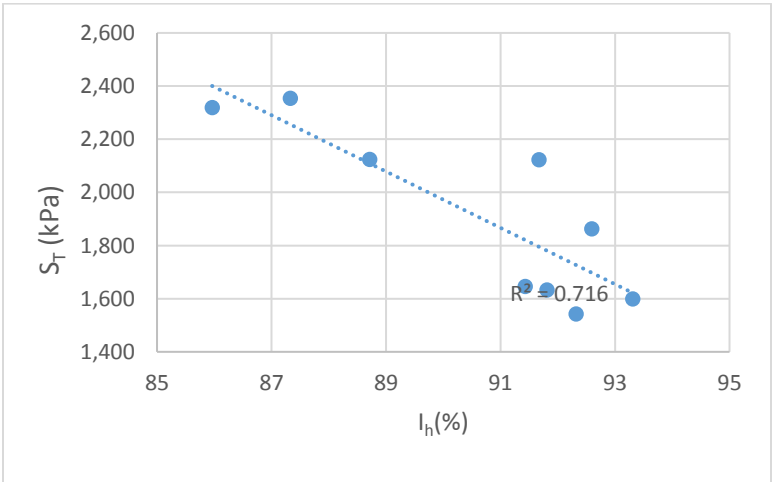

Figure 5-31. Correlation between I_h and S_T for the Samples with Initial HTPG 74.2°C ± 1°C (n=9).

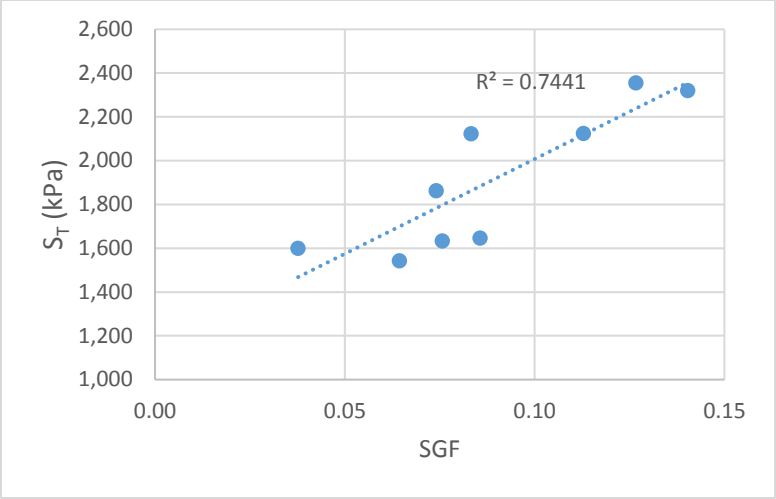

Figure 5-32. Correlation between SGF and D(t) for the Samples with Initial HTPG 74.2°C ± 1°C (n=9).

5.5 Summary of Test Results

Table 5-17 presents a statistical comparison of ranking of laboratory test results LWT, SCB, and Florida IDT test for rejuvenated recycled mixes evaluated compared to the virgin mix at each aging level considered. Test results from LWT, SCB, and IDT tests were statistically analyzed using the T-Test procedure provided in the Statistical Analysis System (SAS) 9.4 program (SAS Institute 1985). A statistical t-Test with a confidence level of 95% was performed on the means. The signs plus (+), minus (-), and equal (=) indicate that the RAP mix showed statistically better, worse or similar performance as compared to the virgin mix, respectively. Generally, short-term aged (1 hour) recycled mixes exhibited less rutting and higher moisture resistance than short-term aged virgin mixes. The test results for 5-day aged mixes were mixed for rutting and moisture resistance. Long-term aged (10-day) recycled mixes presented similar rutting and moisture resistance as the virgin mixes. This may indicate that long-term aging (5 to 10 days) of the recycled mixes resulted in a decrease of rutting and moisture resistance of the recycled mixes to a level similar to the virgin mix. Short-term aged virgin mixes showed higher intermediate temperature fracture resistance than the short-term aged recycled mixes, as measured by the $DCSE_f$ value at 10°C and the SCB Jc value at 25°C. Generally, long-term aged (10 days) virgin mixes exhibited higher $DCSE_f$ values than long-term aged (10 days) recycled mixes. However, long-term aged (5 to 10 days) recycled mixes tended to show SCB J_c values similar to the long-term aged (5 to 10 days) virgin mixes.

Table 5-17. Summary of the Test Results

Mix Composition/Test Parameter	Rut Depth 20,000 passes, 25°C Wet	SIP, 25°C Wet	$DCSE_f$	SCB Jc value, 25°C	ER, 10°C
	1hr. At 165°C				
RAP+7.9% RA1	+	+	-	-	+
RAP+15.7% RA1	=	=	-	-	-
RAP+6.5% RA2	+	+	-	-	+
RAP+11.3% RA2	+	+	-	-	+
	5-Days at 85°C				
RAP+7.9% RA1	+	=	=	=	+
RAP+15.7% RA1	-	-	=	=	-
RAP+6.5% RA2	+	=	-	=	-
RAP+11.3% RA2	=	-	=	=	+
	10-Days at 85°C				
RAP+7.9% RA1	NM	NM	-	=	+
RAP+15.7% RA1	=	=	=	=	-
RAP+6.5% RA2	=	=	-	=	+
RAP+11.3% RA2	=	=	-	=	-

SIP: Stripping Inflection point; NM: Not measured as sample was damaged; Statistical groupings were based on a t-Test at a 95% confidence level; +: Higher performance than virgin mix; -: Lower performance than virgin mix; =: Similar performance as the virgin mix; ER: Energy ratio

Chapter 6 : EVALUATION OF SIMULATED AGING PROTOCOLS

6.1 Introduction

The results from Task 3 (Chapter 3), indicated that both natural and oven aging cause heterogeneous aging in the asphalt film surrounding aggregates. However, the stiffness gradient of the naturally aged Mixes (Reclaimed Asphalt Pavement or RAP) was different from the oven-aged Mixes. This difference can potentially influence the performance of the Mix and be a source of error for tests that are based on simulated aging. The purpose of this task is to evaluate and compare different simulated aging protocols.

There are fewer studies on the aging of asphalt Mixes than on the aging of binders. The AASHTO Standard Practice for Mix Conditioning of Hot Mix Asphalt (AASHTO R30) was developed based on the work of Von Quintus et al. (Quintus et. al, 1991). The protocol covers Mix conditioning for volumetric Mix design, and for short- and long-term conditioning. The Mix is conditioned in a forced draft oven for various periods of time and temperatures, as shown in Table 6-1.

Table 6-1. Various Aging Conditions According to AASHTO R30

Conditioning type	Temperature	Time
Mix design conditioning	Varies*	2 hours
Short-term aging	135 °C	4 hours
Long-term aging	85 °C	5 days

*A Mix's specified compaction temperature and type of Mix (reheat, produced, plant, etc.).

Oven aging of compacted samples is a common method used to simulate long-term aging conditions. However, it may promote the formation of an oxidation gradient along the depth of the specimen. On the other hand, loose Mixes are aged more homogeneously compared to compacted Mixes. But it also has the problem of increased exposure to air and heat, compared to in-service pavements. (Bell et al., 1994).

Bell et al. evaluated the AASHTO R30 short-term aging protocol. The results of the study showed that this protocol has the ability to simulate and predict asphalt Mix short aging quite well. Another researcher also confirmed the accuracy of the short-term aging protocol by evaluating the resilient modulus and indirect tensile test results (Mohammadafzali et al., 2017). However, many studies show that the long-term conditioning protocol (85°C for 5 days) does not account for different climate conditions, traffic volume, and mix properties. According to the work of Sirin et al., severe environmental conditions, such as in the Middle East region, would need 45 to 75 days at 85°C on

the compacted samples to simulate 5 years of field aging, compared to 1-2 days at 135°C to achieve the same field aging (Sirin et al., 2018).

6.2 Sample Preparation

A single source of RAP was used in this study. The average pavement age in South Florida prior to milling is approximately 18 years. One type of virgin binder and aggregate were used to prepare the Mix. The gradation of the loose Mix was the same as that of the RAP, with a 7 percent binder content (by the weight of the Mix). Virgin asphalt binder was obtained from a local asphalt producer in Miami. The high-temperature Performance Grade (HTPG) of this binder was 74.2ºC, as determined by Dynamic Shear Rheometer (DSR) testing.

6.3.1 Test Methodology

The typical stiffness gradient caused by natural aging was identified by performing staged extraction for three RAP Mixes. Stiffness gradient factors and homogeneity indices were obtained for these samples and the average values were determined. Aged samples were prepared by exposing virgin mixes to different aging protocols (Table 6-2). A sample of loose Mix was produced and placed in several pans. A thin layer of the Mix with the approximate thickness equal to the Nominal Maximum Aggregate Size (13mm-16mm) was placed into each pan. To minimize the effect of an oven temperature gradient, the loose mix was agitated once a day during the oven aging process. After the mix was aged, the pans were taken out of the oven and mixed together to obtain a uniform Mix. Then, the mix was left at room temperature to cool. Finally, parameters obtained from each aging protocol were compared to those determined for naturally aged samples to identify the best protocol.

The procedures used to prepare the mix, extract the binder and measure the homogeneity index and stiffness gradient were explained in Chapter 3.

Table 6-2. Results of DSR tests on the staged extracted binder.

	Temp (° C)	Days	Sample Number	Extraction No.	Binder Recocvred (grmas)	Binder Recocvred (%)	Continious High Temperature Grade	Weighted Average	Bias	Normalized PG	(Max - Min)	Ih	SGF
Virgin mixture	85	5	1	X1	40.23	0.55	86.86	83.51	3.35	1.04	10.58	0.87	12.7%
				X2	21.35	0.29	81.00		-2.50	0.97			
				X3	11.28	0.15	76.28		-7.23	0.91			
		10	2	X1	39.60	0.56	88.25	84.69	3.26	1.04	11.93	0.86	14.1%
				X2	19.66	0.28	82.15		-2.54	0.97			
				X3	10.87	0.15	76.32		-8.37	0.90			
	110	2	3	X1	43.25	0.57	87.24	85.09	2.15	1.03	12.03	0.86	14.1%
				X2	22.20	0.29	85.45		0.36	1.00			
				X3	10.20	0.13	75.21		-9.88	0.88			
		4	4	X1	37.98	0.55	91.58	89.64	1.94	1.02	8.34	0.91	9.3%
				X2	20.14	0.29	89.54		-0.10	1.00			
				X3	11.24	0.16	83.24		-6.40	0.93			
		6	5	X1	40.21	0.57	94.54	92.95	1.59	1.02	8.22	0.91	8.8%
				X2	19.63	0.28	93.25		0.30	1.00			
				X3	10.56	0.15	86.32		-6.63	0.93			
	135	1	6	X1	40.25	0.55	88.21	85.99	2.22	1.03	12.89	0.85	15.0%
				X2	23.17	0.32	86.32		0.33	1.00			
				X3	9.12	0.13	75.32		-10.67	0.88			
		2	7	X1	39.25	0.53	93.00	90.33	2.67	1.03	13.77	0.85	15.2%
				X2	25.36	0.34	90.28		-0.05	1.00			
				X3	9.30	0.13	79.23		-11.10	0.88			
		3	8	X1	35.26	0.50	95.46	93.26	2.20	1.02	10.23	0.89	11.0%
				X2	20.35	0.29	95.21		1.95	1.02			
				X3	14.63	0.21	85.23		-8.03	0.91			
RAP Material			9	X1	45.21	0.62	92.25	91.49	0.76	1.01	4.01	0.96	4.4%
				X2	18.50	0.25	91.25		91.25	1.00			
				X3	9.30	0.13	88.24		88.24	0.96			
RAP Material			10	X1	42.14	0.56	89.88	89.58	0.30	1.00	3.13	0.97	3.1%
				X2	22.33	0.29	90.25		90.25	1.01			
				X3	11.23	0.15	87.12		87.12	0.97			
RAP Material			11	X1	55	0.68	89.25	89.08	0.17	1.00	2.51	0.97	2.4%
				X2	16.35	0.20	89.63		89.63	1.01			
				X3	9.3	0.12	87.12		87.12	0.98			

6.4 Analysis

Table 6-2 shows SGF and I_h values for each sample. Figure 6-1 shows the PG of the X1 (outer) layer was higher than the other layers, and the PG of the X3 (inner) layer was lower than the other layers. Therefore, PG_{max} corresponds to the X1 layer, and PG_{min} corresponds to the X3 layer. As expected, the average I_h of the RAP samples was higher than that of the artificially aged samples, which indicates a more homogenous binder layer for RAP samples (Figure 6-1).

According to the results shown in Table 6-2, the average I_h of the RAP Mixes was 0.97, and the average I_h for loose oven-aged Mixes was 0.87. In Figures 6-1 and 6-2, all values shown for RAP samples are the average of the three replicates (samples 9, 10 and 11). Also, the SGF values of the RAP samples were lower compared to artificially aged samples (Figure 6-2). In oven aging, the high temperature exposure that occurs in a relatively short period of time ages the outer layer significantly faster than the inner layer and results in a stiffness gradient through the depth of the binder layer coating the aggregates. The protocol that results in a larger I_h, a smaller SGF in a shorter period of time, and a PG closer to that of RAP should be a better option for aging simulation.

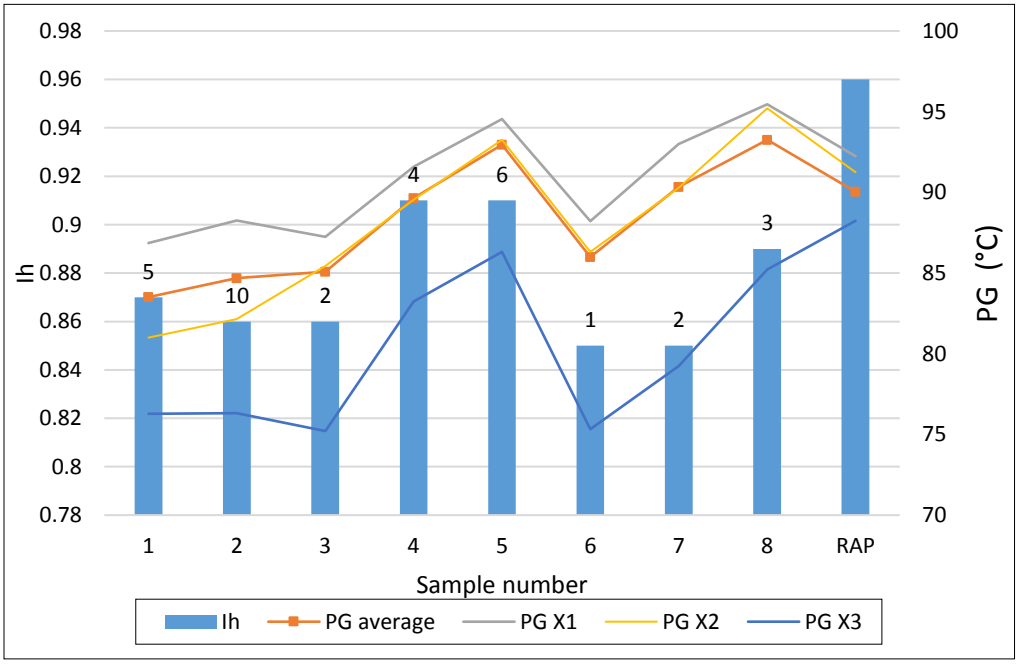

Figure 6-1. Homogeneity Index, PG average and each layer's PG for all samples (The duration of aging for each sample is written at the top of each bar as the number of days.).

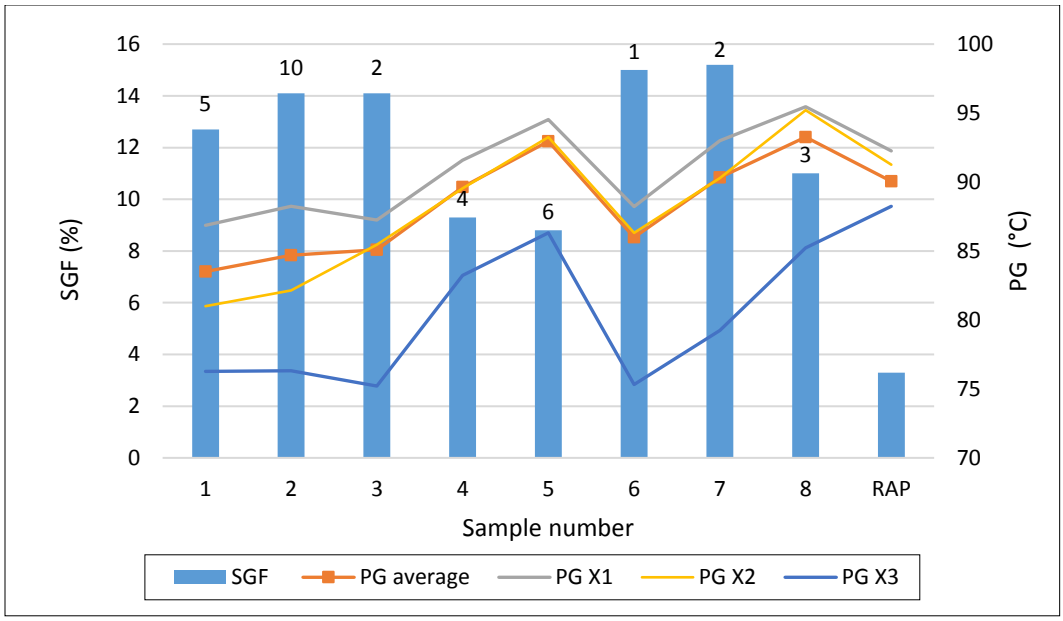

Figure 6-2. SGF, PG and I_h for All Samples

The duration of aging for each sample is written at the top of each bar as the number of the days.

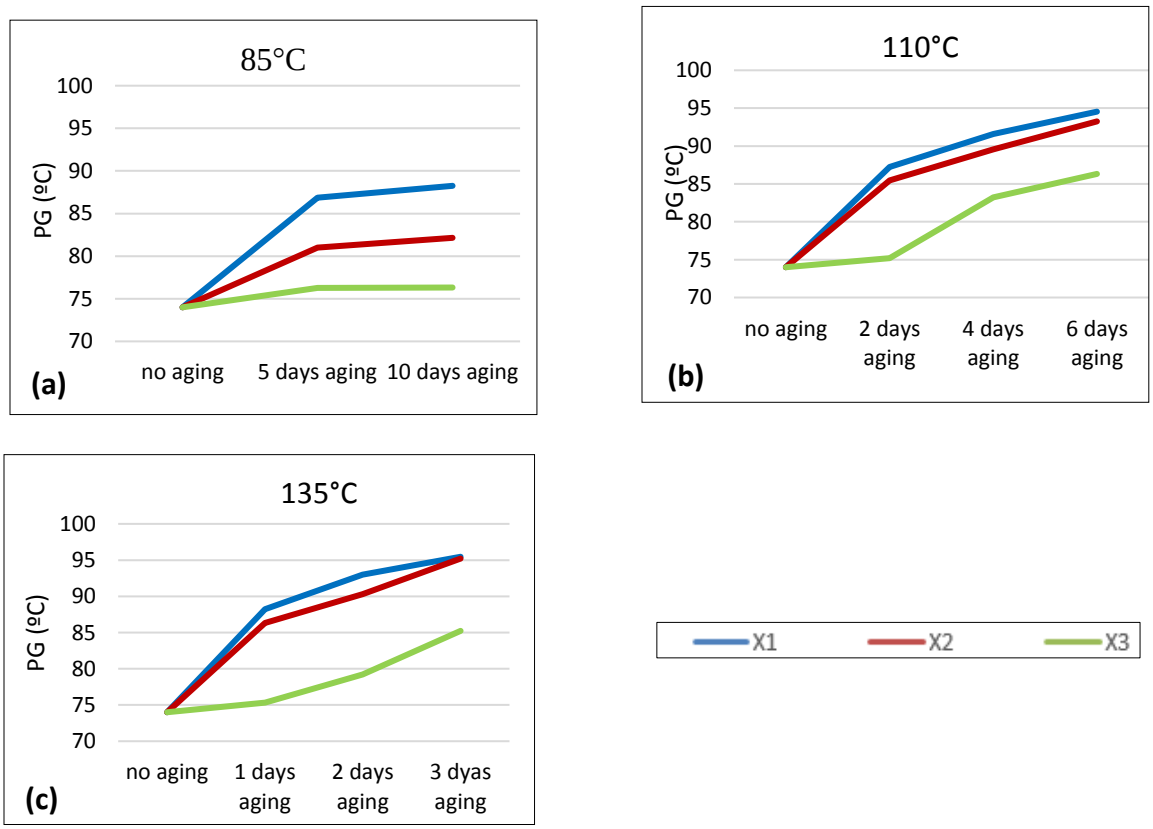

Figure 6-3. High-temperature PG of Samples 1 to 8. (a) Samples 1 and 2 (b) Samples 3, 4 and 5 (c) Samples 6, 7 and 8.

An increase in the aging duration did not considerably change the I_h of samples aged at 85°C. However, the I_h significantly increased for samples exposed to higher temperatures. One reason for this trend could be that the stiffness of the inner layer at a lower temperature (85°C) does not increase considerably, while the stiffness of the outer layer increases significantly (Figure 6-3. (a)). Thus, the difference of PG between the two layers increases. For example, in sample 2, after ten days of aging, the PG of the outer layer increases by 19%, while there is only a 3% increase in the PG of the inner layer. However, for samples that experienced higher temperatures (110°C and 135°C), the rate of increase of the PG of the outer and inner layers is not that much different. For example, for sample 5, after five days of aging at 110°C, the PG of the outer layer increases by 27.4%, and the inner layer PG increases by 16%. The other reason for this observation could be that the outer layer loses most of its volatile material during the first days of aging in the oven and its PG increases quickly, but after initial aging (1 or two days), the rate of increase in PG decreases as the less volatile material in the binder starts to evaporate. For instance, in one day of aging at a temperature of 135°C, the PG of the outer layer increased by 19%, but after only one more day of aging at the same temperature, the X1 PG increased by only 6% in samples 6 and 7.

The average PG of the three RAP samples tested in this study is 90.05°C. According to the results of different protocols, and considering a 3°C of tolerance, samples 4, 5 and 7 have the closest PG_{ave} to 90.05. Additionally, the protocol with a higher I_h and lower SGF is the most favorable one for the simulation of natural aging. Among samples 4, 5 and 7, sample 4 with the I_h of 0.91 and SGF of 9.3% are the best options comparatively.

By comparing the samples with a similar overall level of aging (average PG), the following trends could be identified:

- Samples 2, 3, and 6 with an average PG of 85 ± 1^{O}C: The homogeneity index and SGF values for these samples were similar. However, the samples aged at 135°C had slightly less homogeneous binder layers.
- Samples 4, and 7 with an average PG of 90 ± 1^{O}C: Using a higher temperature (135°C compared to 110°C) resulted in a significantly less homogeneous binder layer.
- Samples 5 and 8 with an average PG of 93 ± 1^{O}C: Using a higher temperature (135°C compared to 110°C) resulted in a significantly less homogeneous binder layer.

Based on these observations, it is concluded that:

- The oven-aged binder is significantly less homogeneous than the naturally aged binder. The outer layer is more intensely affected by the oven's heat and therefore is stiffer. In this study, the difference in the PG of the outer and inner layers was higher than 12°C in several cases, especially when a high temperature (135°C) was used. This can affect the Mix's behavior and performance.

- In this study, while no significant difference was observed between the binder stiffness gradient exposed to the 85°C and 110°C temperatures, increasing the temperature to 135°C adversely affected the homogeneity of the binder. Therefore, it is recommended that the oven-aging temperature be limited to 110°C.
- Out of the eight protocols examined, aging for 4 days at 110°C (sample 4) produced the closest resemblance to natural aging, as determined by the average binder PG grade and stiffness gradient.

Chapter 7 : SUMMARY AND CONCLUSION

This study evaluated the effects of binder homogeneity and durability on the performance of recycled mixes. Five mixes and two rejuvenator types were considered in this study. Mix 1 was the control with the virgin binder and aggregate. Mixes R1 and R2 included 100% RAP materials with two levels of RA1 rejuvenator at a dosage of 7.9% and 15.7%, respectively. Furthermore, mixes R3 and R4 also included 100% RAP materials with two levels of RA2 rejuvenator at a dosage of 6.5% and 11.3%, respectively. These mixes were subjected to three levels of aging: short-term aging at 165°C for 1 hour, and long-term aging at 5 and 10 days (85°C). Performance tests were conducted on rejuvenated RAP specimens and compared to virgin asphalt concrete specimens. High and intermediate temperature properties of the asphalt mixes were evaluated using the Hamburg Type Loaded Wheel Tracking test and the Semi-Circular Bending test, respectively. The Florida Indirect Tension Test was conducted to determine the tensile failure limits and the dissipated creep strain energy density. The following observations were made:

- The short-term aged recycled mix in this study exhibited better rutting resistance than the virgin mix when its high-temperature PG (HTPG) was 6°C higher than the virgin mix. When it had the same HTPG, the rutting resistance was similar. Long-term aged (10-day) recycled mixes recorded rutting and moisture resistance similar to the virgin mixes.
- Short-term aged virgin mix showed higher intermediate temperature fracture resistance than the short-term aged recycled mixes, as measured by the $DCSE_f$ value at 10°C and SCB Jc value at 25°C.
- Long-term aged (10 days) virgin mixes exhibited higher $DCSE_f$ values than long-term aged (10 days) recycled mixes.
- Long-term aged (5 to 10 days) recycled mixes recorded SCB J_c values statistically similar to the long-term aged (5 to 10 days) virgin mixes.
- Short-term aged virgin mixes and recycled mixes with high rejuvenator dosage rates (RAP+15.7% RA1 and RAP + 11.3% RA2) exhibited higher rut depths than similar mixes long-term aged at 5 and 10 days.
- Aging levels did not affect the rut depths for recycled mixes at lower rejuvenator dosage levels (RAP+7.9% RA1 and RAP + 6.5% RA2).
- All mixes except recycled mixes with a higher dosage of RA1 showed a better cracking performance for short-aged samples than long-term aging. RA1 at a high dosage seemed to improve crack performance with aging.
- The virgin (control) mix had an average rut depth of 10 mm. The average rut depth for recycled mixes with HTPG of the same as virgin mix was 10.46 mm and with recycled mixes with 6°C higher HTPG was 2.84 mm. This indicates that overall rutting performance of the control mix was almost the same as recycled mix when the HTPG are the same. Also, this indicates that recycled mix had an overall better rutting resistance than the virgin mix when its HTPG was 6°C higher than the virgin mix.

- Rut depths for mixes recycled to a 6ºC higher HTPG than the control mix using RA1 and RA2 were 2 and 3.37 mm, respectively. The rut depth for mixes recycled to the same HTPG of the control mix using RA1 was 12 mm, and 9 mm using RA2 as compared to 10 mm of rutting for the control.
- Aging levels evaluated resulted in a progressive increase in the SCB Jc values of the recycled mixes at higher rejuvenator dosage levels (RAP+15.7% RA1 and RAP + 11.3% RA2).
- Only the short-term aged virgin mix had SCB Jc values equal to or greater than the specified minimum value of 0.5kJ/m^2.
- Only the short-term aged virgin mix had a Jc value equal to or greater than the specified minimum value of 0.5 kJ/m^2 (10, 11). This is an indication that the virgin mix had a better crack propagation resistance compared to recycled mixes.
- The average Jc for mixes rejuvenated to 6ºC higher than the HTPG of the control was 0.34 kJ/m^2. The average Jc for mixes rejuvenated to the same HTPG of the control was 0.30 kJ/m^2. This is possibly an indication that no performance benefit is gained by increasing the amount of rejuvenator beyond the amount needed to achieve 6ºC above that of the HTPG of the virgin mix.
- Short-term aged virgin mix and recycled mixes with the low dosage rate of rejuvenator RA1 (RAP+7.9% RA1) exhibited higher $DCSE_f$ values than similar mixes that were long-term aged at 5 and 10 days.
- Low and high dosage rates of recycled mixes with rejuvenator RA2 (RAP+6.5% RA2 and RAP+11.3% RA2) also showed higher $DCSE_f$ values than similar mixes long-term aged at 5 and 10 days.
- Per the $DCSE_f$ values, the virgin mix had the best performance, with an average $DCSE_f$ value of 4.36 kJ/m^3, followed by mixes recycled with RA1, with an average $DCSE_f$ value of 2.58 kJ/m^3, followed by mixes recycled with RA2, with an average $DCSE_f$ value of 2.48 kJ/m^3. This order of performance is the same as that established by the SCB Jc. All mixes had a $DCSE_f$ value higher than the critical value of 0.75 kJ/m^3, indicating a satisfactory crack initiation resistance behavior.
- According to ER values, the mix recycled with RA1 had the best performance, with an average ER value of 5.87, followed by the virgin mix, with an average ER value of 4.86, followed by mixes recycled with RA2, with an average ER value of 4.83. All mixes had an ER value higher than the critical value of 1, indicating a satisfactory crack initiation resistance behavior.
- Recycled binder's Homogeneity Index and Stiffness Gradient Factor were found to correlate with cracking parameters, but not with rutting.
- Generally, short-term aged (1 hour) recycled mixes with a higher HTPG (6°C higher than that of virgin binder) exhibited less rutting and higher moisture resistance than short-term aged virgin mixes. The test results for 5-day aged mixes were mixed for rutting and

moisture resistance. Long-term aged (10-day) recycled mixes presented similar rutting and moisture resistance as the virgin mixes.

- Short-term aged virgin mixes showed higher intermediate temperature fracture resistance than the short-term aged recycled mixes, as measured by the $DCSE_f$ value at 10°C and the SCB Jc value at 25°C. Generally, long-term aged (10 days) virgin mixes exhibited higher $DCSE_f$ values than long-term aged (10 days) recycled mixes. However, long-term aged (5 to 10 days) recycled mixes tended to exhibit SCB J_c values similar to the long-term aged (5 to 10 days) virgin mixes.
- While no significant difference was observed between the binder stiffness gradient exposed to the 85°C and 110°C temperatures, increasing the temperature to 135°C adversely affected the homogeneity of the binder. Therefore, it is recommended that the oven-aging temperature be limited to 110°C.
- Out of the eight protocols examined, aging for 4 days at 110°C (sample 4) produced the closest resemblance to natural aging, as determined by the average binder PG grade and stiffness gradient.

7.1 Hypothesis Evaluation

The results of the analysis are used to examine each hypothesis listed in Section 1.5:

Hypothesis #1: The effectiveness of rejuvenation can be evaluated using critical PAV time and homogeneity index. The acceptable limits for these parameters should be determined after further studies with more rejuvenators. However, the following tentative limits are used to distinguish between proper and improper rejuvenators in this study:

- Critical PAV Time $\geq$ 50 hours
- Ih $\geq$ 0.9
- Rejuvenator dosage is determined to achieve a target HTPG for the recycled binder, as described in #3 below.

Rutting performance: Both rejuvenators used in this study had a PAV critical time of more than 50 hours and homogeneity index of more than 0.9. However, RA1 had a higher homogeneity index than RA2. Based on average trends, RA1 had a rutting performance similar to RA2, and both performed better than the virgin mix when they had a higher HTPG.

Cracking performance: Based on SCB J_c and IDT $DCSE_f$ parameters, RA1 had a better cracking performance than RA2, but the virgin mix had better cracking performance than the recycled mixes. However, the ER parameter shows that the mix with the RA1 rejuvenator shows better cracking performance than the virgin mix, which supports this hypothesis.

Hypothesis # 2: A recycled mix rejuvenated by a proper rejuvenator has a better long-term mix performance compared to a new mix with a virgin binder with a similar HTPG.

RA1 is considered a proper rejuvenator compared to RA2. A mix with a 15.7 % RA1 has the same HTPG as the virgin mix.

Rutting performance: The virgin mix showed equal rutting performance compared to the RAP mix containing the 15.7 % RA1.

Cracking performance: Cracking performance was better for the virgin mix, and RA1 did better than RA2 based on $DCSE_f$ and J_c results. RA1 did better than the virgin mix and better than RA2 based on ER. The results seem to partially support the hypothesis. Further research may be needed.

Hypothesis # 3: The target HTPG for a recycled mix can be set 6°C higher than virgin mixes without compromising the mix performance. A recycled mix can have a long-term performance similar to a virgin mix, with a 6°C lower HTPG compared to the recycled mix.

From a performance standpoint, mixes rejuvenated at a 6°C higher HTPG than the virgin mix performed better in rutting and similarly in cracking, which support this hypothesis.

Hypothesis #4: In the case of improper rejuvenation, the recycled mix will have worse long-term performance compared to a virgin mix.

Rutting performance: This held true for rutting.

Cracking performance: Cracking performance was better for the virgin mix, and RA1 did better than RA2 based on $DCSE_f$ and J_c results. RA1 did better than the virgin mix and better than RA2 based on ER. The results seem to partially support the hypothesis. Further research may be needed.

7.2 Mix Design Implications

Based on the analysis results, we can plot both the rutting performance (as a function of the binder PG grade, Figure 5-2), and the cracking performance (using ER as an example, Figure 5-11) on the same chart. Figure 7-1 is a schematic showing an acceptable range of HTPG based on rutting and cracking criteria. It is clear that the acceptable HTPG of the recycled mix has to be greater than 75 °C. The use of rejuvenators is mainly to improve workability and activate the old binder. Any additional use of rejuvenators that results in binder grade less than HTPG 75 °C is counterproductive. In fact, an optimum design can be to the right of that point, near ER=2.0 (HTPG 77) to provide a good factor of safety against cracking. This type of analysis is mix-specific and should be conducted during the mix design process.

It should be noted that this analysis was based on good mixing in the lab using a rotary mixer. In practice, mixing can be compromised by the speed of production in drum mix plants and in in-place recycling methods.

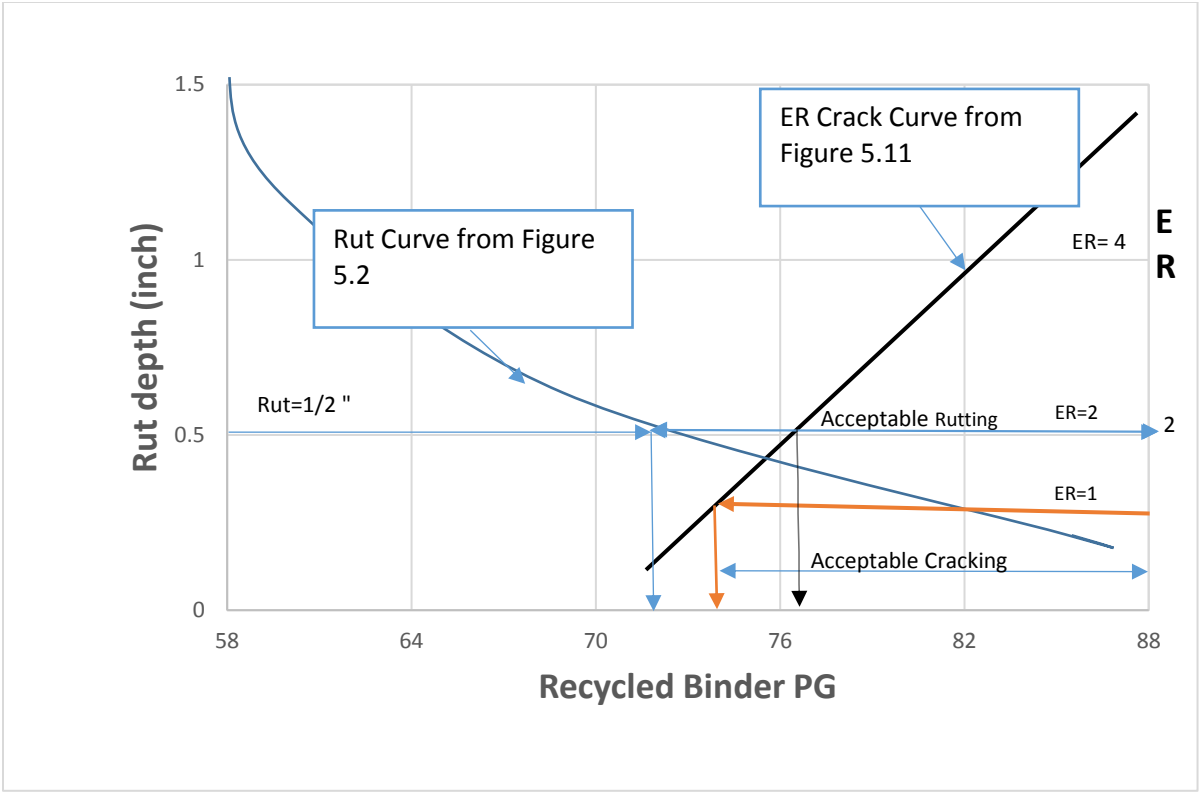

Figure 7-1. Recycled Mix HTPG Grade Selection

References

AASHTO M320 (2017). Standard Specification for Performance-Graded Asphalt Binder. American Association of State Highway and Transportation Officials, Washington, DC.

AASHTO PP (2016). Standard Method of Test for Tensile Creep Compliance, Tensile Failure Limits and Energy Ratio of Asphalt Mixtures Using the Superpave Indirect Tension Test. American Association of State Highway and Transportation Officials, Washington, DC.

AASHTO R30 (2002). Standard Practice for Mixture Conditioning of Hot-Mix Asphalt (HMA). American Association of State Highway and Transportation Officials, Washington, DC.

ASHTO T 315 (2012). Standard Method of Test for Determining the Rheological Properties of Asphalt Binder Using a Dynamic Shear Rheometer (DSR). American Association of State Highway and Transportation Officials, Washington, DC.

AASHTO T 324 (2017). S Standard Method of Test for Hamburg Wheel-Track Testing of Compacted Asphalt Mixtures. American Association of State Highway and Transportation Officials, Washington, DC.

Ali, Hesham, and Khaled Sobhan. 2012. "On the Road to Sustainability: Properties of Hot in-Place Recycled Superpave Mix." Transportation Research Record: Journal of the Transportation Research Board, no. 2292: 88–93.

Ali, Hesham, and Mojtaba Mohammadafzali. "Long-term aging of recycled binders." Final Report Submitted to Florida Department of Transportation, Contract BDV29 Two 977-01 July 2015.

Alkins, Andrew, Becca Lane, and Tom Kazmierowski. 2008. "Sustainable Pavements: Environmental, Economic, and Social Benefits of in Situ Pavement Recycling." Transportation Research Record: Journal of the Transportation Research Board, no. 2084: 100–103.

Allen, R Grover, Dallas N Little, and Amit Bhasin. 2012. "Structural Characterization of Micromechanical Properties in Asphalt Using Atomic Force Microscopy." Journal of Materials in Civil Engineering 24 (10): 1317–27.

Al-Qadi, Imad L, Mostafa Elseifi, and Samuel H Carpenter. 2007. "Reclaimed Asphalt Pavement—a Literature Review." Federal Highway Administration, IL, USA Report No.: FHWA-ICT-07-001. Contract No.: ICT R27-11.

ASTM D 2041 (2011). Standard Test Method for Theoretical Maximum Specific Gravity and Density of Bituminous Paving Mixtures. ASTM International, West Conshohocken, Pennsylvania United States.

ASTM-D2172 (2017). Standard Test Methods for Quantitative Extraction of Asphalt Binder from Asphalt Mixtures. ASTM International, West Conshohocken, Pennsylvania United States.

ASTM-D5404 (2017). Standard Practice for Recovery of Asphalt from Solution Using the Rotary Evaporator. ASTM International, West Conshohocken, Pennsylvania United States.

ASTM-D6307 (2019). Standard Test Method for Asphalt Content of Asphalt Mixture by Ignition Method. ASTM International, West Conshohocken, Pennsylvania United States.

ASTM-D8044 (2016). Standard Test Method for Evaluation of Asphalt Mixture Cracking Resistance Using the Semi-Circular Bend Test (SCB) at Intermediate Temperatures. ASTM International, West Conshohocken, Pennsylvania United States.

Bell, Chris A, Alan J Wieder, and Marco J Fellin. 1994. "Laboratory Aging of Asphalt-Aggregate Mixtures: Field Validation" No. SHRP-A-390.

Bowers, B. F., Huang, B., He, Q., Shu, X., Jia, X., & Miller, B. C. 2014. "Investigation of sequential dissolution of asphalt binder in common solvents by FTIR and binder fractionation." Journal of Materials in Civil Engineering, 27(8), 04014233.

Bowers, B. F., 2013. "Investigation of asphalt pavement mixture blending utilizing analytical chemistry techniques". Doctoral Thesis, The University of Tennessee

Buttlar, W.G., and R. Roque. 1994. "Experimental Development and Evaluation of the New SHRP Measurement and Analysis System for Indirect Tensile Testing at Low Temperature." Transportation Research Record 1454: 163–71.

Carpenter, Samuel H, and John R Wolosick. 1980. "Modifier Influence in the Characterization of Hot-Mix Recycled Material." Transportation Research Record, no. 777, pp.15-22.

Cavalli, M.C., M. Griffa, S. Bressi, M.N. Partl, G. Tebaldi, and L.D. Poulikakos. 2016. "Multiscale Imaging and Characterization of the Effect of Mixing Temperature on Asphalt Concrete Containing Recycled Components." Journal of Microscopy 264 (1): 22–33.

Coffey, Sean, Eric DuBois, Yusuf Mehta, Aaron Nolan, and Caitlin Purdy. 2013. "Determining the Impact of Degree of Blending and Quality of Reclaimed Asphalt Pavement on Predicted Pavement Performance Using Pavement ME Design." Construction and Building Materials 48: 473–78.

Cooper III, S. B., Mohammad, L. N., and Elseifi, M. A. (2011). Laboratory performance characteristics of sulfur-modified warm-mix asphalt. Journal of Materials in Civil Engineering, 23(9), 1338-1345.

Ding, Yongjie, Baoshan Huang, and Xiang Shu. 2016. "Characterizing Blending Efficiency of Plant Produced Asphalt Paving Mixtures Containing High RAP." Construction and Building Materials 126: 172–78.

Dony, A, J Colin, D Bruneau, I Drouadaine, and J Navaro. 2013. "Reclaimed Asphalt Concretes with High Recycling Rates: Changes in Reclaimed Binder Properties According to Rejuvenating Agent." Construction and Building Materials 41: 175–81.

Huang, Baoshan, Guoqiang Li, Dragan Vukosavljevic, Xiang Shu, and Brian K Egan. 2005. "Laboratory Investigation of Mixing Hot-Mix Asphalt with Reclaimed Asphalt Pavement." Transportation Research Record 1929 (1): 37–45.

Karlsson, Robert, and Ulf Isacsson. 2003. "Application of FTIR-ATR to Characterization of Bitumen Rejuvenator Diffusion." Journal of Materials in Civil Engineering 15 (2): 157–65.

Kim, Y Richard, Youngguk Seo, Mark King, and Mostafa Momen. 2004. “Dynamic Modulus Testing of Asphalt Concrete in Indirect Tension Mode.” Transportation Research Record 1891 (1): 163–73.

Kooij, V. D., & Verburg, H. A. 1996. "Mixing of high penetration bitumen with aged bitumen during hot-mix recycling of porous asphalt'. In Eurasphalt and Eurobitume congress, Strasbourg, 7-10 May 1996. Volume 3. Paper E&E. 5.137..

Lee, Teh-Chang, Ronald L Terrel, and Joe P Mahoney. 1983. Test for Efficiency of Mixing of Recycled Asphalt Paving Mixtures.

Masson, JF, GM Polomark, and P Collins. 2002. “Time-Dependent Microstructure of Bitumen and Its Fractions by Modulated Differential Scanning Calorimetry.” Energy & Fuels 16 (2): 470–76.

McDaniel, Rebecca S, Hamid Soleymani, R Michael Anderson, Pamela Turner, and Robert Peterson. 2000. “Recommended Use of Reclaimed Asphalt Pavement in the Superpave Mix Design Method.” NCHRP Web Document 30.

Mohammad, Louay N, Minkyum Kim, and Mostafa Elseifi. 2012. “Characterization of Asphalt Mixture’s Fracture Resistance Using the Semi-Circular Bending (SCB) Test.” In , 1–10. Springer.

Mohammadafzali, Mojtaba. 2017. “Evaluation of Durability and Homogeneity of Rejuvenated Asphalt Binders.” Florida International University. https://digitalcommons.fiu.edu/etd/3167/.

Mohammadafzali, Mojtaba, Hesham Ali, James A Musselman, Gregory A Sholar, and Aidin Massahi. 2017. “The Effect of Aging on the Cracking Resistance of Recycled Asphalt.” Advances in Civil Engineering 2017.

Navaro, Julien, Denis Bruneau, Ivan Drouadaine, Johan Colin, Anne Dony, and Jérôme Cournet. 2012. “Observation and Evaluation of the Degree of Blending of Reclaimed Asphalt Concretes Using Microscopy Image Analysis.” Construction and Building Materials 37: 135–43.

Nguyen, Viet Hung. 2009. “Effects of Laboratory Mixing Methods and RAP Materials on Performance of Hot Recycled Asphalt Mixtures.”

Noureldin, Ahmed S, and Leonard E Wood. 1987. “Rejuvenator Diffusion in Binder Film for Hot-Mix Recycled Asphalt Pavement.” Transportation Research Record, no. 1115.

Quintus, HL Von, JA Scherocman, CS Hughes, and TW Kennedy. 1991. “Asphalt Aggregate Mixture Analysis System.” National Cooperative Highway Research Program Report 338.

Rad, Farhad Yousefi, Nima Roohi Sefidmazgi, and Hussain Bahia. 2014. “Application of Diffusion Mechanism: Degree of Blending between Fresh and Recycled Asphalt Pavement Binder in Dynamic Shear Rheometer.” Transportation Research Record 2444 (1): 71–77.

Roque, Reynaldo, Bjorn Birgisson, Christos Drakos, and Bruce Dietrich. 2004. “Development and Field Evaluation of Energy-Based Criteria for Top-down Cracking Performance of Hot Mix Asphalt (with Discussion).” Journal of the Association of Asphalt Paving Technologists 73.

Roque, Reynaldo, and William G Buttlar. 1992. "The Development of a Measurement and Analysis System to Accurately Determine Asphalt Concrete Properties Using the Indirect Tensile Mode (with Discussion)." Journal of the Association of Asphalt Paving Technologists 61.

SAS Institute. 1985. SAS User's Guide: Statistics. Vol. 2. Sas Inst.

Sholar, G., Page, G., Musselman, J. and Moseley, H. 2004. "Evaluating the Use of Lower VMA Requirements for Superpave Mixtures." FDOT/SMO/04–479, Florida DOT.

Shu, Xiang, Baoshan Huang, and Dragon Vukosavljevic. 2008. "Laboratory Evaluation of Fatigue Characteristics of Recycled Asphalt Mixture." Construction and Building Materials 22 (7): 1323–30.

Silva, Hugo MRD, Joel RM Oliveira, and Carlos MG Jesus. 2012. "Are Totally Recycled Hot Mix Asphalts a Sustainable Alternative for Road Paving?" Resources, Conservation and Recycling 60: 38–48.

Sirin, Okan, Dalim K Paul, and Emad Kassem. 2018. "State of the Art Study on Aging of Asphalt Mixtures and Use of Antioxidant Additives." Advances in Civil Engineering 2018.

Tang, Bing, and Ulf Isacsson. 2005. "Determination of Aromatic Hydrocarbons in Asphalt Release Agents Using Headspace Solid-Phase Microextraction and Gas Chromatography–Mass Spectrometry." Journal of Chromatography A 1069 (2): 235–44.

Xu, Ying, Shifa Xu, and Jie Ji. 2014. "Measurement Method of Blending Status between Virgin and Aged Binder in Recycled Asphalt Mixtures—A Literature Review." In Challenges and Advances in Sustainable Transportation Systems, 311–18.

Yan, Yu, Sanghyun Chun, Reynaldo Roque, and Sungho Kim. 2016. "Effects of Alternative Polymer Modifications on Cracking Performance of Asphalt Binders and Resultant Mixtures." Construction and Building Materials 121 (September): 569–75. https://doi.org/10.1016/j.conbuildmat.2016.06.049.

Zaumanis, Martins, Rajib B Mallick, and Robert Frank. 2014a. "100% Recycled Hot Mix Asphalt: A Review and Analysis." Resources, Conservation and Recycling 92: 230–45.

Zaumanis, Martins, Rajib B Mallick, Lily Poulikakos, and Robert Frank. 2014b. "Influence of Six Rejuvenators on the Performance Properties of Reclaimed Asphalt Pavement (RAP) Binder and 100% Recycled Asphalt Mixtures." Construction and Building Materials 71: 538–50.

Zearley, Lowell J. 1979. "Penetration Characteristics of Asphalt in a Recycled Mixture."

Zhang, Kun, and Balasingam Muhunthan. 2017. "Effects of Production Stages on Blending and Mechanical Properties of Asphalt Mixtures with Reclaimed Asphalt Pavement." Construction and Building Materials 149: 679–89.

Zhao, Sheng, Baoshan Huang, Xiang Shu, and Mark E Woods. 2016. "Quantitative Evaluation of Blending and Diffusion in High RAP and RAS Mixtures." Materials & Design 89: 1161–70.

Zhi-ling, H.U. Guo-ling ZHU, and GUO Xiao-ling. 2005. “Differential Scanning Calorimetry (DSC) and Its Application in Asphalt Study [J].” Shanxi Architecture,Year 2005, Issue 8, Page 113-114